GEOPHYSICAL TRANSACTIONS
GEOFIZIKAI KÖZLEMÉNYEK
ГЕОФИЗИЧЕСКИЙ БЮЛЛЕТЕНЪ

XX. 3—4.

CONTENTS

TARTALOM

4

СОДЕРЖАНИЕ

A Geofizikai Közlemények Szerkesztő Bizottsága úgy határozott, hogy az 1. Pót-füzetben jelzett monográfiákat különkiadásként jelenteti meg. A lap rendes számai a szokásos módon jelennek meg.

SZERKESZTŐSÉG

The Editorial Board of the Geophysical Transactions has decided to issue the monographs announced in Supplement 1 in the form of Special Editions. The serial ordinary members of the paper will be published in the usual way.

THE EDITORIAL OFFICE

Редакция журнала «Геофизический буллетень» решила издать монографии, объявленные в дополнительном выпуске N 1, в отдельном номере. Очеред-ные номера журнала выпускаются по обычному порядку.

РЕДАКЦИЯ

AN ANALYSIS OF THE INITIAL SEISMIC PULSE NEAR UNDERGROUND EXPLOSIONS

T. BODOKY–G. KORVIN–I. LIPTAI–J. SIPOS*

The experiments were carried out in 1968 and 1969, in the Nyir-region, Hungary, in a nearsurface sandy complex characteristic of this area. The primary aim of the investigations was to determine the basic characteristics of the seismic pulse, its dependence on depth and charge weight, further its change during propagation. A detailed knowledge of these parameters has been rendered necessary by digital seismic data processing, where a realistic initial wave shape is indispensable for the deconvolution process.

The method and instrument of experiment

A barium-titanate crystal was used as detector, for the measurements. The unit-amplification matching member was mounted in a water-proof sonde-case holding the crystal. Signals from the crystal passed through this member to the recorder. The latter was a storage-system Textronix oscilloscope provided with a photoadapter.

The main data of the sensing head: material: $BaTiO_3$ ceramics; diameter 20 mm; natural frequency 500 kcps; measuring range 0,1–100,0 atm; capacity 1670 pF; sensitivity 230 mV/atm; attenuating block: epoxiresin. The recording oscilloscope permitted the input signal to start the ray with an extremely short delay ($1,6 \cdot 10^{-7}$ sec), to realize the amplification and time-expansion in calibrated stages, and to store the signal on the oscilloscope screen long enough to be photographed. The sensitivity of this oscilloscope hardly varies between 0 and 10 kcps. The calibration of amplitude and frequency is provided by an internal calibrating unit. Voltage limits: 1 mV/div, resp. 300 mV/div peak to peak; time limits: 10^{-6} s/div, resp. 1 s/div, (LÁNYI–RÁKÓCZY, 1969).

For the explosions, usual seismic hole-shooting with Paxit IV explosive was used. (Paxit IV is a mixture of trinitro-toluol, dinitro-toluol and ammon-saltpeter. Its parameters are similar to Nobel's Explosive No. 704, Ammonal No. 3 and Blasting Abelite).

Partly to attain a better coupling, partly for the elimination of the effect of the low-velocity layer, the sensing sonde was placed, in general, in hole. When investigating the effect of the low-velocity layer, the sonde was placed on the bottom of the mud-pit, on the surface. Shots recorded in a hole are shown in Fig. 11, shots recorded on the surface, in Fig. 1.

Manuscript received 5, 5, 1971.
* Roland Eötvös Geophysical Institute, Budapest.
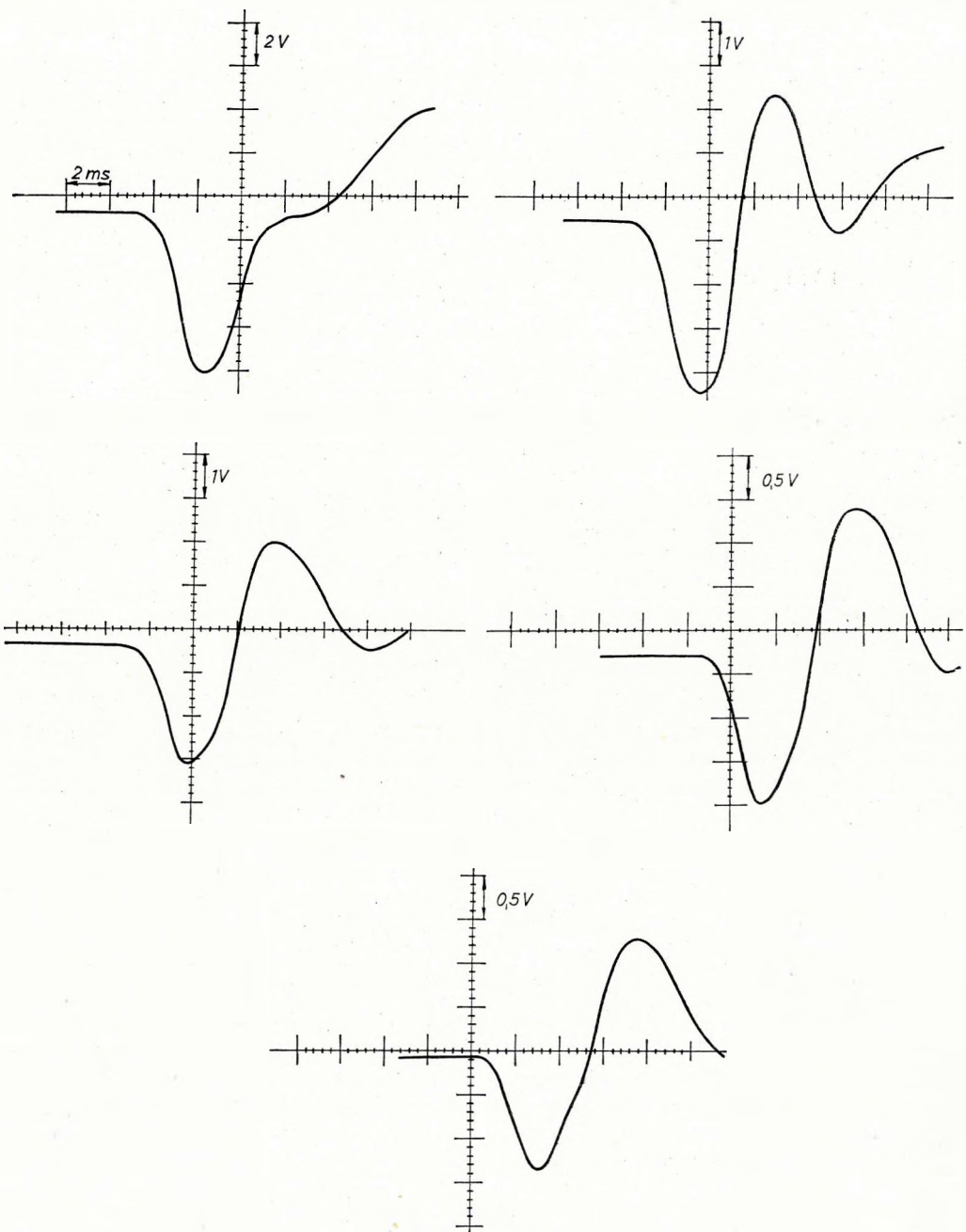
Fig. 1 Series of records observed at increasing source-detector distances (Cf. Table I, Rec. Nos. 5, 4, 3, 2, 1)

1. ábra. Felszínen mért jelsorozat növekvő töltet—szonda-távolság mellett (v. ö. I-es táblázat 5., 4., 3., 2., 1. felvétel)

Рис. 1. Серия сигналов, записанных на дневной поверхности при увеличивающихся расстояниях до пункта возбуждения (см. табл. I. записи 5, 4, 3, 2, 1)

Table I.

List of records

Date	Charge weight, kg	Charge depth, m	Detector depth, m	Charge-detector horizontal distance, (m)	Charge-detector distance, m	Observation	Remark
1. 1969 11 05	1	15	0,3	3,6	15,13	on the surface	
2. 1969 11 05	1	10,5	0,3	3,6	10,82	on the surface	
3. 1969 11 05	1	8,0	0,3	3,6	8,5	on the surface	
4. 1969 11 05	1	5	0,3	3,6	5,92	on the surface	
5. 1969 11 05	1	3	0,3	3,6	4,5	on the surface	
6. 1969 11 05	1	15	0,3	3,1	15,02	on the surface	
7. 1969 11 05	1	9	0,3	3,1	9,24	on the surface	
8. 1969 11 05	1	3,5	0,3	3,1	4,46	on the surface	
9. 1969 11 05	1	12	0,3	2,6	11,99	on the surface	
10. 1969 11 05	1	6	0,3	2,6	6,26	on the surface	
11. 1968 10 10	1	10	10	10	10,0	in hole	ghost
12. 1968 10 10	1	15	10	10	11,18	in hole	ghost
13. 1968 10 10	1	30	10	10	22,36	in hole	ghost
14. 1968 10 10	1	40	10	10	31,62	in hole	ghost
15. 1968 10 10	1	50	10	10	41,23	in hole	ghost
16. 1968 10 10	1	20	0	10	22,36	in hole	ghost
17. 1969 04 24	0,125	15	12	17	17,26	in hole	ghost
18. 1969 04 23	0,25	15	12	16	16,28	in hole	ghost
19. 1969 04 23	0,5	15	12	16	16,28	in hole	ghost
20. 1969 04 23	1	15	12	17	17,26	in hole	ghost
21. 1969 04 24	2	15	12	17	17,26	in hole	ghost
22. 1969 04 24	4	15	12	17	17,26	in hole	ghost
23. 1969 04 24	1	10	0	1	10,05	in hole	ghost

Interpretation of records

Records were sampled manually at equidistant rates $\Delta t = 0,0002$ sec, resp. $\Delta t = 0,00025$ sec. The computations were performed with a MINSK-2 computer. The beginning of the analysed interval of the pulse was the first onset of the pressure wave and the end of the interval was identical with the end of the first period.

The computer program determined for each pulse:

a) the pulse-shape, reduced to zero average and normalized with respect to the amplification used;

b) the minimum and maximum amplitude (A_{min} and A_{max}), the time interval between them (T_1), the pulse width (T), and the average energy of the pulse (Fig. 2).

The spectrum was computed with the well-known formula of the transfer function of digital filters (ROBINSON–TREITEL, 1964).

23 records were analysed altogether (Table I). In case of ghosts the primary pulse and its ghost were analysed separately as well as the composite wave-form.
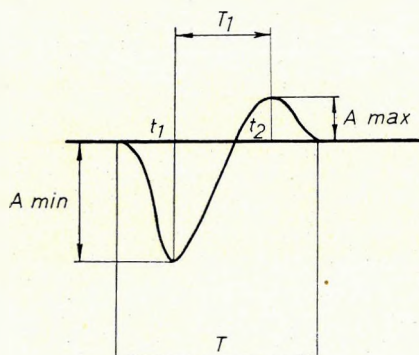
Fig. 2 Characteristics of the primary pulse

2. *ábra.* A jelalak jellemzöi

Рис. 2. Характеристики формы сигналов

Results

The following relations were analysed:

1. the change in pulse shape during propagation;

2. dependence of pulse shape on charge weight;

3. the mechanism of ghost generation.

The results of analysis will be compared with already published theoretical and experimental data, and discrepancies will be tried to be explained. Pulses observed on the surface and those observed in hole will be separately treated, since they show rather different properties, due to the filtering effect of the weathered layer.

Change in pulse shape during propagation

The dependence of amplitude on distance

Pulse amplitudes, when observed on the surface, decreased with increasing shot-detector distance, according to the law

$A_{min} = \text{const.} \, r^{-1}$

$A_{max} = \text{const.} \, r^{-1,1}$

The results apply to a distance interval $r = 4,5 - 15$ m and a constant charge weight $W = 1$ kg (Fig. 3.a). The series, recorded in hole, showed a significant, although not regular, decrease.

Dependence of pulse energy on distance

The average energy was found to depend on distance as

$$E = \text{const.} \, r^{-2,32},$$

when measured on the surface. The hole measurements gave

$$E = \text{const.} \, r^{-2,02}, \qquad \text{(Fig. 3.b)}$$

There is a considerable discrepancy among experimental data published on amplitude decrease (Table II). The relatively small exponent found is closest to that observed in water (GRINDA, 1959; LÁNYI–RÁKÓCZY, 1969). This is due to the small range of distances considered. Indeed, the law $E \sim r^{-2,32}$, describing the decrease of energy in the weathered layer, can be written as $E \sim r^{-2} \cdot r^{-0,32}$, where the first factor describes spherical divergence, while the second corresponds to absorption, since, in the range of distances in question, $r^{-0,32} \approx e^{-2\alpha r}$ with $\alpha = 0,14$ m^{-1} being the
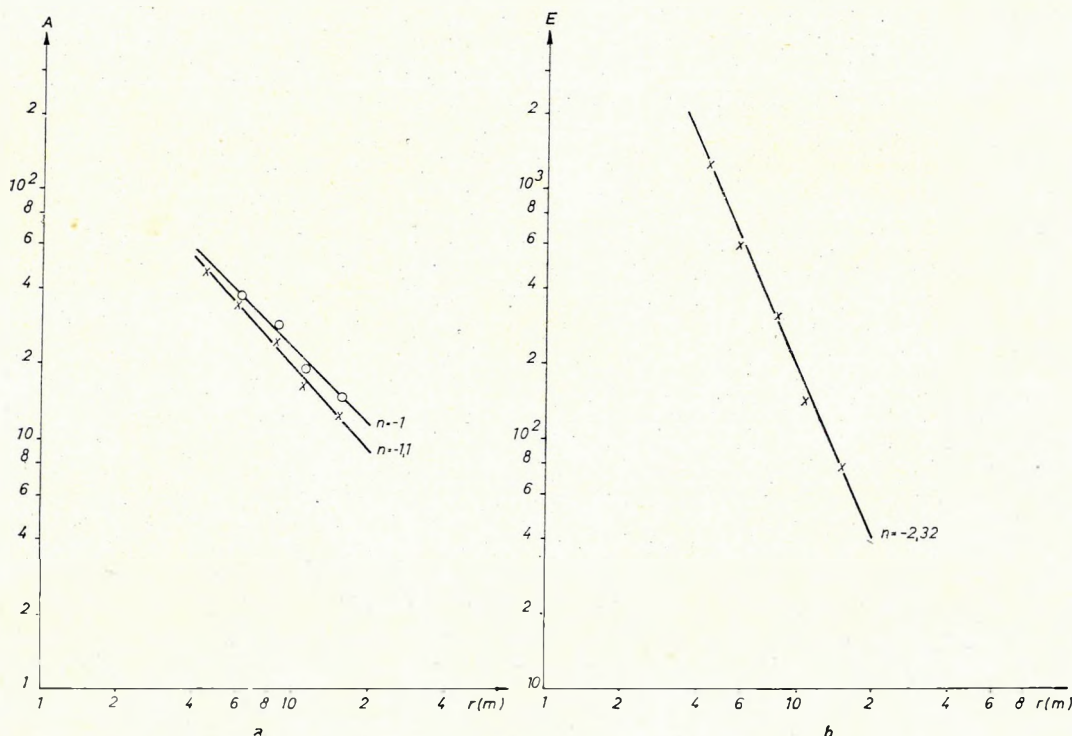
Fig. 3 Amplitude *(a)* and average energy *(b)* values observed on the surface, as functions of distance

3. ábra. Felszínen mért amplitúdó *(a)* ill. átlagenergia *(b)* értékek a távolság függvényében, állandó töltetsúly mellett

Рис. 3. Зависимость амплитуды *(a)* и средней интенсивности *(б)* от расстояния, при равных величинах заряда

Table II.

Dependence of amplitude on distance

	Author	Year	Medium	Range of distance, m	Exponent of divergence	Relation
1.	Ricker	1953	clay	15 – 488	$-2.5 \pm 3\%$	$A \sim t^n$
2.	Jolly	1953	clay	50 – 152	-2.6	$A \sim t^n$
3.	Levin-Lynn	1958	—		$-2.26 \div -2.38$	$A \sim t^n$
4.	McDonal et al.	1958	—	30 – 150	$-1.98 \div -2.26$	$A \sim t^n$
5.	Duvall	1953	sandy clay resp. granite	1.5 – 5,1	$-1.6 \div -2.5$	$A \sim r^n$
6.	Grinda	1959	water		-1.13	$A \sim r^n$
7.	Fogelson et al.	1959	granite gneiss	0.7 – 32	-1	$A \sim r^n$
8.	Kogan	1961	—	r larg᷍	-2	$A \sim r^n$
9.	Lányi-Rákóczy	1969	water	50 – 830	-0.9727	$A \sim r^n$
10.	O'Brien	1969	clay	3 – 80	$-1.01 \div -1.66$	$A \sim r^n$
11.	O'Brien	1969	sandstone	3 – 80	$-1.14 \div -1.69$	$A \sim r^n$

Dependence of energy on distance

	Author	Year	Medium	Range of distance, m	Exponent of divergence	Relation
12.	Howell-Kaukonen	1954	—		-2.3	$E \sim r^n$
13.	Howell, Jr.–Budenstein	1955	—	3.08 – 357	-1.3; -2.6; -3 -4.4, near shot: -6.9	$E \sim r^n$
14.	Fogelson et al.	1959	granite gneiss	0.7 – 32	-2	$E \sim r^n$

absorption coefficient for the dominant frequency of the pulse. It is a general experience that for greater distances the exponent increases, owing to energy losses in reflection, absorption and scattering phenomena.

Relation between pulse-width and distance

The pulse width T and the time interval T_1 between amplitude minimum and amplitude maximum increases during propagation according to the laws

$T = \text{const.} \, r^{0,24}$

$T_1 = \text{const.} \, r^{0,35}$

(detector on surface) and

$T = \text{const.} \, r^{0,42}$

$T = \text{const.} \, r^{0,80}$

(detector in hole; Fig. 4). The results obtained are in conformity with literary data:

$T = \text{const.} \, t^{0,5}$ (RICKER, 1953),

$T = \text{const.} \, r^{0,37-0,16}$ (O'BRIEN, 1969),

$T = \text{const.} \, t^{0,25}$ (McDONAL et al., 1958).

Change of the pulse spectrum during propagation

Each pulse was Fourier-analysed between 0–1000 cps. The computed spectra can be considered as reliable between 10–300 cps (below 10 cps the spectrum is distorted by the shortness of records, while above 300 cps it becomes noisy due to reading errors).

It was assumed that the detector's transfer function is not influenced by its orientation and that the initial spectrum of the explosion does not depend on source depth. Fig. 5 shows the spectra of records observed at different source—detector distances. The analysis of these spectra have led to the following conclusions:

From inspecting the spectra of pulses recorded on the surface it is apparent that the total spectral energy decreases with increasing source—detector distance and the dominant frequency shifts toward the lower range during propagation. The decrease of spectral energy can be attributed to the combined effect of spherical divergence and absorption, while frequency shift is due to a frequency-dependent mechanism of the latter. One among the spectra shown in Fig. 5a has a unique shape, it looks like the spectrum of two interfering wavelets. The corresponding record was made above the ground-water table.

Fig. 5b shows spectra of the pulses recorded in hole. The same shift of frequencies can be observed again, the decrease of energy, however, is not so unambiguous, since in these measurements the explosions were performed under slightly different conditions. The spectrum of Rec. No 6 in this series corresponds to an explosion at the same depth but recorded on the surface. It gives, correspondingly, the transfer function of the weathered layer. The weathered layer behaves as a low-pass filter with 90 cps cut-off frequency and 12 dB/octave slope, approximately.
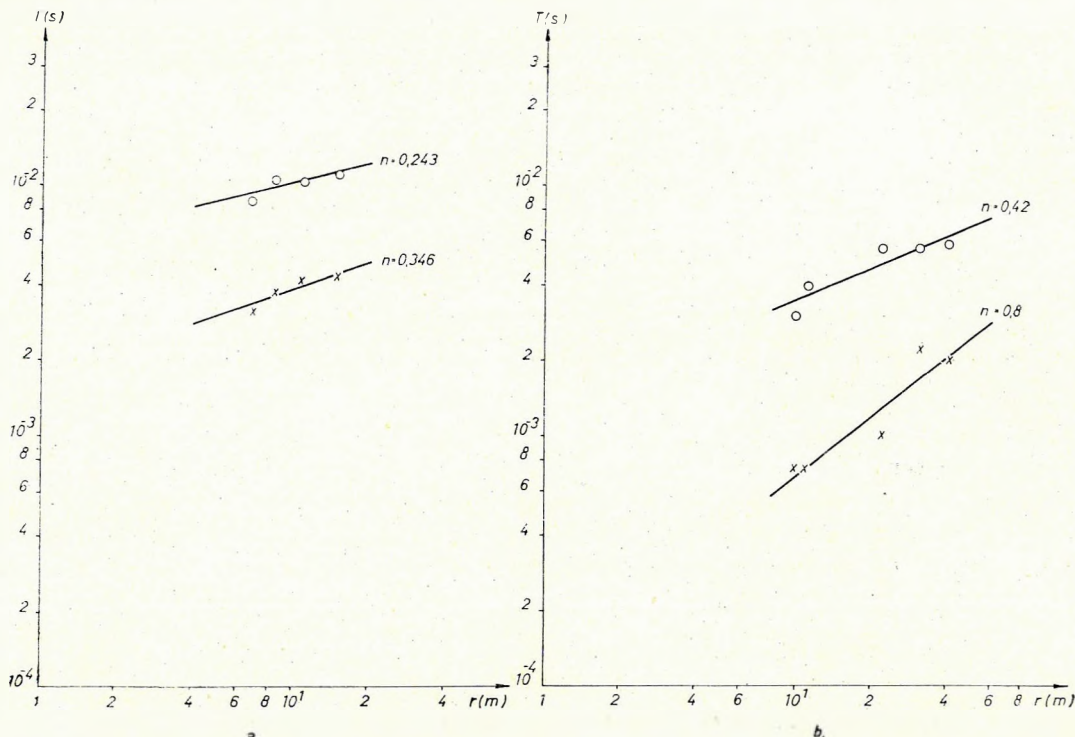
Fig. 4 Pulse width *(e)* and time difference between minimum and maximum amplitudes *(x)*, as functions of distance. Recorded on the surface *(a)*, and in hole *(b)*

4. ábra. Jelszélesség *(e)* illetve maximum—minimum távolság *(x)* a megtett út függ-vényében *a* — felszínen; *b* — lyukban észlelve

Puc. 4. Зависимость ширины *(e)* и разноса экстремумов сигнала *(x)* от пути пробега, при *a* — наземных; *δ* — скважинных наблюдениях

The dominant frequency decreases with increasing source—detector distances, in the order of $r^{-1/3}$ (measured on the surface) and $r^{-2/3}$ (measured in hole). The small deviation from the law describing pulse-broadening is due to the fact that for pulses of not exactly sinusoidal shape, the relation $T = 1/f_{\text{peak}}$ is only approximately valid.

Dependence of absorption on frequency

A frequency-dependent absorption coefficient was determined from the computed spectra of the pulses. We assume that these spectra can be written as

$$Y(\omega) = R(\omega)\cdot S(\omega)\cdot X(r, \omega)\cdot r^{-1} \tag{1}$$

where $R(\omega)$ the source spectrum

$\quad\quad S(\omega)$ amplitude characteristics of the detector

$\quad\quad X(r, \omega)$ attenuation of a harmonic component of angular frequency $\omega = 2\pi f$, after a path of length r.

Let us assume, further, that

$$X(r_1 + r_2; \omega) = X(r_1, \omega) \cdot X(r_2, \omega), \qquad (2)$$

$$X(r, 0) = 1$$

Eq. (2) expresses the homogeneity of the medium and prescribes the usual normalizing constraint. The solution for the functional equation (2) is given by

$$X(r, \omega) = e^{-\alpha(\omega)r}, \quad \alpha(0) = 0,$$

where $\alpha(\omega)$ is some non-negative function of frequency called the (frequency-dependent) absorption coefficient.
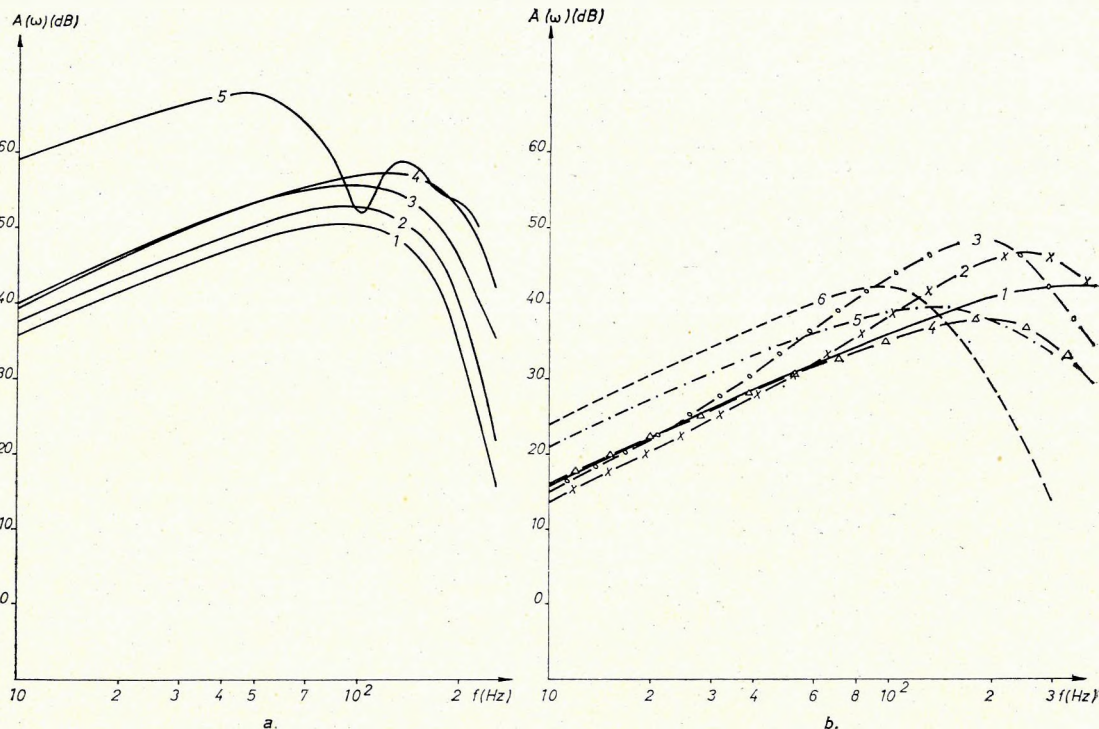
Fig. 5 Amplitude spectra of pulses for different source-detector distances. *a.* Observation on the surface; source-detector distance: *1* 15.13 m, *2* 10.82 m, *3* 8.5 m, *4* 5.92 m, *5* 4.5 m; *b.* Observation in hole; source-detector distance: *1* 10 m, *2* 11.18 m, *3* 22.36 m, *4* 31.62 m, *5* 41.23 m, *6* 22.36 m

5. ábra. Jelek amplitúdó-spekrumai különböző töltet-szonda-távolság esetén, állandó töltetsúly mellett *a)* felszínen észlelve; töltet—szonda-távolság: 1 — 15,13 m; 2 — 10,82 m; 3 — 8,5 m; 4 — 5,92 m; 5 — 4,5 m. *b)* lyukban észlelve; töltet—szonda-távolság: 1 — 10 m; 2 — 11,18 m; 3 — 22,36 m; 4 — 31,62 m; 5 — 41,23 m; 6 — 22,36 m

Рис. 5. Амплитудные спектры сигналов при различных расстояниях до пункта возбуждения и равных величинах заряда

а) наземные наблюдения при расстояниях до пункта возбуждения: *1* — 15,13 м; *2* — 10,82 м; *3* — 8,5 м; *4* — 5,92 м; *5* — 4,5 м;

д) скважинные наблюдения при расстояниях до пункта возбуждения: *1* — 10 м; *2* — 11,18 м; *3* — 22,36 м; *4* — 31,62 м; *5* — 41,23 м; *6* — 22,36 м

Using spectra of pulses recorded at different distances r_1 and r_2 from the source. the detector's transfer function $S(\omega)$ can be eliminated and, assuming that $R(\omega)$ is independent of shot depth, the absorption coefficient can be determined.

In conformity with published theoretical and experimental findings it was found that α obeys the law

$$\alpha(\omega) = \text{const. } \omega^n,$$

where, in our case, $n = 2$ for the weathered layer, the attenuation being

$$2,3 \cdot 10^{-5} f^2 \ \text{dB/m};$$

while measurements performed in hole gave a smaller value $n = 1,2$ (Fig. 6). Exponent $n = 1,2$ is close to the values usually encountered in literature (Table III), while the f^2 law, describing attenuation in the weathered layer, reproduces Ricker's classic, much debated, result.
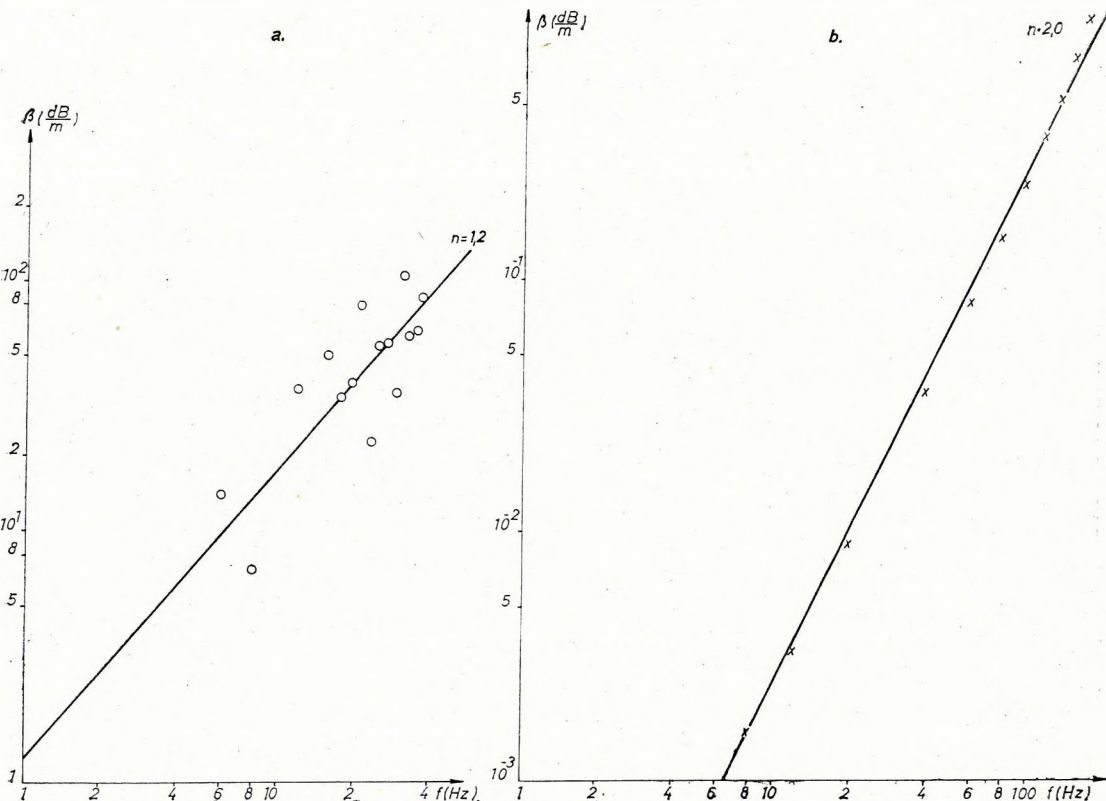
Fig. 6 Coefficient of absorption in function of frequency, *a* in hole, *b* on the surface

6. ábra. Abszorpciós koefficiens a frekvencia függvényében, *a* — lyukban, *b* — felszínen észlelve

Рис. 6. Зависимость коэффициента поглощения от частоты при *a* — скважинных; *б* — наземных наблюдениях

Table III.

Dependence of absorption on frequency

Author	Year	Medium	Range of frequency, cps	Law of absorption
1. Born	1941		22 – 48	$e^{-\delta ft}$; $\delta = 0.023 \div 0.041$
2. Ricker	1953			$e^{-\alpha x}$; $\alpha = \pi f^2/f_0 c$
3. Karusz	1958	sandy clay	80 resp. 200	$e^{-\alpha x}$; $\alpha = 0.19/m$ resp. $\alpha = 0.67/m$
4. McDonal et al.	1958		50 – 450	$\alpha = 0.65\,f^{1.1}$ dB/1000 ft $= 2.13 \cdot 10^{-4} f^{1.1}$ dB/m
5. Huang Jen-Hu	1961	clay, sand	20 – 80	$e^{-\alpha x}$; $\alpha = x f^\beta$ where: $\beta = 1$; $x = 7.8 \cdot 10^{-5}$/Hzm
6. Attewell–Ramana	1966		$1 - 10^8$	$\alpha = 1.012 \cdot 10^{-5} \cdot f^{0.911}$ dB/cm
7. Mack	1966	sandy clay		$e^{-\frac{\pi \cdot x \cdot f}{Q \cdot c}}$ where $\frac{1}{Q} = 0.012 \pm 0.004$
8. Tullos–Reid	1969			$e^{\alpha f^\beta t}$; $\beta = 1 - 1.3$

The dependence of pulse shape on charge weight

In this series of experiments the charge weight varied from 1/8 to 4 kg, the detector was placed in holes at a constant distance $r = 17$ m from the source. The following relations were established:

amplitude vs. charge-weight dependence:

$A_{min} = \text{const. } W^{0,54}$;

energy vs. charge-weight dependence:

$E = \text{const. } W^{1,07}$.

These relations are illustrated on Fig. 7.
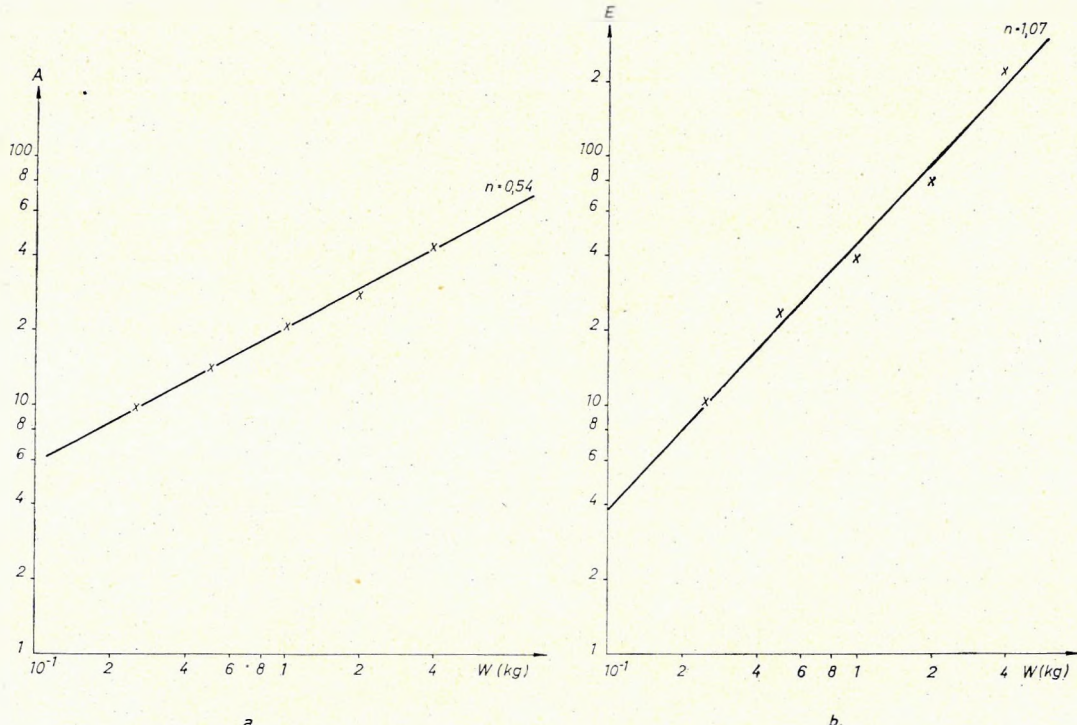
Fig. 7 Amplitude *(a)* and average energy *(b)* values measured in hole, in function of charge weight, for constant source-detector distance

7. ábra. Lyukban mért amplitúdó *(a)* illetve átlagenergia *(b)* értékek a töltetsúly függvényében, állandó töltet—szonda-távolság mellett

Puc. 7. Зависимость величин амплитуд (а) и интенсивности (д) от величины заряда при постоянных расстояниях зонда до пункта возбуждения, при скважинных наблюдениях

The literature concerning amplitude vs. charge weight relations unanimously accepts the $A = \text{const.}W^n$ law. The exponent n, however, greatly depends on the explosion itself (charge weight, shape and quality of explosive, properties of the surrounding medium, etc.), so a variety of values covering the range $n = 0{,}33 - 1{,}2$ have been reported (Table IV). The exponent found by us is close to that of O'BRIEN, 1969.

Pulse-width vs. charge weight dependence

Pulse width T was found to increase with the 0,13th power of charge weight (see also O'BRIEN, 1969). T_1 showed no significant change (Fig. 8).
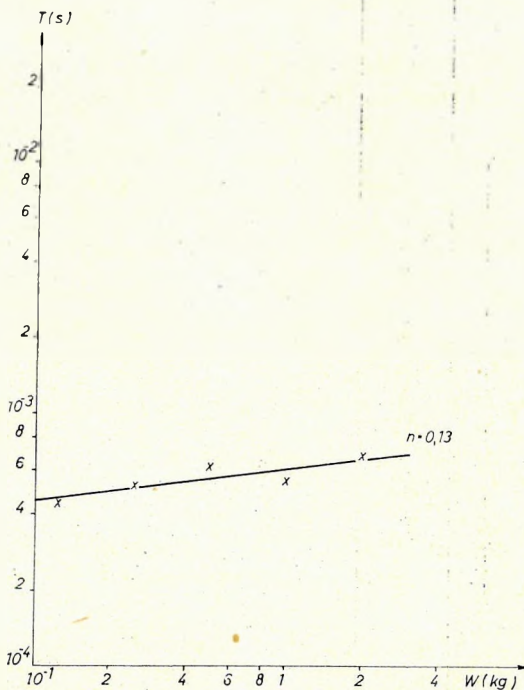
Fig. 8 Pulse width in function of charge-weight

8. ábra. Jelszélesség a töltetsúly függvényében

Рис. 8. Зависимость ширины сигнала от величины заряда

Pulse spectrum vs. charge weight dependence

Fig. 9 illustrates the spectra corresponding to different (1/8–2 kg) charge weights in a constant depth, recorded at a constant distance ($r = 17$ m) from the source. From the analysis of these spectra one may draw the following conclusions:

By increasing the weight of charge the pulse spectrum shifts toward lower frequencies.

2*

Table IV.

Dependence of amplitude on charge weight

Author	Year	Medium	Range of charge weight, kg	Exponent	Remark
1. Barnhard	1967			1/3, 1/2, 2/3, 3/4, 5/6, 1, 7/6	data collected from literature
2. Habberjam—Whetton	1952		2 – 90	0.805	
3. Gaskell	1956	sandstone	9 – 90	1.11	
4. O'Brien	1957		1 – 136	1.12	
5. O'Brien	1960		1 – 200	2/3	
6. Lányi–Rákóczy	1969	water	0.2 – 30	0.3294	
7. O'Brien	1969	clay	0.8 – 9.5	0.336 – 0.55	
8. O'Brien	1969	sandstone	0.8 – 9.5	0.38 – 0.56	

According to PEET's (1960) theory the peak values of the spectra vs. frequency, in case of different charges are located on a hyperbola $A_{peak} = \text{const.} f^{-2}$. We found $A_{peak} = \text{const.} f^{-0,85}$, the smaller exponent can be attributed to the low-pass character of the weathered layer (cf. PEET, 1960, Section IV).
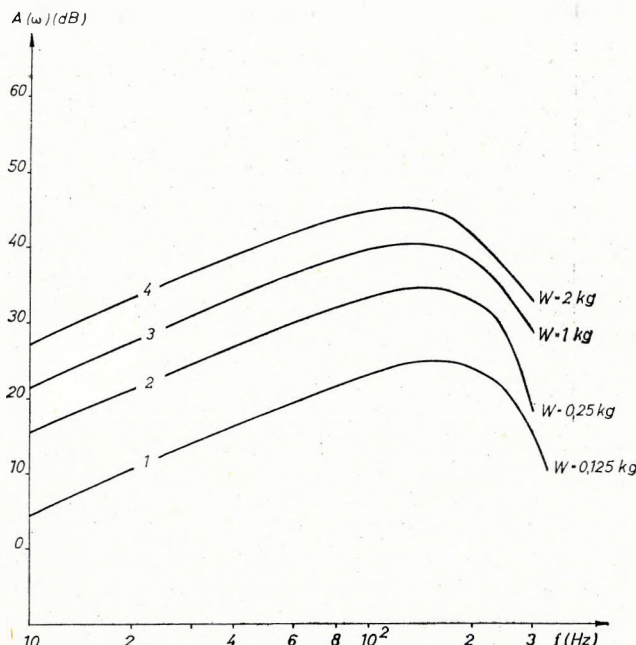

Fig. 9 Amplitude-spectra of pulses for different charge weights (source-detector distance constant)

9. ábra. Jelek amplitúdó-spektrumai különbözö töltet-súlyok esetén, állandó töltet—szonda-távolság mellett

Рис. 9. Амплитудные спектры сигналов при разных величинах заряда и равных расстояниях между зондом и зарядом

The dominant frequency was found to depend on charge weight as $f_{peak} = \text{const.} W^{-0,09}$ (Fig. 10). A recent paper of SCHENK (1971) lists experimental and literary data ranging from $n = 0,12$ to $n = 0,28$. It is of interest to note that all experimental values hitherto reported are lower than the theoretical exponent, $n = 1/3$ (PEET, 1960; BLAKE, 1952) which would correspond to the equivalent radiator hypothesis. The spectral amplitude corresponding to dominant frequencies was found to be proportional with $W^{0,5}$. According to PEET (1960) the theoretical exponent is 2/3.
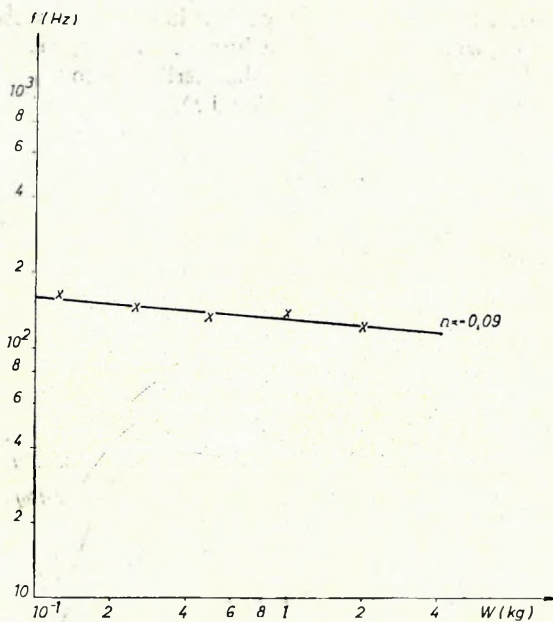
Fig. 10 The dominant frequency in function of charge weight

10. ábra. Csúcsfrekvencia a töltetsúly függvényében

Рис. 10. Зависимость предельных частот от величины заряда

Mechanism of ghost-generation

On certain records (Nos. 11–16, in Table I) the primary pulse was followed by a ghost-arrival. Typical records are shown in Fig. 11.

Figure 12 illustrates the geometry involved in searching for the surface which generates ghosts. From this figure it is obvious that

$$v \cdot t_p = \sqrt{(h_s - h_d)^2 + d^2},$$

$$v \cdot t_g = \sqrt{(h_s - 2h_g + h_d)^2 + d^2},$$

where we have introduced the notations

h_g depth of the ghost-generating surface,

h_d detector depth,

h_s shot depth,

d horizontal source–detector distance,

v average velocity,

t_p, t_g primary and ghost arrival times, respectively.
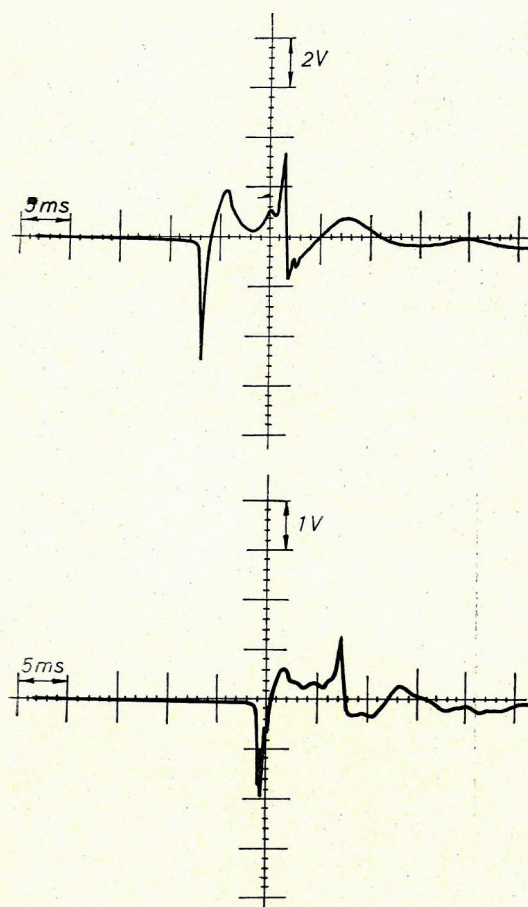
Fig. 11 Typical ghost arrivals
11. ábra. Ghostos felvételek
*Рис. 11.* Записи с отражениями-спутниками
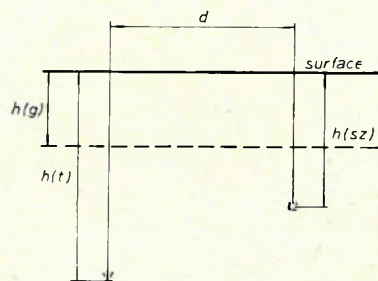
Fig. 12 The geometry of ghost generation
12. ábra. Ghostképződés geometriája
Рис. 12. Геометрия образования отражений-спутников

Using observed values of t_g and t_p, the unknown depth h_g of the surface can be determined. Calculations gave the fair estimation $h_g = 3{-}6$ m, suggesting that ghost pulses originate from top of the ground-water table. In order to check this hypothesis in another way, we computed the angle of incidence Θ of the ghosts and estimated the corresponding reflection coefficients from the ghost/primary amplitude ratios. The plot of reflection coefficient versus angle of incidence is illustrated in Figure 13. Extrapolating for the case of normal incidence, that is, for $\Theta = 0$, a reflection coefficient $-0{,}45$ is obtained which seems to be realistic for a moist clayey sand—dry sand boundary. Indeed, denoting the acoustic impedances of dry sand and moist clayey sand by Z_1 and Z_2, respectively, we have (cf. GÁLFI et al. 1961, p. 233) $Z_1 \approx 15 \cdot 10^4$ gr cm^{-2} sec^{-1}; $Z_2 \approx 40 \cdot 10^4$ gr cm^{-2} sec^{-1}, and

$$R = \frac{Z_1 - Z_2}{Z_1 + Z_2} = -0{,}45.$$
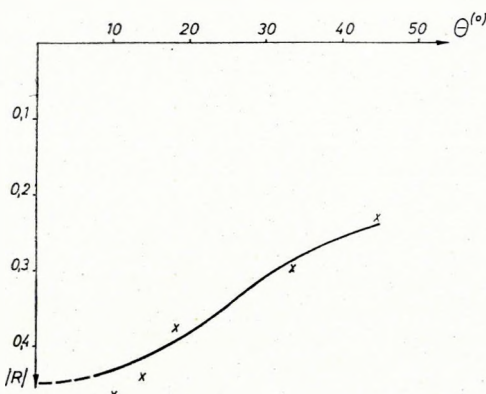
Fig. 13 Dependence of the reflection coefficient on the angle of incidence

13. ábra. Reflexiós együttható a beesési szög függvényében

Рис. 13. Зависимость коэффициента отражения от углов падения

Differences between primary and ghost spectra

As shown in Fig. 14, the spectrum of the composite waveform possesses two isolated peaks indicating that primary and ghost pulses have different spectra. Individual primary and ghost spectra were also determined. The main difference between them is the energy decrease of ghost spectrum, due to spherical and reflection losses and its shift toward lower frequencies, caused by absorption. We have experimental data as yet not enough to elucidate the (presumably frequency-dependent) mechanism of ghost production.

In areas under exploration, measurements of this kind may yield valuable informations for digital processing, since the exact knowledge of ghost/primary amplitude ratio and the time-delay involved is a prerequisite for ghost suppression.
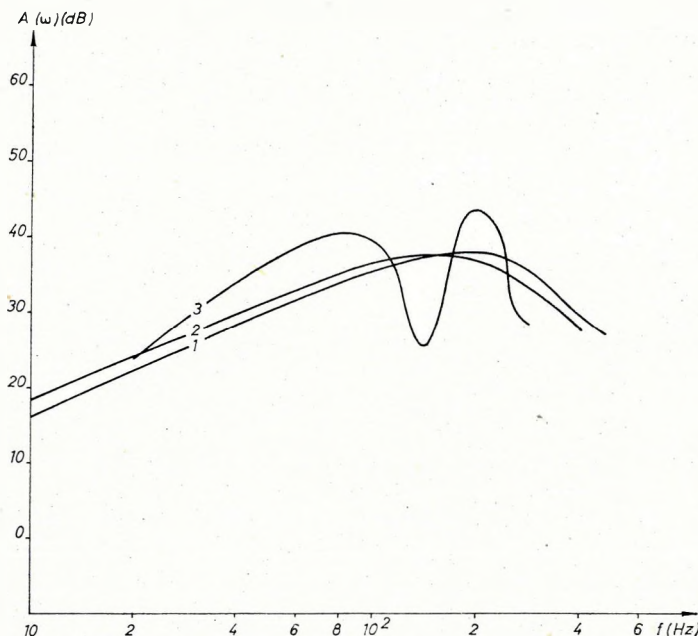
*Fig. 14* Amplitude spectra of primary and ghost pulses *1* primary, *2* ghost, *3* combined spectrum

14. ábra. Ghostos felvétel amplitudó-spektruma *1* — jel spektruma, *2* — ghost spektruma, *3* — jel és gost együttes spektruma

Рис. 14. Амплитудный спектр записей с отражениями-спутниками *1* — спектр исгнала *2* — спектр отражения-спутника; *3* — совместный спектр сигнала и отражения-спутника

REFERENCES

ATTEWELL, P. B.–RAMANA, Y. V., 1966: Wave attenuation and internal friction as functions of frequency in rocks. Geophysics, XXXI. 6., pp. 1049-1056.

BARNHARD, P., 1967: Signal strength of marine explosives. Geophysics, XXXII. 5., pp. 827-832.

BLAKE, F. G., 1952: Spherical wave propagation in solid media. J. Acoust. Soc. Am. XXIV. 2., pp. 211-215.

BORN, W. T., 1941: The attenuation constant of earth materials. Geophysics, VI. 1., pp. 132-148.

DUVALL, W. I., 1953: Strain-wave shapes in rock near explosions. Geophysics, XVIII., 2., pp. 310-324.

FOGELSON, D. E.–ATCHISON, T. C.–DUVALL, W. I., 1959: Propagation of peak strain and strain energy for explosion-generated strain pulses in rock. Colorado School of Mines Quarterly, LIV. 3., pp. 271-284.

GÁLFI, J.–MÁRTON, P.–MESKÓ, A.–STEGENA, L., 1967: Geofizikai Kutatási Módszerek I. Szeizmika. (Methods of Geophysical Exploration I. Seismic methods). Tankönyvkiadó, Budapest.

GASKELL, T. F., 1956: The relation between size of charge and amplitude of refracted wave. Geophysical Prospecting, IV. 2., pp. 185–194.

GRINDA, L., 1959: Influence de la profondeur de l'amplitude des ondes sismiques engendrées par une explosion sous-marine. Bolletino di Geofisica, I. 2., pp. 161–174.

HABBERJAM, G. M.–WHETTON, J. T., 1952: On the relationship between seismic amplitude and charge of explosive fired in routine blasting operations. Geophysics, XVII. 1., pp. 116–128.

HOWELL, B. F. JR.–KAUKONEN, E. K., 1954: Attenuation of seismic wave near an explosion. Bull. Seism. Sec. Am., XLIV., pp. 481–492.

HOWELL, B. F., JR.–BUDENSTEIN, D., 1955: Energy-distribution in explosion generated seismic pulses. Geophysics, XX. 1., 33–52.

HUANG JEN–HU, 1961: A szeizmikus hullám frekvencia spektrumának kialakulása a gerjesztés, tovaterjedés és észlelés folyamán. Kandidátusi értekezés, Budapest. (Change in the spectral properties of seismic waves during generation, propagation and recording. C. Sc. Thesis, Budapest).

JOLLY, R. N., 1953: Deep-hole geophone studies in Garvin County, Oklahoma. Geophysics, XVIII. 3., pp. 662–670.

Карус, Е. В. 1958: Поглощение упругих колебаний в горных породах при стационарном возбуждении. Известия АН СССР, Серия геофизическая, 4, 438—448. (Attenuation of elastic vibrations in solid media)

Коган, С. Я. 1961: Об определении коэффициента поглощения сейсмических волн. Известия АН СССР, Серия геофизическая, 12, 1738—1749. (Determination of the absorbtion coefficient of seismic waves)

LÁNYI J.–RÁKÓCZY I., 1969: Vízben, robbantással keltett nyomáshullámok terjedésének mérése. Geofizikai Közlemények, XVIII. 3., pp. 97–102. (Investigations of pressure-waves generated by explosion in water).

LEVIN, F. K.–LYNN, R. D., 1958: Deep hole geophone studies. Geophysics, XXIII. 4., pp. 639–664.

MACK, H., 1966: Attenuation of controlled wave seismograph signals observed in cased boreholes. Geophysics, XXX. 1., pp. 243–252.

McDONAL, F. J.–ANGONA, F. A.–MILLS, R. L.–SENGBUSH, R. L.–VAN NOSTRAND, R. G.–WHITE, J. E., 1958 : Attenuation of shear and compressional waves in Pierre Shale. Geophysics, XXIII. 3., pp. 421–439.

O'BRIEN, P. N. S., 1957: The relationship between seismic amplitude and weight of charge. Geophysical Prospecting, V. 3., pp. 349.

O'BRIEN, P. N. S., 1960: Seismic energy from explosions. Geophysical Journal, III. pp. 29-44.

O'BRIEN, P. N. S., 1969: Some experiments concerning the primary seismic pulse. Geophysical Prospecting, XVII. 4., pp. 511–547.

PEET, W. E., 1960: A shock wave theory for the generation of the seismic signal around a spherical shot hole. Geophysical Prospecting, XVII. 4., pp. 509–533.

RICKER, N., 1953: The form and laws of propagation of seismic wavelets. Geophysics XVIII. 1.

ROBINSON, E. A.–TREITEL, S., 1964: Principles of digital filtering. Geophysics, XXIX. 3., pp. 395–404.

SCHENK, V., 1971: The predominant frequency of stress waves in non-elastic zone near an explosive source. Geophys. J. R. Astr. Soc. XXII. 4., pp. 347–352.

TULLOS, F. N.–Reid, A. C., 1969: Seismic attenuation of Gulf Coast sediments. Geophysics, XXXIV. 4., pp. 516–528.

BODOKY TAMÁS—KORVIN GÁBOR—LIPTAI ISTVÁN—SIPOS JÓZSEF

ROBBANTÁSSAL KELTETT NYOMÁSHULLÁMOK JELLEMZŐINEK VIZSGÁLATA

A dolgozatban ismertetjük az 1968—69-es évben a Nyírségben végzett robbanáshullám kísérletek eredményeit. A méréseket elsősorban az teszi szükségessé, hogy a digitális szeizmikus feldolgozásban, különösen a dekonvolúciós művelet során, elengedhetetlen a jelalak és a jelalak időbeli változásának pontos ismerete. A méréseket homokos összletben végeztük, az észlelést piezoelektromos érzékelővel és Tektronix típusú oszcilloszkóppal hajtottuk végre. A kísérletsorozatban a jelalak változását vizsgáltuk a töltetszonda-távolság és a töltetsúly függvényében. Megállapítottuk, hogy a jelalak amplitúdója r^{-1}; átlagenergiája $r^{-2,3}$; szélessége $r^{0,2-0,4}$; csúcsfrekvenciája $r^{0,3-0,6}$ törvényszerűség szerint függ a távolságtól, a töltetsúly függvényében a jel amplitúdója a $W^{0,5}$, energiája $W^{1,1}$, szélessége $W^{0,13}$, csúcsfrekvenciája $W^{-0,1}$ szerint változik. Az eredmények $W = 1/8 - 4$ kg töltetsúlyokra, és $r = 5 - 50$ m távolságra vonatkoznak. Az eredményeket külön tárgyaljuk lyukban, illetve felszínen végzett észlelés esetére, mert az empirikus kitevők — a laza réteg szűrő hatása miatt — az utóbbi esetben módosulnak. Meghatároztuk az adott közegre jellemző frekvenciafüggő abszorpciós törvényt: felszínközeli összletben a teljes csillapodás $2,3 \cdot 10^{-5,2} f^2$ dB/m. Az elsődleges jelet több esetben ghost beérkezés követte (11. ábra). A ghost követési távolságának és amplitúdójának elemzésével bebizonyítottuk, hogy a ghost a talajvízszint határán képződik. Az elsődleges jel és a ghost frekvenciatartalmának eltérése az abszorpció jelenségére utal. A kísérleti eredmények összhangban vannak az irodalmi adatokkal, az esetleges eltéréseket elemezzük.

A dolgozathoz négy táblázat csatlakozik, az első táblázat a mérés körülményeit foglalja össze, a I., III., IV. Táblázatokban összefoglaljuk az amplitúdótávolság függésére, a frekvenciafüggő abszorpcióra és az amplitúdó töltetsúly függésére vonatkozó irodalmi adatokat.

Т. БОДОКИ – Г. КОРВИН — И. ЛИПТАИ — И. ШИПОШ

АНАЛИЗ ХАРАКТЕРНЫХ СВОЙСТВ ПРОДОЛЬНЫХ ВОЛН, ВОЗБУЖДЕННЫХ ВЗРЫВАМИ

В работе описываются результаты опытных работ, проведенных в 1968—1969 гг. в районе Ниршег (Северо-восточная Венгрия) для анализа продольных волн, возбужденных взрывами. Постановка подобного рода исследований была обусловлена тем, что при цифровой обработке сейсмических данных, в частности, при операциях деконволюции, необходимо точно знать формы сигналов и их изменения во времени. Наблюдения проводились в песчаной толще с использованием пьезоэлектрического приемника и осциллоскопа типа Тектроникс. В процессе исследований анализировались изменения формы сигналов в зависимости от расстояния до пункта возбуждения и от величины зарядов. Обнаружено, что для амплитуды сигнала характерна закономерность изменения с расстоянием r^{-1}, для средней его интенсивности — $r^{-2,3}$, для ширины — $r^{0,2-0,4}$ и для предельной частоты — $r^{0,3-0,6}$, а закономерность изменения с величиной заряда выражается для амплитуды — $W^{0,5}$, для интенсивности — $W^{1,1}$, для ширины — $W^{0,13}$ и для предельной частоты — $W^{-0,1}$. Результаты действительны для величин заряда $W = 1/8 - 4$ кг и для расстояний $r = 5 - 50$ м. Раздельно рассматриваются результаты наблюдений, проведенных на дневной поверхности и в скважинах, поскольку эмпирические показатели неодинаковы в связи с фильтрующим эффектом зоны выветривания. Был определен закон изменения поглощения в зависимости от частоты, характерный для данной среды: затухание волн в приповерхностной толще равно $2,3 \cdot 10^{-5,2} f^2$ дб/м. За первичным сигналом во многих случаях следовали отражения-спутники (см. рис. 11). Анализ протяженности и амплитуды отражения-спутника позволил сделать вывод о том, что последнее образуется на границе грунтовых вод. Отклонение частотных характеристик первого сигнала и отражения-спутника свидетельствует о наличии поглощения. Полученные результаты согласуются с литературными данными, а причины возможных отклонений анализируются.

К работе прилагаются 4 таблицы, в первой из которых приведены данные об условиях наблюдений, а во второй, третьей и четвертой таблицах представлены литературные данные о зависимостях амплитуды от расстояния, поглощения от частоты и амплитуды от величины заряда, соответственно.

APPROXIMATION OF THE OPTIMUM-FILTERS USED IN SEISMIC DATA PROCESSING

A. MESKÓ* P.–ZSELLÉR**

Introduction

It is well known that optimum filter theory has found a wide application in many stages of seismic data processing ($S/S + N$ filters, deconvolution filters and, in special problems, OVS or OHS filters). In the actual design of filters various approximations must be made and in most cases the necessary filter parameters are estimated from the recorded data (by means, e.g., of correlation analysis). The filter is only optimum if all approximations made are justified and even then only with respect to the parameters used. The filter finally applied to a given channel is, even in the best case, a good approximation.

In the usual derivation of $S/S + N$ filters, for example, it is assumed that signal and noise are non-correlated and both are realizations of stationary stochastic processes. Power spectra are estimated from the autocorrelation functions. It is well-known, however, that the frequency content of the seismic signal changes during propagation, i.e. stationarity which is assumed may hold only within reasonable short time gates. The coefficients figuring in the correlation functions are random variables and if one estimates them from a small number of samples, the corresponding confidence intervals become rather wide. Consequently, the estimation of correlation functions becomes the less reliable the narrower is the time gate. If we strive at the fulfilment of one of the criteria (stationarity), the indeterminacy of the estimation of the parameters will be increased and vice versa.

Similar difficulties are encountered in case of other problems of optimum filtering. These problems do not make the computation of optimum filters superfluous since their application results in much clearer seismic sections. It is, however, reasonable to try to design sub-optimum filters if these lead to an ease in the computations or a substantial saving in computer time.

The methods of sub-optimum filter design can be classified in two large groups. In the first of them the design model is chosen in such a way that the determination of the transfer function or weight function of the filter be simple. Investigations of this kind were reported by FOSTER and SENGBUSH (1965). But, in reality, also the OHS and OVS filters —although they are termed as optimum by the authors (SCHNEIDER et al. 1964, 1965) — were designed under such assumptions on the input channels which were meant to make the filters suitable for computation.

Manuscript received 30, 6, 1971.
  * University, Budapest.
 ** National Oil and Gas Trust Budapest.

Another type of sub-optimum filters is obtained if we approximate in the frequency domain some filter which had been designed according to the theory of optimum filters. The approximating function (i.e. the transfer function of the sub-optimum filter) has only a few parameters. Its form assures that the corresponding weight-function be computable with a closed formula from the parameters given. The actual values of the parameters can be determined by fitting the sub-optimum transfer function to the optimum one.

The computation of sub-optimum filters is justified, among others, by the convenient properties of the weight functions: smoothness, shortness. Consequently, the otherwise necessary smoothing and truncation may be omitted.

This paper will treat a special group of sub-optimum filters of the second type. After a brief discussion of the algorithm of design, a concrete application will be dealt with.

Determination of the transfer function of the sub-optimum filter

Let us denote by $S_0(f)$ the transfer function of some optimum filter and by $S(f, \alpha_1, \alpha_2, \ldots, \alpha_n)$ that of the suboptimum filter, where $\alpha_1, \alpha_2, \ldots, \alpha_n$ are parameters which are to be determined.

In order to fit the transfer function we determine the series of parameters for which

$$\frac{1}{2F} \int_{-F}^{F} |S_0(f) - S(f, \alpha_1, \alpha_2, \ldots, \alpha_n)|^2 \, df = \text{minimum.} \tag{1}$$

In practical cases instead of $S_0(f)$ its sampled version

$$S_0(if_0) \qquad (i = 0, \pm 1, \pm 2, \ldots \pm N)$$

is given and instead of integral (1) the sum

$$I = \frac{1}{2N+1} \sum_{i=-N}^{N} |S_0(if_0) - S(if_0, \alpha_1, \alpha_2, \ldots, \alpha_n)|^2 \tag{2}$$

must be minimum. If the transfer functions of the optimum filter and of the approximating sub-optimum filters are real, the modulus sign can be omitted. In what follows, we shall be concerned with this simpler case.

By virtue of the condition of optimality the partial derivatives with respect to the parameters α_k are zero:

$$\frac{\partial I}{\partial \alpha_k} = 0; \qquad (k = 1, 2, \ldots, n). \tag{3}$$

After performing differentiation we obtain a system of equations for the unknown parameters $\alpha_1, \alpha_2, \ldots, \alpha_n$:

$$\sum_{i=-N}^{N} [S_0(if_0) - S(if_0, \alpha_1, \alpha_2, \ldots, \alpha_n)] \frac{\partial S}{\partial \alpha_k} = 0. \tag{4}$$

This system of equations is generally non-linear. We shall attempt to solve it after linearization, by an iterative procedure. Let us introduce for sake of simplicity the notations:

$$S(if_0, \alpha_1, \ldots, \alpha_n) = S(if_0, \alpha),$$

$$\text{grad}_\alpha S = \left(\frac{\partial S}{\partial \alpha_1}, \ldots, \frac{\partial S}{\partial \alpha_n} \right).$$

The order of approximations in the course of the iteration will be shown by the upper index of the parameters. Let the initial n-tuple of parameters be

$$\alpha_1^{(0)}, \alpha_2^{(0)}, \ldots, \alpha_n^{(0)},$$

while in the j-th step

$$\alpha_1^{(j)}, \alpha_2^{(j)}, \ldots, \alpha_n^{(j)}.$$

The $(j+1)$-st approximation can be constructed from the j-th one as follows. Let us introduce the notation $\Delta_k^{(j)}$ for the differences (corrections) between successive approximations, i.e.

$$\alpha_k^{(j+1)} = \alpha_k^{(j)} + \Delta_k^{(j)}. \tag{5}$$

Developing the function $S(f, \alpha_1^{(j+1)}, \alpha_2^{(j+1)}, \ldots, \alpha_n^{(j+1)})$ in a Taylor-series at the neighbourhood of $\alpha_k^{(j)}$:

$$S(if_0, \alpha_k^{(j+1)}) = S(if_0, \alpha_k^{(j)}) + (\overline{\Delta}^{(j)}, \text{grad}_\alpha S) + O[(\Delta_k^{(j)})^2] \tag{6}$$

—where the components of vector $\overline{\Delta}^{(j)}$ are the values defined by (5);
the arguments of vector $\text{grad}_\alpha S$ are the parameters of the j-th approximation.

Assuming that the terms which are of the second order in the corrections $\Delta_k^{(j)}$ are sufficiently small:

$$S(if_0, \alpha_k^{(j+1)}) = S(if_0, \alpha_k^{(j)}) + (\overline{\Delta}^{(j)}, \text{grad}_\alpha S) \tag{7}$$

Substituting this to Eq. (2) and differentiating with respect to the corrections $\Delta_k^{(j)}$ we obtain that

$$\sum_{i=-N}^{N} \left[S_0(if_0) - S(if_0, \alpha_k^{(j)}) - (\overline{\Delta}, \text{grad}_\alpha S|_{\alpha_k = \alpha_k^{(j)}}) \right] = \frac{\partial S}{\partial \alpha_k} \bigg|_{\alpha_k = \alpha_k^{(j)}}. \tag{8}$$

This last system of equations is already linear in the corrections $\Delta_k^{(j)}$. After solving it, the $(j+1)$-st approximation of the parameters are obtained by means of Eq. (5).

We have not established the convergence of the procedure theoretically. It was found in practice, however, that for an appropriate initial n-tuple of parameters, the corrections $\Delta_k^{(j)}$ become small after a few iterative steps. The choice of initial parameters has a crucial role since it has been always assumed that corrections are small.

The brief description of the above iterative method was thought appropriate since this algorithm had been used throughout our investigations. Analyses of other methods and a detailed investigation of the convergence problems involved will be subject matters of our further research work.

An application example

We shall proceed to approximate the transfer function illustrated by Fig. 1a The corresponding weight function is also given, Fig. 1b.
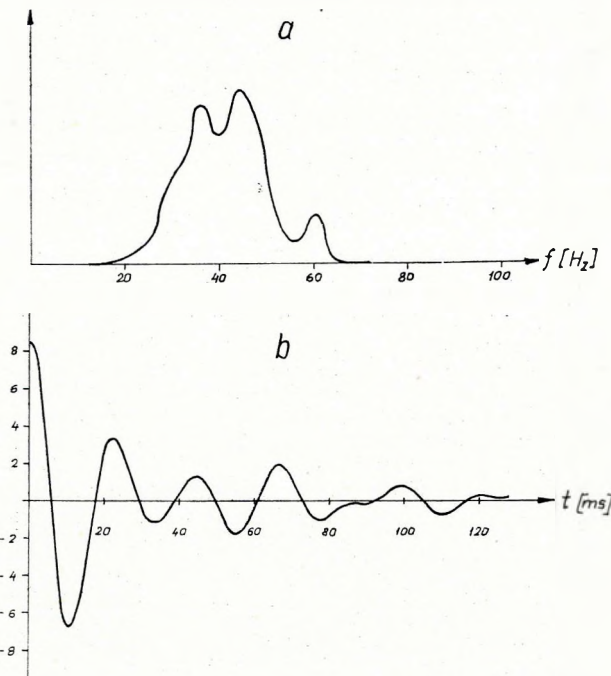

Fig. 1 Transfer function *(a)* and weight function
(b) of the optimum filter

1. ábra. A közelítendö optimumszűrö átviteli függ-
vénye *(a)* és súlyfüggvénye *(b)*

Рис. 1. Характеристика *(а)* и весовая функция *(д)*
аппроксимируемого оптимального фильтра

Considering the shape of the transfer function which is to be approximated it seems appropriate to seek for an approximating function of the form

$$S(f, \alpha_k) = \alpha_1 [e^{-\alpha_2(f-\alpha_3)^2} + e^{-\alpha_2(f+\alpha_3)^2}], \qquad (9)$$

that is, the transfer function of the sub-optimum filter consists of two Gaussian curves, placed symmetrically to the origin of the co-ordinate system. Parameter α_1 determines the amplitude, and α_2 the distance of the centres from the origin. Parameter α_3 is in connection with the slope of cut-off. (The transfer function of the optimum filters has the same properties. The imaginary part is identically zero).

The inverse Fourier transform of (9) is given by a closed formula:

$$S(t, \alpha_k) = \alpha_1 \sqrt{\frac{\pi}{\alpha_2}} \, e^{-\frac{\pi^2}{\alpha_2^2} t^2} \cos 2\pi\alpha_3 t. \qquad (10)$$

It is evident that the weight-function is smooth and automatically truncated. The initial choice of parameters for the iterative procedure described above was

$$\alpha_k^{(0)} = (0.7; \, 0.005; \, 10.0).$$

The change of parameters in course of the iterative procedure and the mean square deviation between the transfer functions of the optimum and sub-optimum filters are shown in Table I. The values of the parameters remain practically unchanged after the first iterative step. The mean square deviation decreases with a jump in the first step and attains nearly the same value afterwards.

Table I.

Change of the values of the parameters and of the mean square error in course of the iterations

Iteration	α_1	α_2	α_3	Mean square deviation
0	0.7	0.00500	10,00000	169.201
1	0.87057	0.00635	10.29375	0.121
2	0.87755	0.00631	10.21597	0.119
3	0.88065	0.00642	10.20840	0.119
4	0.87827	0.00633	10.21633	0.119
5	0.87947	0.00637	10.21249	0.119
6	0.87829	0.00633	10.21648	0.119
7	0.87829	0.00633	10.21659	0.119

Table II.

Values of optimum filter $S_0(if_0)$ and of the sub-optimum filter ($f_0 = 4$ cps)

i	$S_0(if_0)$	$S(if_0)$	i	$S_0(if_0)$	$S(if_0)$
0	0.00001	0.00004			
1	0.00000	0.00016	11	0.92376	0.82540
2	0.00000	0.00095	12	0.73508	0.63654
3	0.00005	0.00451	13	0.28234	0.40095
4	0.01496	0.01757	14	0.12135	0.20626
5	0.04185	0.05590			
6	0.09131	0.14524	16	0.02846	0.02974
7	0.34375	0.30820	17	0.00019	0.00834
8	0.53016	0.53415	18	0.00008	0.00191
9	0.85302	0.75609	19	0.00015	0.00036
10	0.68332	0.87413	20	0.00000	0.00005
			21	0.00000	0.00001

The values of the original (optimum) and of the approximating (sub-optimum) transfer function are given in Table II. Figure 2a illustrates the transfer function of the sub-optimum filter while Fig. 2b the corresponding weight function. The transfer function and weight function approximated are plotted in these same Figures by
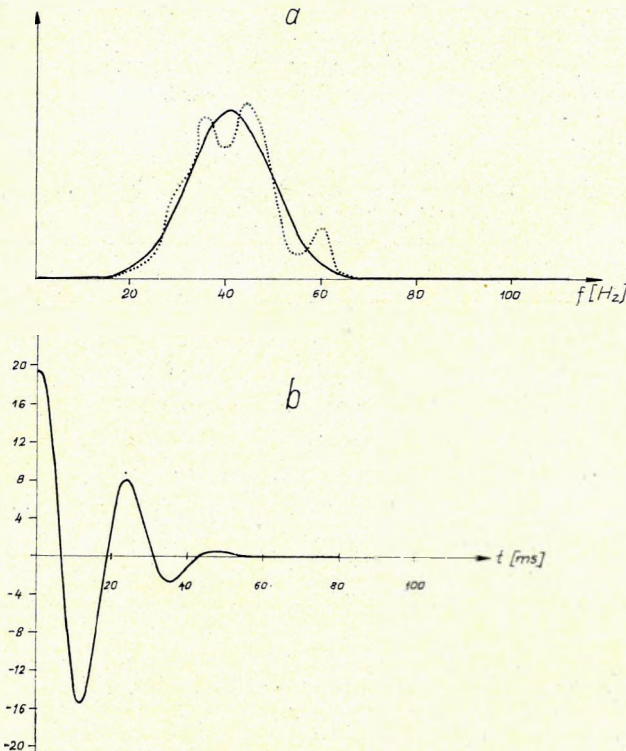

Fig. 2 Transfer function *(a)* and weight function *(b)* of the sub-optimum filter. Curves plotted with dotted lines are the transfer resp. weight functions of the optimum filter

2. ábra. A szuboptimumszűrő átviteli függvénye *(a)* és súlyfüggvénye *(b)*. A szaggatott vonallal rajzolt görbék az optimumszűrő átviteli függvényét illetve súlyfüggvényét ábrázolják

Рис. 2. Характеристика (*a*) и весовая функция (*∂*) субоптимального фильтра. Кривые, проведенные пунктиром, соответствуют характеристике и весовой функции оптимального фильтра

dotted lines. We emphasize again the fact that the approximating weight function is automatically truncated due to the proper choice of the form of approximation (9); the weight-function of the sub-optimum filter is some two and a half times shorter than the original one.

Acknowledgement

REFERENCES

Forster, M. R.–Sengbush, R. L.–Watson, R. J., 1964: Design of sub-optimum filter systems. Geophys. Prosp. Vol. XII. pp. 173-192.
Schneider, W. A.–Larner, L. K.–Burg, J.–Backus, M., 1964: A new data processing technique for the elimination of ghost arrivals on reflection seismograms. Geophysics, Vol. 29.
Schneider, W. A.–Prince, E. R.–Giles, B. F., 1965: A new processing technique for multiple attenuation exploiting differential normal moveout. Geophysics, Vol. 30.

MESKÓ ATTILA—ZSELLÉR PÉTER

A DIGITÁLIS SZEIZMIKUS ADATFELDOLGOZÁSBAN ALKALMAZOTT OPTIMUMSZŰRŐK KÖZELÍTÉSÉRŐL

Az optimumszűrők tervezésének korlátai (az alkalmazott elhanyagolások és paraméterbecslések hibái) indokolttá teszik közelítések alkalmazását. A szuboptimumszűrő használatának további előnye, hogy eltávolítja az eredeti átviteli függvényből a stochasztikus ingadozásokat. A dolgozat az optimumszűrő átviteli függvényéhez néhány paraméteres szuboptimumszűrő illesztését javasolja. A szuboptimumszűrőt úgy választjuk, hogy a hozzá tartozó súlyfüggvény zárt alakban előállítható, simított és csonkított legyen.

Az eredeti, és a szuboptimumszűrő átviteli függvénye közötti átlagnégyzetes különbséget írjuk fel. Az átlagnégyzetes eltérés minimalizálásával a szuboptimumszűrő meghatározandó paramétereire nem-lineáris egyenletrendszert kapunk. Az egyenletrendszert iterációs módszerrel oldjuk meg. A javasolt eljárás szerint a szűrőtervezés az illesztésben alkalmazott iterációs algoritmussal bővül; a numerikus inverz Fourier transzformáció-számítás és csonkítás elmarad.

Az eljárás alkalmazását szuboptimális simítószűrő tervezésével illusztráljuk.

А. МЕШКО—П. ЖЕЛЛЕР

ОБ АППРОКСИМАЦИИ ОПТИМАЛЬНЫХ ФИЛЬТРОВ, ПРИМЕНЯЕМЫХ ПРИ ЦИФРОВОЙ ОБРАБОТКЕ СЕЙСМИЧЕСКИХ ДАННЫХ

В связи с ограничениями, характерными для разработки оптимальных фильтров (погрешности применяемых пренебрежений и оценки параметров) обосновано применять аппроксимации. Дополнительное достоинство субоптимальных фильтров заключается в возможности исключения стохастических колебаний из первоначальной переходной характеристики. В работе предлагается разработать субоптимальный фильтр с несколькими параметрами для переходной характеристики оптимального фильтра. Субоптимальный фильтр выбирается с таким расчетом, чтобы соответствующая весовая функция была получена в замкнутой, выравненной и усеченной форме.

Записывается среднеквадратичная разница между первоначальной переходной характеристикой и переходной характеристикой субоптимального фильтра. Посредством минимализации среднеквадратичного расхождения получается система нелинейных уравнений для определения параметров субоптимального фильтра. Система уравнений решается итерационным методом. По предлагаемому способу разработка фильтра расширяется итерационным алгоритмом, применяемым для согласования; отпадают выравнивание и усечение численной обратной трансформацией Фурье.

Применение метода иллюстрируется на примере разработки субоптимального выравнивающего фильтра.

The effect of dip of the reflecting boundary on the stacking of common-depth-point channels

T. BODOKY*

In seismic exploration, the aim of applying common-depth-point systems is the suppression of random noises and multiple reflexions. The filtering of random noises is based upon the statistical filtering effect of stacking independently recorded channels; the filtering-out of multiples, however, is determined by transfer functions derivable also in a deterministic way.

The filtering effect of common-depth-point systems on multiples was discussed in detail in a previous paper by the author (BODOKY, 1970), where the following relation has been established for the multiply reflected energy, resp. for its attenuation produced by the stacking channel type given:

$$\Phi(t_0, d) = \frac{\int_0^\infty [A(\omega)S(\omega, t_0, d)]^2 \, d\omega}{\int_0^\infty [nA(\omega)]^2 \, d\omega} \tag{1}$$

where

Φ	the ratio of attenuated and unattenuated multiple energy
t_0	arrival time
d	seismometer spacing
ω	circular frequency
$A(\omega)$	spectrum of the arrival
$S(\omega, t_0, d)$	the transfer function of the stacking channel in question
n	stacking number

The form of the transfer function $S(\omega, t_0, d)$ is

$$S(\omega, t_0, d) = \sum_{i=1}^{n} e^{j\omega\tau_i(t_0, d)} \tag{2}$$

where

$\tau_i(t_0, d)$ the value of the "residual moveout" belonging to the i-eth channel to be stacked, on the place (t_0, d).

The value of the residual moveout on a given channel is the difference between the moveouts of the multiple arrival related to the same t_0, resp. of the primary arrival:

$$\tau(t_0, d) = \delta \Delta t(t_0, d) = \Delta t_{\mathrm{T}}(t_0, d) - \Delta t(t_0, d) \tag{3}$$

where

$\delta \Delta t$ the residual moveout
Δt_T the moveout of the multiple arrival
Δt the moveout of the primary arrival

In principle, the value of geometrical correction agrees with the moveout of the primary arrival; consequently the right-hand side of the relation (3) may be considered as the difference of the moveout of any arrival and of the value of geometrical correction. From this interpretation of (3) it is clear that the primary arrivals are stacked with mutual reinforcement and in right phase, the multiples, however, with a phase difference of $\delta \Delta t$, mutually attenuating each other.

The value of geometrical correction is computed under the assumption of horizontal reflecting planes, consequently Δt signifies the moveout of a reflexion from a horizontal boundary.

In the majority of cases, however, the reflecting boundaries are not horizontal, but dipping. Therefore it is in place to examine the question, what effect has the dip on stacking. The investigation will be carried out both for primary arrivals and multiples.

Primary arrivals from dipping boundaries

According to CRESSMAN (1968), if the dip angle in profile direction is α then

$$\Delta t(\alpha) = \Delta t \cos^2 \alpha \tag{4}$$

where $\Delta t(\alpha)$ is the value of the moveout of a primary arrival from a boundary dipping at an angle of α.

If this is substituted in (3), as the actual moveout of a primary arrival, also primary arrivals from a dipping boundary have their residual moveouts,

$$\delta \Delta t(\alpha) = \Delta t \cos^2 \alpha - \Delta t = - \Delta t \sin^2 \alpha. \tag{5}$$

In case of dipping reflectors, then, the phase-difference-free stacking of simple primaries will not be fulfilled.

In order to investigate the effect of dip-caused phase-difference also numerically, let us substitute relation (5) in the transfer function of (2), resp. in formula (1). The relation established in this way permits the computation of the attenuation function of three variables $\Phi(t_0, \alpha, d)$. For illustrativeness sake let us compute functions $\Phi(t_0, \alpha)$, resp. $\Phi(\alpha, d)$ keeping one of the variables fixed.

According to the points of view of the paper mentioned in the beginning, let us choose the stacking-channel types, denoting them, in the way mentioned there, with a series of shotpoint-distances, of the channels figuring there, given in seismometer spacing units.

The stacking-channel types selected are:

the (1.5 2.5 5.5 6.5 9.5 10.5) type stacking channel of the split-spread system,
the (12 16 20 24 28 32) type stacking channel of the offset shotpoint system.

With these selected stacking-channel types the attenuation function computations $\Phi(t_0, \alpha, d)$ were carried out with the spectrum and velocity function used also in the paper mentioned in the introduction, according to the formulas (5), (2) and (1).

In the following, the value of the Φ functions will always be given in decibels.

The $\Phi(\alpha, d)$ functions obtained for $t_0 = 2$ sec are visible, in a sequence corresponding to the enumeration of channel types, in the first two figures (Fig. 1–2).
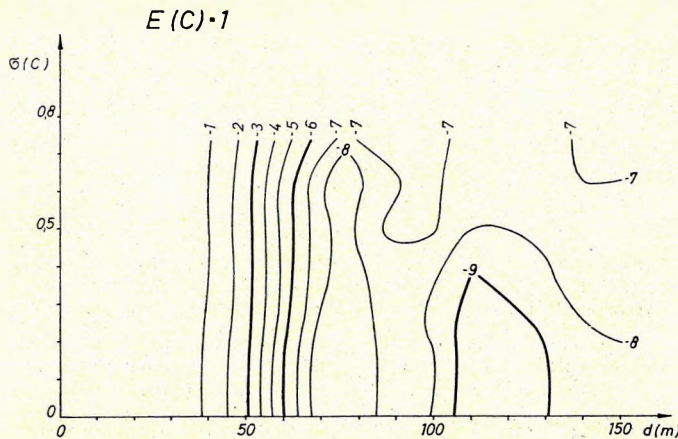
Fig. 1 The $\Phi(\alpha, d)$ attenuation function of the (1,5; 2,5; 5,5; 6,5; 9,5; 10,5) stack channel type, calculated for primary reflexions (represented in dB; $d =$ seismometer-spacing; $\alpha =$ dip-angle)

1. ábra. az (1,5; 2,5; 5,5; 6,5; 9,5; 10,5) összegcsatorna típus $\Phi(\alpha, d)$ csillapítási függvénye egyszeres reflexiókra számítva (dB-ben ábrázolva; $d =$ geofonköz; $\alpha =$ dőlésszög)

Рис. 1. Функция затухания $\Phi(\alpha, d)$ суммотрассы типа (1,5; 2,5; 5,5; 6,5; 9,5; 10,5) для однократных отражений (в дб; $d -$ шаг сейсмоприемников; $\alpha -$ угол наклона)

An examination of these figures shows that the attenuation of primary arrivals, caused by the dipping of the reflecting boundaries, determines, for a given stacking-channel type, the maximum permitted seismometer spacing, and the maximum permitted seismometer spacing decreases with the increase of both the dip and the distance of recording.

Figs. 3 and 4 present the $\Phi(t_0, \alpha)$ functions of the same channel types. The seismometer spacing is fixed at the multiple-suppression optimum of the individual channels, i.e. $d = 110$ and $d = 50$, in turn.

According to these figures, our statements can be completed by the following:

— at low t_0 values, especially with such large seismometer spacing, the primary arrivals are very sensitive against dip. With an increase of t_0, this sensitivity rapidly decreases, and the cut-off zone rapidly shifts towards greater dips.

— if the seismometer spacing is selected for an optimum as to multiple-suppression, the place of the cut-off-zone is practically independent of recording distance;

— the steepness of cut-off and the value of maximum attenuation increases with an increasing recording distance.

E (C)·1
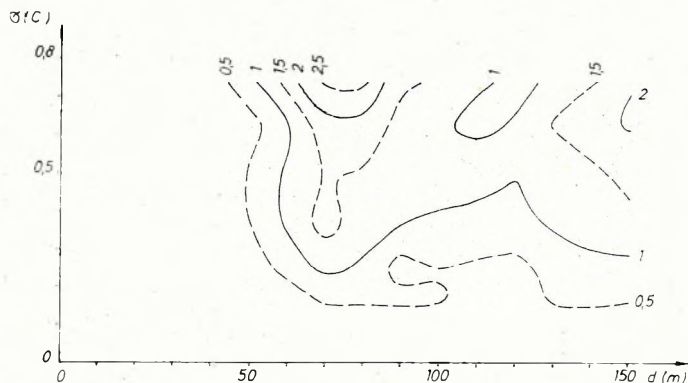
Fig. 2 The $\Phi(\alpha, d)$ attenuation function of the (12, 16, 20, 24, 28, 32) stack channel type, calculated for primary reflexions (represented in dB; d = seismometer-spacing; α = dipangle)

2. ábra. A (12, 16, 20, 24, 28, 32) összegcsatorna típus $\Phi(\alpha, d)$ csillapítási függvénye egyszeres reflexiókra számítva (dB-ben ábrázolva; d = geofonköz; α = dőlésszög)

Рис. 2. Функция затухания $\Phi(\alpha, d)$ суммотрассы типа (12, 16, 20, 25, 28, 32) для однократных отражений (в дб; d — шаг сейсмоприемников; α — угол наклона)

E (C)·1

Fig. 3 The $\Phi(t_0, \alpha)$ attenuation functionfo the (1,5; 2,5; 5,5; 6,5; 9,5; 10,5) stack channel type, calculated for primary reflexions (represented in dB; α = dip-angle; seismometer spacing = 110 m)

3. ábra. Az (1,5; 2,5; 5,5; 6,5; 9,5; 10,5) összegcsatorna típus $\Phi(t_0, \alpha)$ csillapítási függvénye egyszeres reflexiókra számítva (dB-ben ábrázolva; α = dőlésszög; geofonköz 110 m)

Рис. 3. Функция затухания $\Phi(t_0, \alpha)$ суммотрассы типа (1,5; 2,5; 5,5; 6.5; 9,5; 10,5) для однократных отражений (в дб; α — угол наклона; шаг сейсмоприемников — 110 м)

E (C)·1
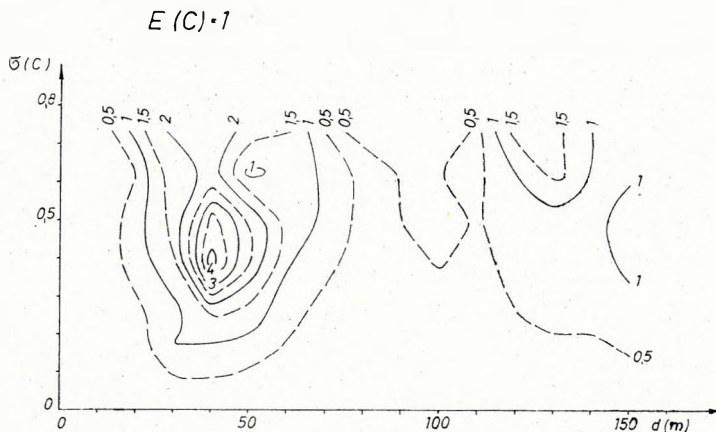
Fig. 4 The $\Phi(t_0, \alpha)$ attenuation function of the (12, 16, 20, 24, 28, 32) stack channel type, calculated for primary reflexions (represented in dB; α = dip-angle; seismometerspacing: 50 m)

4. ábra. A (12, 16, 20, 24, 28, 32) összegcsatorna típus $\Phi(t_0, \alpha)$ csillapítási függvénye egyszeres reflexiókra számítva (dBben ábrázolva; α = dőlésszög; geofonköz 50 m)

Рис. 4. Функция затухания $\Phi(t_0, \alpha)$ суммотрассы типа (12, 16, 20, 24, 28, 32) для однократных отражений (в дб; α — угол наклона; шаг сейсмоприемников — 50 м)

Dipping boundaries and multiple reflexions

Next, the effect of dip upon the multiple attenuation of individual stacking channels will be discussed.

If merely the simplest, i.e. double-way multiple reflexion is considered, this behaves, according to the laws of geometrical optics, as a primary reflexion from a boundary dipping at 2α.

Its moveout is:

$$\Delta t_T(\alpha) = \Delta t_T \cos^2 (2\alpha).$$

Hence, the residual moveout:

$$\delta \Delta t(\alpha) = \Delta t_T \cos^2 (2\alpha) - \Delta t. \tag{6}$$

The expression of $\delta \Delta t(\alpha)$ will be substituted in (2), further the obtained function $S(\omega, \alpha, t_0, d)$ in formula (1). With the formula obtained in this way, the attenuation function $\Phi(t_0, \alpha, d)$ is computed also for the multiple reflexion.

The $\Phi(\alpha, d)$ functions of the two stacking channels figuring also in the previous computations are presented in the figures 5 and 6 in due order, calculated for multiples at $t_0 = 2$ sec. In the next two figures, again, (7 and 8), the $\Phi(t_0, \alpha)$ functions of the same channel types are visible, with the calculation of seismometer spacing as optimum for multiple-suppression, i.e. for $d = 110$ m and $d = 50$ m, in due order.
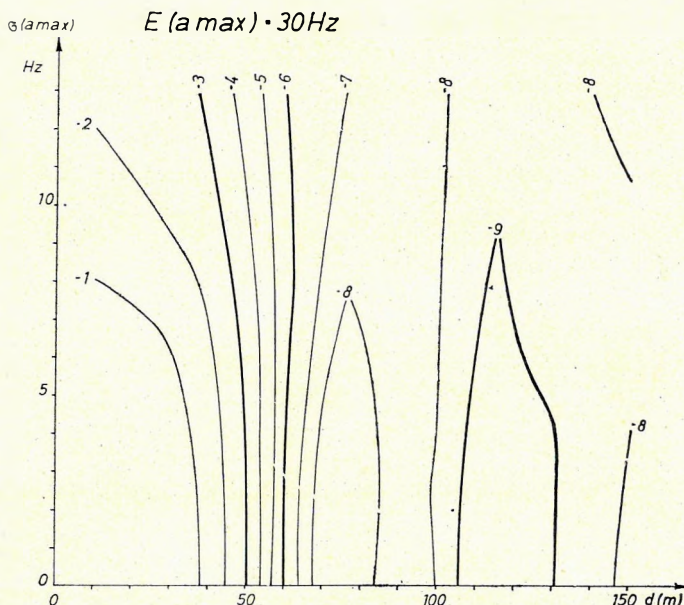
Fig. 5 The Φ (α, d) attenuation function of the (1,5; 2,5; 5,5; 6,5; 9,5; 10,5) stack channel type, calculated for primary reflexions (represented in dB; d = seismometer-spacing; α = dip-angle)

5. ábra. Az (1,5; 2,5; 5,5; 6,5; 9,5; 10,5) összegcsatorna típus Φ(α, d) csillapítási függvénye többszörös reflexiókra számítva (dB-ben ábrázolva; d = geofonköz; α = dőlésszög)

Рис. 5. Функция затухания Φ(α, d) суммотрассы типа (1,5; 2,5; 5,5; 6,5; 9,5; 10,5) для кратных; отражений (в дб; d — шаг сейсмоприемников; α — угол наклона)

It is visible from the figures that

— the value of multiple-attenuation, as expectable according to (6), decreases on account of the dip of the reflecting boundary, becoming zero at a critical dip value. With a further increase of the dip, it starts to improve again.

— The place of the zone with zero attenuation depends on recording time only. It does not depend on either seismometer spacing or offset value, consequently no means are given to influence it.

*

The results presented throw up two problems

One of them is: how to solve, in case of a dipping boundary, the stacking of simple reflections without phase-difference? The other: what can be done, in this case, against multiples?

The stacking of primary reflexions without phase-difference is ensured, if the value of geometrical correction is, instead of Δt, $\Delta t \cos^2 \alpha$. For this, however, the accurate position of the reflecting boundaries must be known in advance, but exactly this is the aim of the measurement. This contradiction is circumvented by up-to-date computer procedures in such a way that they determine the value of the geometrical correction in an empirical way from the measurement materials. This operation, the "velocity-analysis", must be made with a "sampling rate" according to the geological build-up of the area under investigation, since the value of corrections depend on the geological structure through dip conditions, and thus the results of one or two analyses cannot always be extended to the entire section.

The suppression of multiples is the harder one of the two tasks. Applying the proper geometrical correction, the value of the residual moveout will be

$$\delta \Delta t = \Delta t_T \cos^2 (2\alpha_1) - \Delta t \cos^2 \alpha_2$$

where α_1 — the dip of the boundary reflecting multiples,

 α_2 — the dip of the boundary reflecting primaries.
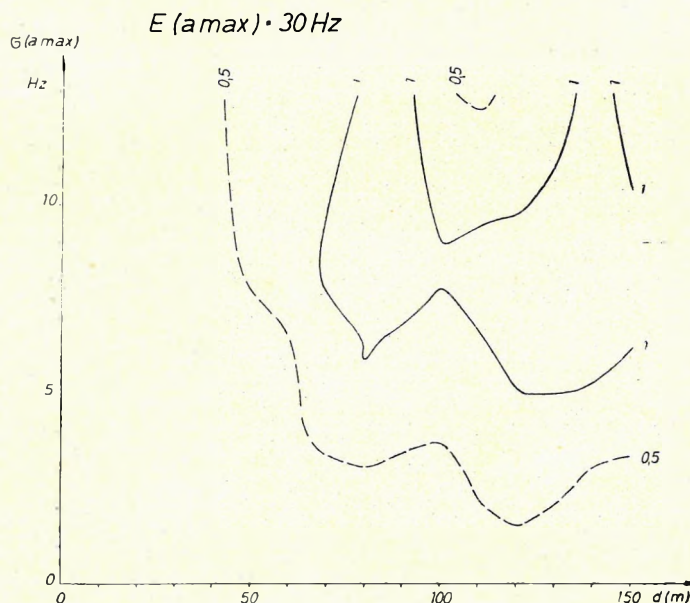
Fig. 6 The $\Phi(\alpha, d)$ attenuation function of the (12, 16, 20, 24, 28, 32) stack channel type, calculated for primary reflexions (represented in dB; d = seismometer-spacing; α = dip-angle)

6. ábra. A (12, 16, 20, 24, 28, 32) összegcsatorna típus $\Phi(\alpha, d)$ csillapítási függvénye többszörös reflexiókra számítva (dB-ben ábrázolva; d = geofonköz; α = dőlésszög)

Рис. 6. Функция затухания $\Phi(\alpha, d)$ суммотрассы типа (12, 16, 20, 24, 28, 32) для кратных отражений (в дб; d — шаг сейсмоприемников; α — угол наклона)
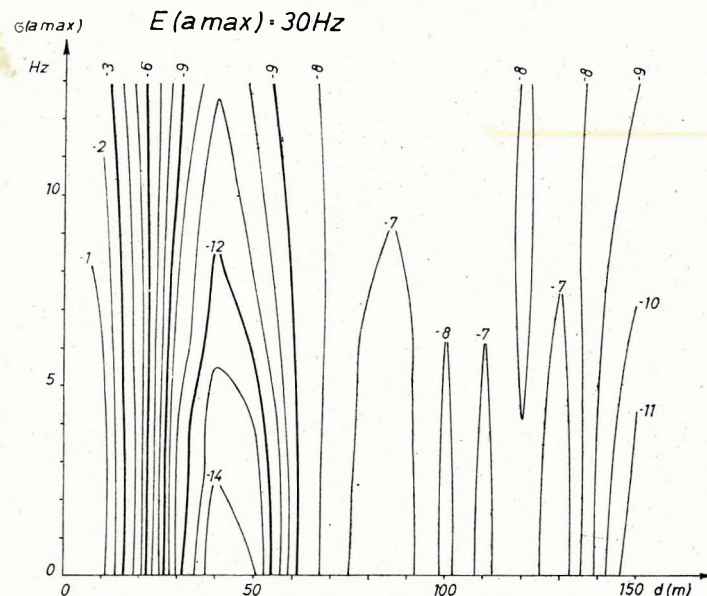
Fig. 7 The $\Phi(t_0, \alpha)$ attenuation function of the (1,5; 2,5; 5,5;
6,5; 9,5; 10,5) stack channel type, calculated for multiple
reflexions (represented in dB; α = dip-angle)

7. ábra. Az (1,5; 2,5; 5,5; 6,5; 9,5; 10,5) összegcsatorna típus
$\Phi(t_0, \alpha)$ csillapítási függvénye többszörös reflexiókra számítva
(dB-ben ábrázolva; α = dölésszög)

Рис. 7. Функция затухания $\Phi(t_0, \alpha)$ для суммотрассы типа (1,5; 2,5;
5,5; 6,5; 9,5; 10,5) для кратных отражений (в дб; α — угол
наклона)

Since no necessary relation exists between α_1 and α_2, the possibility of the
following case may always exist:

$$\Delta t_T \cos^2 (2\alpha_1) \approx \Delta t \cos^2 \alpha_2$$

that is,

$$\delta \Delta t \approx 0$$

meaning zero multiple-attenuation.

With up-to-date computer procedures, with the computer modelling of actual
wave-paths, this problem, too, can be solved, according to literary data. In our home
practice, however, for the time being this is not yet possible, consequently this eventuality must be taken into account.

REFERENCES

BODOKY, T., 1970: A közös mélységpontos (CDP) rendszerek szűrőhatása és átviteli
függvényeik. The filtering effect and transfer function of common-depth-point
(CDP) systems (in Hungarian), Magyar Geofizika, Vol. XI. No. 6., pp. 209–218.
CRESSMAN, K. S., 1968: How Velocity Layering and Steep Dip Affect CDP. Geophysics,
Vo. 33, No. 3, pp. 399–411.
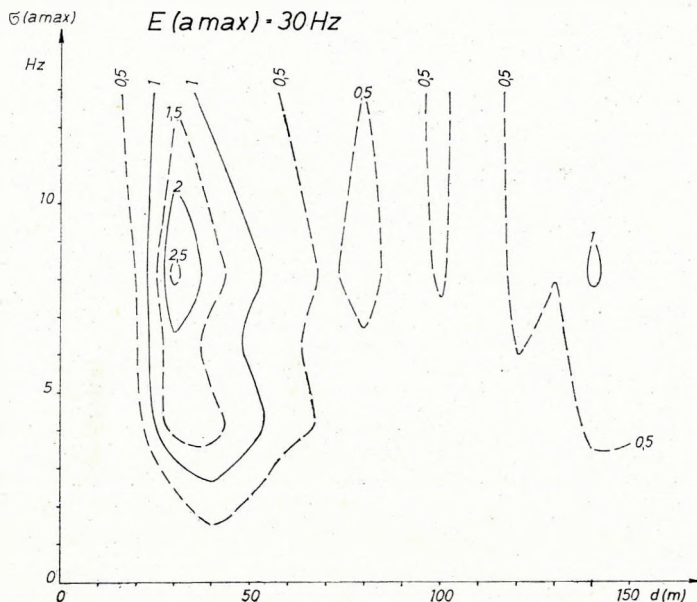
Fig. 8 The $\Phi(t_0, \alpha)$ attenuation function of the (12, 16, 20, 24, 28, 32) stack channel type, calculated for multiple reflexions (represented in dB; $\alpha =$ dip-angle)

8. ábra. A (12, 16, 20, 24, 28, 32) összegcsatorna típus $\Phi(t_0, \alpha)$ csillapítási függvénye többszörös reflexióra számítva (dB-ben ábrázolva; $\alpha =$ dölésszög)

Рис. 8. Функция затухания $\Phi(t_0, \alpha)$ для суммотрассы типа (12, 16, 20, 24, 28, 32) для кратных отражений (в дб; α — угол наклона)

BODOKY TAMÁS

A VISSZAVERŐ FELÜLET DŐLÉSÉNEK HATÁSA A KÖZÖS MÉLYSÉGPONTOS CSATORNÁK ÖSSZEGEZÉSÉNÉL

A tanulmány a reflektáló felületelemek dőlésének a közös mélységpontos összegezés végrehajtásakor fellépő hatását vizsgálja. Két különböző offsetű összegcsatorna típusra kiszámítja az összegezés átviteli függvényét a terjedési idő és a dőlés, illetve a dőlés és a geofontávolság függvényében. A számításokat mind egyszeres, mind többszörös reflexiókra elvégzi.

A számítások eredményeként megállapítható, hogy az egyszeres beérkezéseknek a dőlés következtében fellépő csillapítása felső határt szab a geofontávolságok hosszának. Mind a dőlés, mind az offsett növekedtével ez a felső határérték csökken.

A kis beérkezési idejű egyszeres reflexiók igen érzékenyek a dőlésre, a beérkezési idő növekedtével az érzékenység rohamosan csökken.

A többszörös reflexió-csillapítás a dőlés következtében csökken, egy kritikus értéknél zérussá válik, majd ismét növekedni kezd.

A zérus kioltással jelentkező zóna helye csak a terjedési időtől függ, a terjedési idő növekedtével ez a zóna a nagyobb geofontávolságok felé tolódik.

т. бодоки

О ВЛИЯНИИ НАКЛОНА ОТРАЖАЮЩЕЙ ПОВЕРХНОСТИ ПРИ СУММИРОВАНИИ ЗАПИСЕЙ ПО МЕТОДУ ОГТ

В работе анализируется влияние наклона отражающих площадок, наблюдаемое при суммировании записей по методу ОГТ. Для двух типов суммотрасс, при различной степени смещения пункта возбуждения вычисляются характеристики в зависимости, соответственно, от времени пробега и углов наклона, а также от углов наклона и шага сейсмоприемников. Вычисления проводятся как для однократных, так и для многократных отражений.

Результаты вычислений показывают, что затуханием однократных волн, связанным с наклоном поверхности, обусловливается максимальный шаг сейсмоприемников. С увеличением как углов наклона, так и степени смещения пункта возбуждения, уменьшается верхний предел шага сейсмоприемников.

Однократные отражения с небольшими временами вступления весьма чувствительны к наклонам, причем с возрастанием времени эта чувствительность резко снижается.

Затухание кратных отражений уменьшается с увеличением углов наклона; при определенной критической величине последнего оно становится равным нулю, а затем снова увеличивается.

Место зоны с нулевым затуханием зависит только от времени пробега; с увеличением последнего эта зона смещается в сторону больших шагов сейсмоприемников.

THE EFFECT OF NORMAL CORRECTION ERRORS ON THE STACKING OF COMMON-DEPTH-POINT TRACES

T. BODOKY–ZS. SZEIDOVITZ*

The analog processing of seismic stacking profiles consists of two basic steps: normal correction of single-coverage profiles and stacking.

When investigating stacking problems from different points of view, it is generally assumed that normal correction can be carried out accurately, i.e. the individual arrivals of the channels to be stacked can be brought into full phase-identity. Experiences gathered in areas with poor energy conditions and high noise-level, however, contradict this assumption. Therefore it will be tried to follow the effect of correction errors throughout the course of the stacking process.

Assuming the traces are normalized, the transfer function of stacking is

$$S(\omega) = \sum_{i=1}^{f} e^{j\omega\tau_i}, \tag{1}$$

where f is the coverage number, τ_i the time-shift between identical phase points of the reference and of the i-th trace.

If the correction itself is considered as free of error, τ will indicate, in an actual case, some fixed phase-shift on each channel. If, however, the correction is considered as burdened with error, this phase-shift may assume various values. Within a certain part of a section, where the signal-to-noise ratio can be regarded as constant, every possible value of error has a cetain probability of occurrence. Let us denote the possible values of the error by x, the corresponding probabilities by $p(x)$, and let us consider $M\{S(\omega)\}$ the expectable value of the transfer function for a given error-distribution. (The treatment of errors as random variables is reasonable due to the great number of single-coverage traces in the profile). In this case, in Relation (1), $(\tau + x)$, i.e. the error-burdened value of the phase-shift must be taken instead of τ, and the expected value of the transfer function will be

$$M\{S(\omega)\} = \int_{-\infty}^{\infty} \dots \int_{-\infty}^{\infty} \sum_{i=1}^{f} e^{j\omega(x_i+\tau_i)} p(x_1) \dots p(x_f) \, dx_1 \dots dx_f =$$

$$= e^{j\omega\tau_1} \int_{-\infty}^{\infty} \dots \int_{-\infty}^{\infty} e^{j\omega x_1} p(x_1) \dots p(x_f) \, dx_1 \dots dx_f + \dots$$

$$\ldots + e^{j\omega\tau_f} \int\limits_{-\infty}^{\infty} \ldots \int\limits_{-\infty}^{\infty} e^{j\omega x_f} p(x_1)\ldots p(x_f)\, dx_1\ldots dx_f =$$

$$= e^{j\omega\tau_1} \int\limits_{-\infty}^{\infty} e^{j\omega x_1} p(x_1)\, dx_1 \int\limits_{-\infty}^{\infty} p(x_2)\, dx_2 \ldots \int\limits_{-\infty}^{\infty} p(x)\, dx_f + \ldots$$

$$\ldots + e^{j\omega\tau_f} \int\limits_{-\infty}^{\infty} p(x_1)\, dx_1 \ldots \int\limits_{-\infty}^{\infty} p(x_{f-1})\, dx_{f-1} \int\limits_{-\infty}^{\infty} e^{j\omega x_1} p(x_f)\, dx =$$

$$= e^{j\omega\tau_1} \int\limits_{-\infty}^{\infty} e^{j\omega x_1} p(x_1)\, dx_1 + \ldots + e^{j\omega\tau_f} \int\limits_{-\infty}^{\infty} e^{j\omega x_f} p(x_f)\, dx_f$$

since

$$\int\limits_{-\infty}^{\infty} p(x)\, dx = 1,$$

assuming that

$$p(x_1) = p(x_2) = \ldots p(x_f) = p(x)$$

$$M\{S(\omega)\} = \left(\sum_{i=1}^{f} e^{j\omega\tau_i}\right) \int\limits_{-\infty}^{\infty} e^{j\omega x} p(x)\, dx.$$

The expected value of the transfer function is consequently the product of the error-free transfer function and of an integral expression depending on the error.

The relation obtained becomes still simple, if only the case of primary reflexion is considered, where

$$\tau_i = 0.$$

For the primary reflexion,

$$M\{S(\omega)\} = f \int\limits_{-\infty}^{\infty} e^{j\omega x} p(x)\, dx.$$

By means of the expected value of the transfer function, the expected signal energy loss as related to the case of error-free correction can be estimated. Denoting the expected loss by

$$\alpha = \frac{\int\limits_{-\infty}^{\infty} [M\{S(\omega)\} A(\omega)]^2\, d\omega}{\int\limits_{-\infty}^{\infty} [S(\omega) A(\omega)]^2\, d\omega}.$$

For a primary reflexion:

$$\alpha = \frac{\int\limits_{-\infty}^{\infty}\left[\left\{f\int\limits_{-\infty}^{\infty}e^{j\omega x}p(x)\,dx\right\}A(\omega)\right]^{2}d\omega}{\int\limits_{-\infty}^{\infty}[fA(\omega)]^{2}d\omega}\tag{2}$$

where $A(\omega)$ is the spectrum of the arrival.

Since constant f can be eliminated from the integrals by division, the expected signal-energy loss does not depend on the number of coverage but only on the error distribution and on the spectrum of the arrival. In what follows, the error distribution will be estimated from actual field material, and the expected energy loss will be given with respect to this distribution, as a function of error scattering for some possible spectra.

Before passing to the actual calculations, a few words are in order regarding multiples. The transfer function for primaries is constant, therefore the expected effect of the error depends, in case of identical input signals, on the scattering of the error alone. Its calculation and representation is, therefore, comparatively simple. The situation is much more complicated for the case of multiple arrivals. Here, the error-free value of the transfer function depends on the RMO series of the stacked trace (Bodoky, 1970). This tansfer function is distorted by the error, and the expected effect upon a multiple is a function of f variables ($f-1$ RMO values, and the scattering of the error). For threefold stacking this was investigated in detail by P. Halász, 1970.

The distribution of correction errors

If one has to treat the correction errors also in practice, the question arises at once: what is to be considered as correction error and how can it be estimated from the actual field records?

In the present investigation the time data of an uncurved good horizon, read out from all coverages, were corrected with static corrections computed and improved in field work with routine methods. dynamic correction prescribed (for analog processing) and compared with the theoretical, statically and dynamically corrected time-distance curves, i.e. with straight lines. The deviations were accepted as correction errors. The investigations were performed on six samples, each including 200–300 traces, from the Nyir region stacking profile of 1969.

The frequency histograms of the correction errors of these samples are shown in Figs. 1–6.

As to the distribution of correction errors it was as reasonable null hypothesis to assume that they obey a normal distribution, since they are presumably results of several smaller, independently acting factors. This is also corroborated by the frequency histograms. In order to avoid sampling errors, the sampled data were put together in seven intervals, each of 3 msec length, and a test of fitting was carried out on them by the χ^{2} test (Vince, 1968).

No - 4
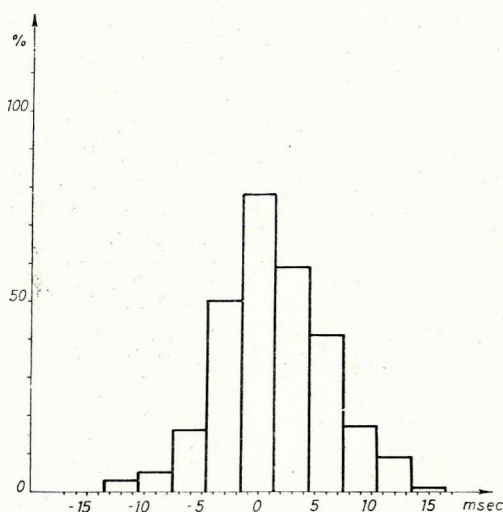
Fig. 1 Frequency histogram of the normal-correction errors, sample taken from the No-4 profile

1. ábra. A normál korrekció hibáinak gyakorisági hisztogramja a No-4 vonalból vett mintánál

Рис. 1. Гистограмма повторяемости погрешностей динамических поправок для выборки записей, полученных по профилю No-4
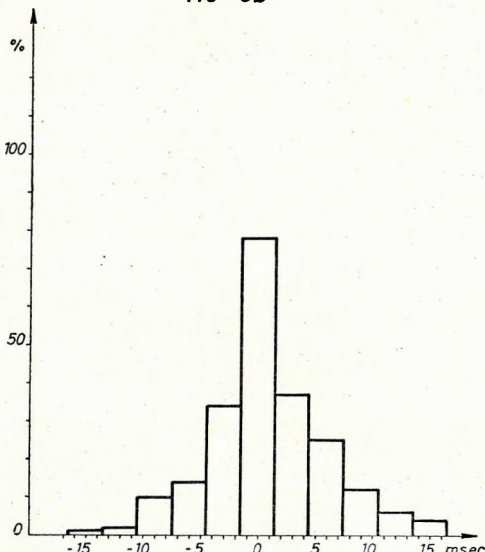
No - 5b

Fig. 2 Frequency histogram of the normal-correction errors, sample taken from the No-5b profile

2. ábra. A normál korrekció hibáinak gyakorisági hisztogramja a No-5b vonalból vett mintánál

Рис. 2. Гистограмма повторяемости погрешностей динамических поправок для выборки записей, полученных по профилю No-5б

Fig. 3 Frequency histogram of the normal-correction errors, sample taken from the No-6 profile (first sample)

3. ábra. A normál korrekció hibáinak gyakorisági hisztogramja a No-6 vonalból vett elsö mintánál

Рис. 3. Гистограмма повторяемости погрешностей динамических поправок для первой выборки записей, полученных по профилю No-6
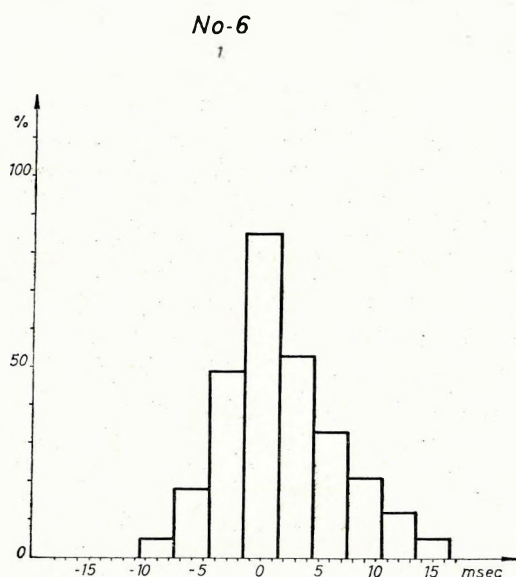
Fig. 4 Frequency histogram of the normal-correction errors, sample taken from the No-6 profile (second sample)

4. ábra. A normál korrekció hibáinak gyakorisági hisztogramja a No-6 vonalból vett második mintánál

Рис. 4. Гистограмма повторяемости погрешностей динамических поправок для второй выборки записей, полученных по профилю No-6
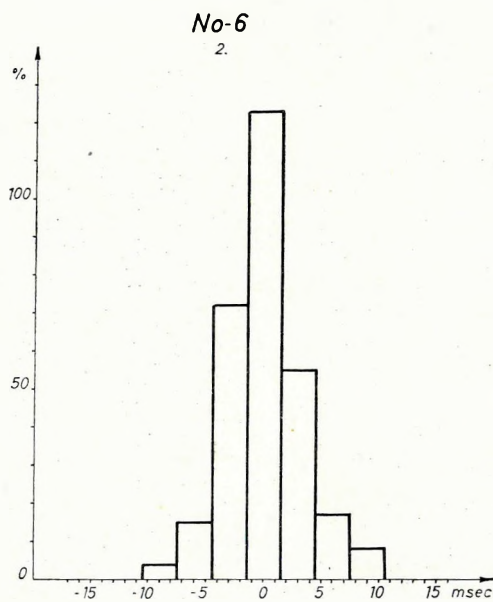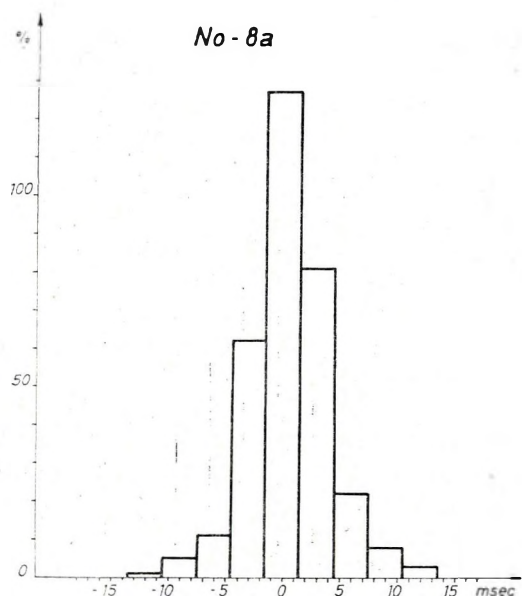
No - 8a
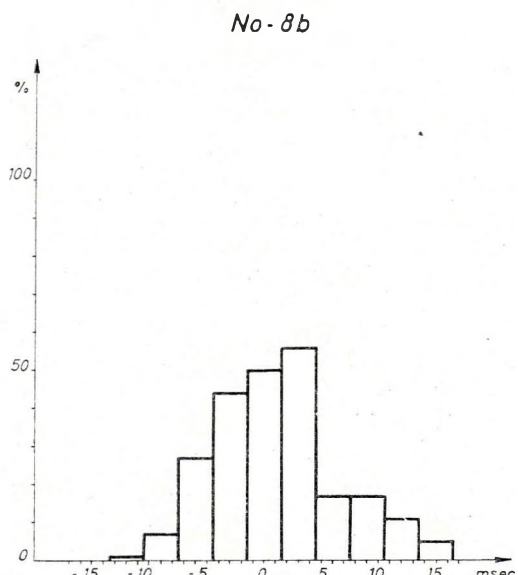
No - 8b

The results of the computations are shown in a tabular form:

Sample	No–4	No–5b	No–6/I	No–6/II	No–8a	No–8b
N	283	228	281	293	319	237
$M(x)$	1,19	0,83	1,68	0,04	0,53	1,22
σ	4,87	5,04	4,81	3,25	3,32	5,75
χ_4^2	3,94	13,78	5,68	10,06	8,42	11,87

where N = number of traces investigated
       $M(x)$ = expected value of the error, msec
       σ = SD of the error
       χ_4^2 = test result

The expected value and the standard deviation were estimated from the data; thus the number degrees of freedom of the test was $7-1-2=4$. For sake of comparison, the critical values of the χ_4^2–test with a degree of freedom of 4 are presented:

Probability in percents	Critical values for the application of the test
90,0	7,78
95,0	9,49
97,5	11,1
99,0	13,3
99,5	14,9
99,9	18,0
99,95	20,0

On the basis of the test, the initial hypothesis was accepted. (If the dynamical correction is erroneous, then the normal error distribution will surely not hold, the symmetry of the histogram will disappear. The analysis of correction errors provides a possible way also for checking the velocity function applied).

The expected signal-energy loss

Accepting error distribution as a normal one, the expected signal-energy loss was determined as a function of the standard deviation. The calculation was carried out for Ricker-wavelet spectra of 30, 40, 50, resp. 60 cps peak frequencies (RICKER. 1953).

The results of the calculation are shown in Figs. 7–10.

The purpose of multifold recording is generally a double one. Multiple reflexions can be filtered, and the signal-to-noise ratio improved, considering random noises alone.
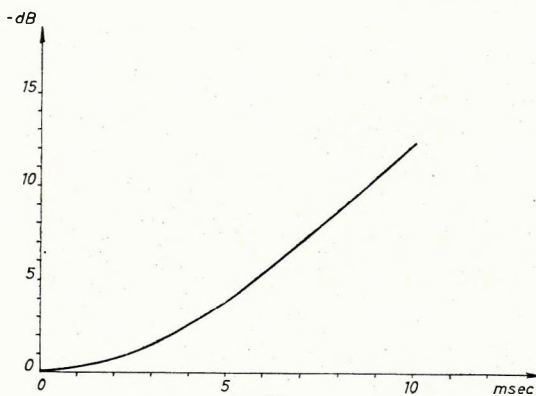
Fig. 7 Signal energy loss in stacking as function
of the standard deviation of correction error, for
input signals of 30 cps peak frequency

7. ábra. Az összegzésnél beálló jel energia veszte-
ség a normál korrekció hiba szórásának függvé-
nyében 30 Hz csúcsfrekvenciájú bemenő jelnél

Рис. 7. Потеря энергии сигнала, намечающаяся при
суммировании, в зависимости от разброса погреш-
ностей динамических поправок при частоте входного
сигнала 30 гц
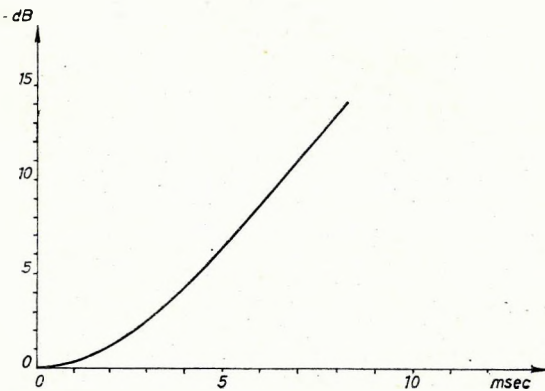
Fig. 8 Signal energy loss in stacking as function
of the standard deviation of correction error, for
input signal of 40 cps peak frequency

8. ábra. Az összegzésnél beálló jel energia veszte-
ség a normál korrekció hiba szórásának függvé-
nyében 40 Hz csúcsfrekvenciájú bemenő jelnél

Рис. 8. Потеря энергии сигнала, намечающаяся при
суммировании, в зависимости от разброса погреш-
ностей динамических поправок при частоте входного
сигнала 40 гц
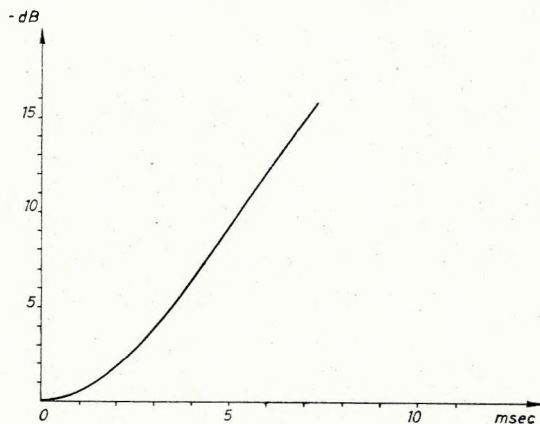
Fig. 9 Signal energy loss in stacking as function of
the standard deviation of correction error, for input
signals of 50 cps peak frequency

9. ábra. Az összegzésnél beálló jel energia veszte-
ség a normál korrekció hiba szórásának függvé-
nyében 50 Hz csúcsfrekvenciájú bemenő jelnél

Рис. 9. Потеря энергии сигнала, намечающаяся при
суммировании, в зависимости от разброса погреш-
ностей динамических поправок при частоте входного
сигнала 50 гц
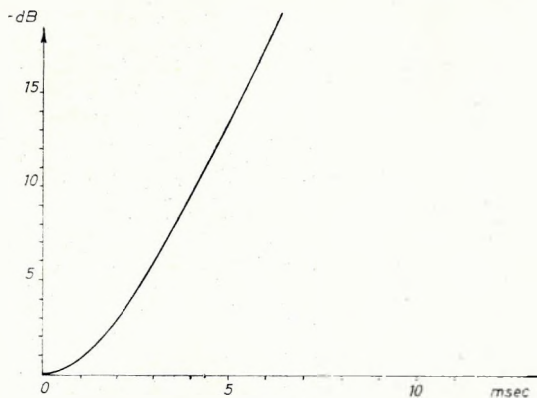
Fig. 10 Signal energy loss in stacking as function
of the standard deviation of correction error, for
input signals of 60 cps peak frequency

10. ábra. Az összegzésnél beálló jel energia veszte-
ség a normál korrekció hiba szórásának függvé-
nyében 60 Hz csúcsfrekcenciájú bemenő jelnél

Рис. 10. Потеря энергии сигнала, намечающаяся при
суммировании, в зависимости от разброса погреш-
ностей динамических поправок при частоте входного
сигнала 60 гц

In noisy areas under poor energy conditions, where even the recording of primary reflexions meets difficulties, the improvement of the signal-to-random noise ratio is of decisive significance. It appears from the calculations that in such areas the signal-to-noise ratio improvement which could be expected from multiple coverage may be lost even in cases of relatively small correction errors, especially in case of high frequency arrivals. Namely

$$\frac{\text{signal}}{\text{noise}} \longrightarrow f\text{-fold stacking} \longrightarrow \frac{f}{\sqrt{f}}\frac{\text{signal}}{\text{noise}} = \sqrt{f}\frac{\text{signal}}{\text{noise}},$$

where f is the number of traces stacked. In three-fold stacking, the expected improvement is 4,8 dB, in six-fold stacking, 7,8 dB, in twelve-fold stacking, 10,8 dB.

Consequently, the advantages of CDP methods can be exploited only if a sufficienty accurate correction, involving not greater error scattering than 1–2 msec is applied. The precondition of the determination of a correction of such a high degree of accuracy is, on the other hand, a good signal-to-noise ratio of single coverages. This can be improved by diminishing the size of spread parameters,—offset, seismometer spacing. The optimum performance of multiple filtering, however, is bound to certain definite sizes of the parameters (Bodoky, 1970).

Consequently, if necessary in the interest of proper signal-to-noise ratio, the optimum multiple filtering effect of CDP systems must be sacrificed.

REFERENCES

Bodoky, T., 1970: A közös mélységpontos rendszerek szűrőhatása és átviteli függvényeik. The filtering effect of common-depth-point systems and their transfer functions; in Hungarian. Magyar Geofizika, XI. 6. pp. 209–218.

Ricker, N., 1953: The form and laws of propagation of seismic wavelets. Geophysics, Vol. 18. No. 1.

Halász, P., 1970: Dinamikus és sztatikus korrekciók megengedhető hibái a közös mélységpontos módszernél. Permissible errors of dynamical and statical corrections in the common-depth-point method; in Hungarian. Magyar Geofizika, XI. 4–5. pp. 176–192.

Vincze J., 1968: Matematikai statisztika ipari alkalmazásokkal. Mathematical statistics with industrial applications; in Hungarian, Műszaki Kiadó, Budapest.

BODOKY TAMÁS—SZEIDOVITZ GYŐZŐNÉ

A NORMÁLKORREKCIÓ HIBÁINAK HATÁSA A KÖZÖS MÉLYSÉGPONTOS CSATORNÁK ÖSSZEGEZÉSÉNÉL

A tanulmány a közös mélységpontos csatornák összegezését korrekciós hiba jelenlétében vizsgálja és az összegezés átviteli függvényét erre az esetre vezeti le. A korrekciós hiba eloszlását konkrét mérési anyagon vizsgálja, és a vizsgálat eredményeképpen normál eloszlásnak fogadja el a hibaeloszlást. Különböző csúcsfrekvenciájú beérkezésekhez a korrekciós hibák okozta jel-energia veszteséget a hiba szórásának függvényében számítja ki. Az eredményekből látható, hogy az összegzés érzékenysége a korrekciós hibákkal szemben nő az összegezett jelek növekvő csúcsfrekvenciájával. A számítások megmutatják a korrekciós hibák szórásának még megengedhető legnagyobb értékét az egyes jelspektrumok esetében.

Т. БОДОКИ—Ж. СЕЙДОВИЦ

О ВЛИЯНИИ ПОГРЕШНОСТЕЙ ДИНАМИЧЕСКИХ ПОПРАВОК НА СУММИРОВАНИЕ ЗАПИСЕЙ ОГТ

В работе рассматривается задача суммирования записей ОГТ при наличии погрешностей в поправках и приводится характеристика суммирования для этого случая. Распределение погрешностей поправок анализируется на фактических материалах. В результате проведенного анализа распределение погрешностей принимается нормальным. Потеря энергии сигналов, вызванная погрешностями поправок вычисляется для волн с различной частотой, в зависимости от разброса погрешностей. Результаты показывают, что чувствительность суммирования к погрешностям поправок увеличивается с повышением частоты сигналов. Вычислениями определяются максимальные допустимые величины разброса погрешностей поправок для различных спектров сигналов.

RECURSION BAND-FILTERS AND THEIR DESIGN

G. GÖNCZ–A. ZELEI*

One phase of data processing in numerous geophysical (seismic, gravimetric, geoelectric) methods is the band-filtering of data. Filtering is frequently performed with the convolution of the input data system and another data system, the weight function of the filter. The filtered data are, depending on the length of the weight function given, a result of a certain number of multiplications and additions. The length of the weight function, and thus the number of operations according to output points is the higher, the narrower the frequency band to be passed or filtered out. In such cases, the application of recursion techniques is very advantageous. Its essence is that it uses, for the production of one output point, not only the input data, but also output data, filtered already earlier too. In this way a filtering effect identical with that of convolution filters is attained with much less operations. The general formula of the recursion algorithm is

$$y_n = \sum_{j=-N}^{M} a_j x_{n-j} - \sum_{i=1}^{L} b_i y_{n-i},\qquad(1)$$

where

  y — the filtered output
  a — the filter affecting the input
  b — the filter affecting the earlier already filtered input
  x — the input

It is assumed that the sampling interval is of unit value.

Formula (1) uses $M + N + 1$ input points and L output points for the production of a single output value. Let us consider now the case $N = 0$, $M = L$ and let us compute the transfer function of the operation. For this purpose (1) has to be written in the frequency domain:

$$F(\{y\}_m) = F(\{a_j\}_{j=0}^{M}) F(\{x\}_l) - F(\{b_i\}_{i=1}^{M}) F(\{y\}_m)\qquad(2)$$

where F indicates the Fourier-transform, and l runs over input points, m runs through every output points. After rearrangement:

$$F(\{y\}_m) = \frac{F(\{a_j\}_{j=0}^{M})}{1 + F(\{b_i\}_{i=1}^{M})}\, F(\{x\}_l).\qquad(3)$$

The transfer function of the operation:

$$F(w) = \frac{F(\{a_j\}_{j=0}^M)}{1 + F(\{b_i\}_{i=1}^M)} = \frac{a_0 + ae^{-jW} + \ldots + a_M e^{-jWM}}{1 + b_1 e^{-jW} + \ldots + b_M e^{-jWM}}. \tag{4}$$

Since the sampling interval is of unit value, $-180° \le W \le 180°$, where $-180°$, $+180°$ is the Nyquist-interval.

If $z = e^{-jW}$ substituted in (4), it is represented in the so-called z-domain:

$$F(z) = \frac{a_0 + az + \ldots + a_M z^M}{1 + b_1 z + \ldots + b_M z^M} = \frac{A_M(z)}{B_M(z)}. \tag{5}$$

$F(z)$ is the ratio of real-coefficient, complex variable, M-th degree polynomials. It is simply visible that the Nyquist-interval is represented on the unit circle of the z-plane, since $|z| = 1$ and, if W varies from $-180°$ to $+180°$, z runs around the unit circle. The $F(z_0)$ value of the transfer function can be ordered to every z_0 point of the unit circle. If $F(z)$ is required to have a definite form, the polynomials $A_M(z)$ and $B_M(z)$ have to be chosen suitably. This can be attained by a proper position of the roots of the polynomials. It must be noted that if a z_i value is the root of any of the polynomials, then also $\bar{z}_i$ must be one. Namely, the coefficients of the polynomials agree with the coefficients of the filter; the latter must be, however, real.

In geophysical literature, the procedure was used for the first time by SHANKS (1967), then by MOONEY (1968) who discussed the design of notch filters, band-cut filters and band-pass filters in detail. As a simple example, a notch filter will be presented here. In the following, the roots of $A_M(z)$ will be called zero places, the roots of $B_M(z)$, on the other hand, poles. Be the zero places $z_0 = e^{-j36°}$ resp. $\bar{z}_0 = e^{+j36°}$, and the poles $z_0 = 1{,}01.e^{-j36°}$, resp. $\bar{z}_0 = 1{,}01.e^{+j36°}$. The amplitude characteristics and the position of the zero places, resp. poles are visible in Fig. 1. R_p indicates the distance of the pole from the origo. The sharpness of the characteristics can be varied. If R_p increases, the steepness decreases. This is shown in Fig. 1, where
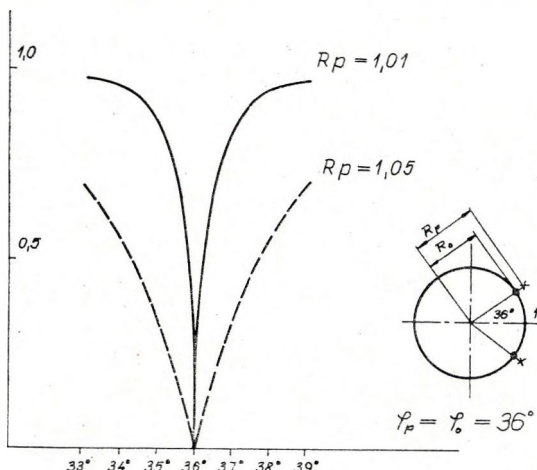

Fig. 1 Amplitude characteristics of notch filters R_p distances 1,05, resp. 1,01

1. ábra. Lyukszűrők amplitúdó-karakterisztikái. A választott R_p távolság 1,05 illetve 1,01

Рис. 1. Амплитудные характеристики фильтров-пробок при расстояниях R_p равных 1,05 и 1,01 соответственно

notch filters of parameters $R_p = 1,05$ and $R_p = 1,01$ are presented. The transfer functions are

$$F(z) = \frac{(z - e^{-j36°})(z - e^{+j36°})}{(z - R_p e^{-j36°})(z - R_p e^{+j36°})} \tag{6}$$

where R_p is 1,01 or 1,05.

The filter has 5 points:

$$F(z) = \frac{\dfrac{1}{R_p^2} - \dfrac{2\cos 36°}{R_p^2} z + \dfrac{1}{R_p^2} z^2}{1 - \dfrac{2\cos 36°}{R_p} z + \dfrac{1}{R_p^2} z^2} \tag{7}$$

the filter points being:

$$a_0 = \frac{1}{R_p^2} \qquad a_1 = \frac{-2\cos 36°}{R_p^2} \qquad a_2 = \frac{1}{R_p^2}$$

resp.

$$b_1 = \frac{-2\cos 36°}{R_p} \qquad b_2 = \frac{1}{R_p^2} .$$
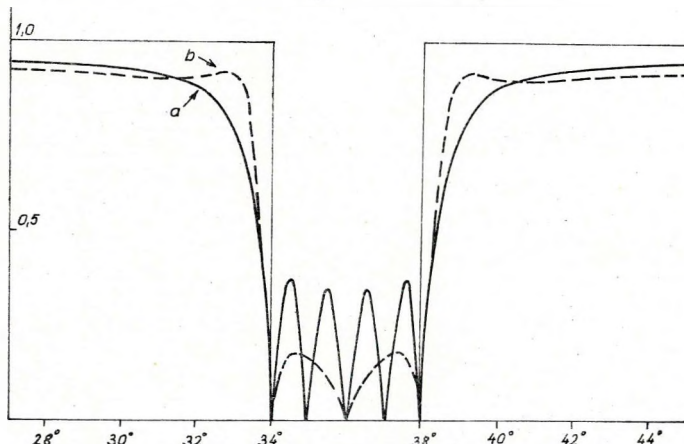
Fig. 2 Amplitude characteristics of band-reject filters; width of filtered-out band: 4° a) Zero/pole pairs established in 1° intervals; $R_p = 1,01$; b) Zero/pole pairs established in 2° intervals; pole places situated at $R_p = 1,008$; 1,05; 1,008 and $\varphi_p = 33,5°$; 36°; 38,5°

2. ábra. Sávvágó szűrők amplitúdókarakterisztikái. A kiszűrt sáv 4° szélességű. *a)* A zérus−pólus párokat 1°-ként helyeztük el. $R_p = 1,01$. *b)* A zérus−pólus párokat 2°-ként, a pólushelyeket $R_p = 1,008$; 1,05; 1.008 és $\varphi_p = 33,5°$; 36°; 38,5° értékeknek megfelelően helyeztük el

Рис. 2. Амплитудные характеристики полосно-заграждающих фильтров. Ширина заграждения полосы —4°. a) Пары нулевых полюсов размещены через 1°. Расстояние $R_p = 1,01$ б) Пары нулевых полюсов размещены через 2°, места полюсов выбраны в соответствии с величинами $R_p = 1,008$; 1,05; 1,008 и $\varphi_p = 35,5°$; 36°; 38,5°

If the filtering of a broader band is wanted, more zero-pole pairs must be placed besides each other. The slope depends also further on the R_p distances; in the exclusion range the amplitude characteristics will be better, the more densely are the zero-pole pairs spaced. This involves, of course, an increase in the number of the filter points. Mooney suggests 0,5°, resp. 1° zero place distances with identical R_p distances. In Fig. 2, the curve denoted by a is the amplitude characteristics of a filter cutting a 4° band. The centre of the band lies at 36°. The zero-pole pairs have been established at each 1°; R_p was 1,01 selected out of the parameters suggested by Mooney. The slope is very steep, but the elimination within the exclusion band is not sufficiently good. This can be improved, if the notch filter placed in the centre of the band is chosen for less steep, and the slope is gradually increased by a suitable selection of the R_p distances. Naturally this will deteriorate the steepness of the filter. This is clearly visible in Fig. 3, where the filtering-out of the afore-mentioned 4° band is our aim, the zero/pole pairs were situated at each 1°; R_p distances were 1,01; 1,025, 1,04; 1,025, 1,01. The zero places in this case, as always, were placed on unit circles.
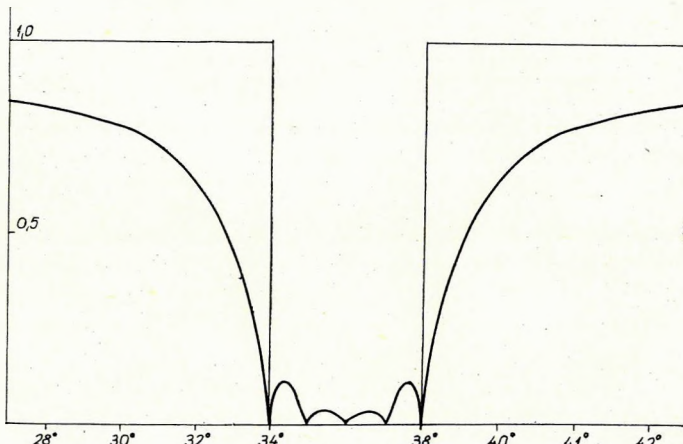
*Fig. 3* Amplitude characteristics of a band-reject filter. Width of filtered-out band: 4°; zero/pole pairs in intervals of 2°; R_p values: 0,01; 1,025; 1,04; 1,025; 1,01

3. ábra. Sávvágó szűrő amplitúdókarakterisztikája. A kiszűrt sáv szélessége 4°. A zérus—pólus párokat 2°-ként helyeztük el. $R_p = 1,01$; 1,025; 1,04; 1,025; 1,01

Рис. 3. Амплитудная характеристика полосно-заграждающего фильтра. Ширина полосы заграждения — 4°. Пары нулевых полюсов размещены через 2°. Расстояния R_p выбирались равными 1,01; 1,025; 1,04; 1,025; 1,01

Another possibility for the improvement of the characteristics would be the densifying of zero, resp. pole places, e.g. to distances of 1/2°. This would, however, as mentioned, increase the number of filter-coefficients. In case of 1° spacing, the filter would consist of 19 points; with 1/2° spacing, of 35 points. This would be, of course, still advantageous if compared with the length of a convolution filterc, by which the same narrow band could be filtered with the same quality. Indeed, in this case a filter of at least 150–200 points should be used.

The amplitude characteristics of the recursive filter, as suggested by MOONEY, might be improved in the following way. If the pole distances are increased when passing towards the centre of the band to be filtered, a good degree of exclusion could be ensured. On the other hand, the slope could be improved if both extreme poles were placed not radially near the corresponding zero-place, but symmetrically, at the lower limit of the band somewhat to the left of it, at the upper one, to the right of it. In this case, namely, the characteristics of both extreme notch filters overshoot at the proper place, compensating the less steepness of the centre filter. Against the previous five pairs, three zero/pole pairs were placed at each 2° in the 4° band. Thus the number of coefficients was decreased from 19 to 11; at the same time, as shown by the curve *b* of Fig. 2, also the properties of the amplitude characteristics have been improved. The parameters chosen were:

R_p	1,008	1,05	1,008
zero places (φ_0)	34°	36°	38°
poles (φ_p)	33,5°	36°	38,5°

The transfer function:

$$F(z) = \frac{(z - e^{-j34°})(z - e^{+j34°})(z - e^{-j36°})(z - e^{+j36°})(z - e^{-j38°})(z - e^{+j38°})}{(z - 1,008\,e^{-j33,5°})(z - 1,008\,e^{+j33,5°})(z - 1,05\,e^{-j36°}) \times (z - 1,05\,e^{j36°})}$$
$$(z - 1,008\,e^{-j38,5°})(z - 1,008\,e^{+j38,5°})$$

$$(8)$$
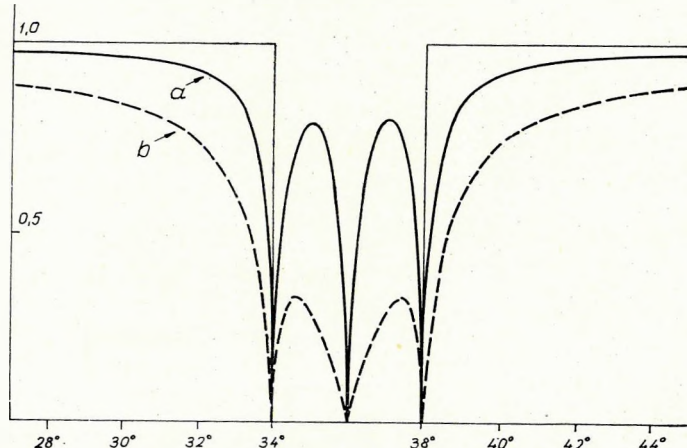
Fig. 4 Amplitude characteristics of band-reject filters. Width of filtered-out band: 4°; zero/pole pairs in intervals of 2°;
  a) $R_p = 1,008$; *b)* $R_p = 1,008$; 1,05; 1,008

4. ábra. Sávvágó szűrők amplitúdókarakterisztikái. A kiszűrt sáv szélessége 4°. A zérus—pólus párokat 2°-ként helyeztük el.
  a) $R_p = 1,008$; *b)* $R_p = 1,008$; 1,05; 1,008

Рис. 4. Амплитудные характеристики полосно-заграждающих фильтров. Ширина полосы заграждения — 4°. Пары нулевых полюсов размещены через 2°; а) $R_p = 1,008$ б) $R_p = 1,008$; 1,05; 1,008

The amplitude characteristics were computed for an $R_p = 1{,}008$, identical with a 2_0 zero/pole pair spacing, in the way suggested by Mooney. The result is shown by curve a of Fig. 4. Comparing it with curve b of Fig. 2, the former is essentially worse. If only the central R_p distance was increased to $1{,}05$, the characteristics represented by the curve b of Fig. 4 were obtained. The exclusion became considerably better, but the steepness decreased at the same time. The conclusion may be drawn that the amplitude characteristics can be improved by a suitable choice of R_p and φ_p values.

The amplitude characteristics presented and the data of the lengths of the necessary weight function show that, in case of narrow-band filtering, recursion filters are more advantageous than convolution filters, the latter being too long in such cases. With an increase of band width, however, also the length of the recursion filter increases, since more and more zero/pole pairs are to be established.

Simultaneously the length of the convolution filter decreases more and more, becoming, in case of broad bands, more advantageous than the recursion filter. In this sense, both procedures are complementing each other. This fact is emphasized and elaborated in details in a forthcoming text-book of MESKO (1971).

The phase distortion of recursion filters

As known, the convolution filters in use are free of phase distortion, but recursion filters are not. Special steps must be taken to make the filtered output free of phase distortion. A simple procedure, known from literature, is, for example, to filter the data system again, from opposite direction. Thus, as additional advantage, the amplitude characteristics will be sharper, while the phase characteristics identically zero. By this procedure, an increase in the number of operations is inevitable, but, recognizing certain symmetry properties of recursion band filters and performing the filtering in two steps, this increase can be kept lower.

Be $X(z)$ the z-transform of the input and $Y(z)$ that of the output. The filter operation in the z-domain is:

$$Y(z) = \frac{A_M(z)}{B_M(z)} X(z). \tag{9}$$

Performing the filtering in two steps:

$$Y(z) = A_M(z)\, \overline{Y}(z) \tag{10}$$

where

$$\overline{Y}(z) = \frac{1}{B_M(z)} X(z). \tag{11}$$

By (10) a convolution filtering, by (11) a recursion filtering is defined, i.e. (9) has been resolved into a convolution and a recursion filtering.

This was done, because it is evident that $A_M(z)$ represents a $2M + 1$-point zero-phase-shift convolution filter.

Let us write $A_M(z)$ in the form:

$$A_M(z) = \prod_{i=1}^{M} a_0(z_{0i} - z)(z_{0i} - z). \tag{12}$$

It is known that $A_M(z)$ is of an even degree, since the number of roots is 2 or 4 or 6, etc. Let us write out the i-th pair of roots separately:

$$(z_{0i} - z)(\bar{z}_{0i} - z) = z_{0i}\bar{z}_{0i} - (z_{0i} + \bar{z}_{0i})z + z^2 = 1 - 2z_{0i,\,\text{real}} + z^2. \tag{13}$$

By (13), a 3-point symmetrical operator is represented:

$$a_{i0} = 1 \qquad a_{i1} = -2z_{0i,\,\text{real}} \qquad a_{i2} = 1. \tag{14}$$

In the z-domain, the $A_M(z)$ filter is produced as a product of such factors; in the time-domain, again, as their convolution:

$$A_M = \{1;\ -2z_{01,\,\text{real}};\ 1\} * \{1;\ -2z_{02,\,\text{real}};\ 1\} * \ldots * \{1;\ -2z_{0\frac{M}{2},\,\text{real}};\ 1\}. \tag{15}$$

The convolution of symmetrical filter operators is similarly symmetrical, i.e. in (15)

$$a_i = a_{2M-i} \qquad 0 \le i \le M-1 \tag{16}$$

Since $A_M(z)$ is symmetrical, it is free of phase distortion.

This can be very illustratively shown in the z-domain. Let us regard $A_M(z)$ as sum of vectors interpreted on the z-plane. Applying (16), $A_M(z)$ can be written as follows:

$$A_M(z) = z^n(a_0 z^{-n} + \ldots + a_{n-1}z^{-1} + a_n + a_{n-1}z + \ldots + a_0 z^n) =$$
$$= z^n(a_0 \bar{z}^n + \ldots + a_{n-1}\bar{z}^1 + a_n + a_{n-1}z + \ldots + a_0 z^n) =$$
$$= |A'_M(z)|e^{-j\varphi} \cdot z^n \qquad \sqrt{n} = M \tag{17}$$

where

$$A'_M(z) = a_0 \bar{z}^n + \ldots + a_{n-1}\bar{z}^1 + a_n + a_{n-1}z + \ldots + a_0 z^n \tag{18}$$

the phase-shift:

$$\varphi = \text{arc tg} \, \frac{I_m A'_M(z)}{R_e A'_M(z)}. \tag{19}$$

The z^n factor is considered by shifting the input data by a sampling interval n. It is easy to see that the value is zero. To prove this, one has only to show that the $A_M(z)$ vector has only real component, show well by Fig. 5. The sum of each pair of vectors fall on the real axis, therefore their resultant similarly falls on the same. Thus, $\text{Im } A'_1(z) = 0$, and from (19), $\varphi = 0$ for every z.

The situation is not similar in the case of $B_M(z)$, since the poles were not placed on the unit circle, thus the 3-point elementary operators will not be symmetric either.
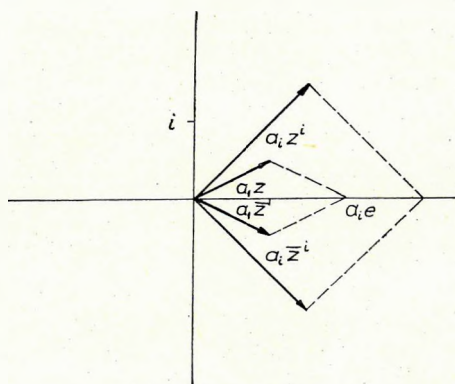
Fig. 5 The $A'_M(z)$ vector in the z-domain
5. ábra. Az $A'_M(z)$ vektor z tartományban
Рис. 5. Вектор $A'_M(z)$ в области z

It is visible, therefore, that phase-distortion is caused only by a recursion filtering with a filter $\dfrac{1}{B_M(z)}$. Merely this has to be corrected, for example in the way mentioned earlier.

The original data system is passed twice across the filter $\dfrac{1}{B_M(z)}$ from opposite directions, then filtered in a non-recursive way with $A_M(z)$. The difference is that the data system had been filtered, until now, with the entire $\dfrac{A_M(z)}{B_M(z)}$ filter, unnecessarily. The block diagram of the filtering suggested is visible in Fig. 6.
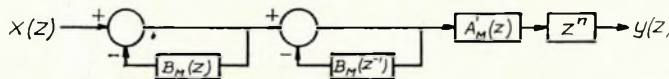
Fig. 6 Block diagram of the filtering suggested
6. ábra. A javasolt szűrés blokksémája
Рис. 6. Предлагаемая схема фильтрации

These two modes of filtering are not fully identical. The amplitude characteristics of the method quoted from literature is

$$|F_1(W)| = \left|\frac{A_M(z)}{B(z)}\right|^2_{\,|z=e^{-jW}} = \frac{|A_M(z)|}{|B_M(z)|^2}\cdot|A_M(z)|_{\,|z=e^{-jW}} \tag{20}$$

while that of the one suggested:

$$|F_2(W)| = \frac{|A_M(z)|}{|B_M(z)|^2}_{\,|z=e^{-jW}} \tag{21}$$

The difference lies in the factor $A_M(z)$. In case of suitably chosen parameters, however, both approach the ideal characteristics fairly well.

Also the number of operations spared was estimated. If the number of established pairs of roots is n, i.e. $A_M(z)$, resp. $B_M(z)$ polynomials are of $M = 2n$-th degree, the number of operations needed for each output point is less by $4n + 1$. Let us assume that a channel of length of $2K$ is filtered, and $n = 6$. The gain is about 51 000 operations. It must be noted that this estimate does not take the increase in computer time, originating from the more complicated data motion, into consideration.

The situation will be somewhat altered when the lower limit of the band to be filtered is zero, i.e. when a low-pass filter is designed. In this case $A_M(z)$ will not be symmetrical, its radical form will be broadened by factor $(c - z)$, filtering out the zero frequency. Here c is real. This corresponds to a non-symmetrical operator $(c_i - 1)$, and the symmetry of the numerator will be destroyed by the convolution made with it. Accordingly, this factor must be detached from $A_M(z)$. The filtering will be modified in such a way that a two-way recursive filtering is made with $\dfrac{c - z}{B_M(z)}$ according to the formula

$$F(z) = \frac{A_M(z)}{B_M(z)} = A_1(z)\,\frac{c - z}{B_M(z)} \tag{22}$$

where

$$A_M(z) = A_1(z) \cdot (c - z) \ .$$

then the convolution filter $A_1(z)$ is applied to the result.

Finally, thanks are due to the Geophysical Exploration Co. of National Oil and Gas Trust for their kind permission to publish this paper.

REFERENCES

Meskó, A. M., 1971: Foundations of digital seismic data processing. University manual (in Hungarian) (in print).

Mooney, H. M., 1968: Pole and zero design of digital filters, Geophysics, Vol. 33, No. 2, pp. 354–360.

Shanks, I., 1967: Recursion filters for digital processing. Geophysics, Vol. 32, No. 1, pp. 33–51.

GÖNCZ GÁBOR—ZELEI ANDRÁS

REKURZÍV SÁVSZŰRŐK TERVEZÉSE

A tanulmány első részében rövid áttekintést ad a rekurzív sávszűrökről, alkalmazásuk előnyeiről és korlátairól, valamint tervezésük egyfajta — az irodalomból jól ismert — módjáról. A módszer alkalmazásával a szűrők amplitúdókarakterisztikája javítható. A rekurzív szűrők fáziskarkterisztikájára vonatkozólag ismeretes, hogy ezen szűrők nem zérus fázistolásúak. Bizonyos eljárással — az egyszer már megszűrt adatok ismételt szűrésével — a fázistorzítást ki lehet küszöbölni. Figyelembe véve a rekurziv szűrők átviteli függvényének bizonyos szimmetria tulajdonságait ez a második szűrés lerövidíthető.

Г. ГЁНЦ—А. ЗЕЛЕИ

РАЗРАБОТКА РЕКУРСИВНЫХ ПОЛОСНЫХ ФИЛЬТРОВ

В первой части работы коротко излагаются существующие виды рекурсивных полосных фильтров, их преимущества и ограничения, а также хорошо известный из литературы метод их разработки. Метод позволяет улучшить амплитудные характеристики фильтров. О фазовой характеристике рекурсивных фильтров известно, что в них фазовое смещение не равняется нулю. С применением определенного способа — путем повторной фильтрации уже отфильтрованных данных — можно исключить фазовые искажения. Учитывая определенные особенности симметрии характеристики рекурсивных фильтров можно сократить вторую фильтрацию.

Függelék

A függelékben a rekurzív szűrők zérus—pólus elhelyezéssel történő tervezését kívánjuk szemléletessé tenni néhány egyszerű példa segítségével.

Tegyük fel, hogy olyan lyukszűrőt akarunk tervezni, z-tartományban, mely a zéró frekvenciát, azaz az egyenkomponenst szűri ki a bemeneti adatrendszerből. Jelöljük ezen szűrő átviteli függvényét $F(z)$-vel. Minthogy definíció szerint $z = e^{-j2\pi f/\tau}$ — ahol τ a mintavételi távolság — olyan $F(z)$-t kell választanunk, melyre fennáll, hogy $F(1) = 0$. Ez teljesül ha:

$$F(z) = \frac{1-z}{2}. \tag{1}$$

Az átviteli függvény zéróhelye $z = 1$-nél van. Az amplitúdókarakterisztika:

$$|F(z)| = \frac{|1-z|}{2}. \tag{2}$$

Az 1. ábrán látható, hogy az $(1-z)$ vektor hossza egyenlő az amplitúdókarakterisztika valamely z helyen felvett értékével. Látható, hogy $F(1) = 0$ és $F(-1) = 1$.
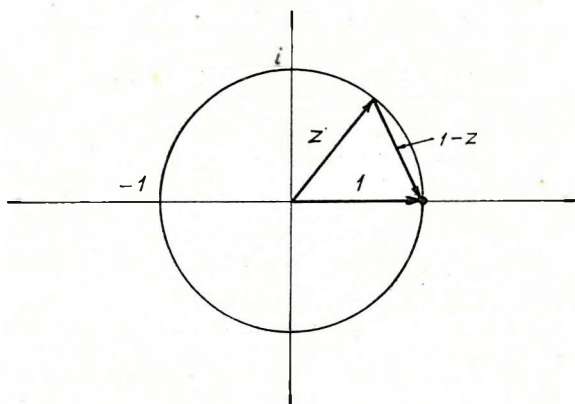
Fig. 1 Transfer function of notch filter $F(z)$ on the z-plane

1. ábra. Az $F(z)$ lyukszűrő átviteli függvénye a z-síkon

Рис. 1. Характеристика фильтра-пробки $F(z)$ на плоскости z

A 2. ábra *a* görbéje mutatja az amplitúdókarakterisztikát a Nyquist-intervallumban. Ez, távolodva a zérus frekvenciától, igen lassan növekszik, emiatt erősen vágja a zérus frekvencia elég tág környezetét is. Ez nemkívánatos hatás. Mindenesetre az (1; − 1) kétpontos szűrő megvalósítja az egyenkomponens kiszűrését. Élesebb amplitúdókarakterisztikájú szűrőre lenne azonban szükségünk. Definiáljuk $G(z)$-t a következőképpen:

$$G(z) = 2\frac{F(z)}{R_p - z},\qquad(3)$$

ahol R_p valós.
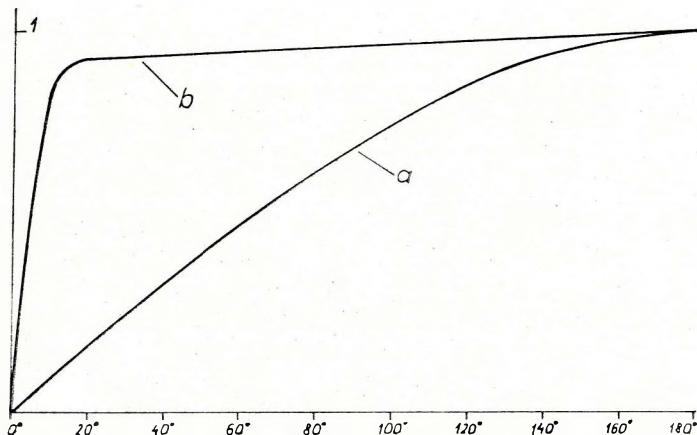
Fig. 2 Amplitude characteristics of filter $F(z)$ (curve a) and of $G(z)$ (curve b)

2. ábra. Az a-val jelölt görbe az $F(z)$ a b-vel jelölt a $G(z)$ szűrő amplitúdókatakterisztikája

Рис. 2. Амплитудные характеристики а) фильтра $F(z)$; б) фильтра $G(z)$

$G(z)$ zéróhelye megegyezik $F(z)$ zéróhelyével, és pólusa van a $z = R_p$ helyen. A 3. ábra szemlélteti az elhelyezett pólus hatását. A $|G(z)|$ az $(1 - z)$ és a $(R_p - z)$ vektorok hosszának hányadosa. Ha $R_p = 1 + a$, ahol $0 < a \ll 1$ akkor $|1 - z|$ és $|R_p - z|$ közelítőleg egyenlő és így $\dfrac{|1 - z|}{|R_p - z|} \simeq 1$ minden z-re, kivéve a $z = 1$ — azaz az $f = 0$ — helyet, ahol $|G(1)| = 0$. Az ábráról leolvasható a fáziskarakterisztika értéke is:

$$\varphi(z) = \Phi(z) - \psi(z).\qquad(4)$$

A 2. ábra *b* görbéje a $G(z)$ szűrő amplitúdókarakterisztikája. Látható tehát, hogy egy zérushely és egy pólus elhelyezésével igen nagy vágási meredekségü szűrőt állíthatunk elő.
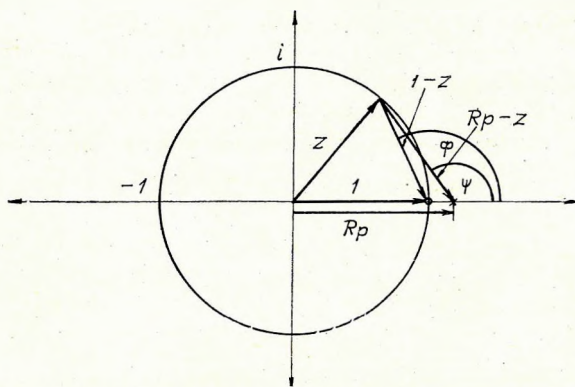
Fig. 3 Transfer function of filter $G(z)$ on the z-plane

3. ábra. A $G(z)$ szűrő átviteli függvénye a z-síkon

Рис. 3. Характеристика фильтра $G(z)$ на плоскости z

Ha $X(z)$-vel jelöljük a bemenet, $Y(z)$-vel a kimenet z-transzformáltját, a szűrést z-tartományban a következő képlet írja le:

$$Y(z) = \frac{\dfrac{1}{R_p} - \dfrac{1}{R_p} \cdot z}{1 - \dfrac{1}{R_p} \cdot z} \cdot X(z), \tag{5}$$

időtartományban pedig:

$$Y_n = \frac{1}{R_p} X_n - \frac{1}{R_p} X_{n-1} + \frac{1}{R_p} Y_{n-1} \tag{6}$$

a szűrő hárompontos, R_p értékeire a szokásos választás $1{,}01 \leq R_p \leq 1{,}1$ ettől függően változik a lyukszűrő meredeksége. Bonyolultabb szűrőket is hasonló meggondolásokkal tervezhetünk.

Felvetődhet a kérdés miért nem tehetők pólusok az egységkör belsejébe. Általánosan bizonyítható, hogy az ily módon kapott szűrő nem lenne stabil. Ismeretes, hogy egy lineáris szűrő akkor stabil, ha az egységimpulzus bemenetre adott válasz — amelyet súlyfüggvénynek is szokás nevezni — időben lecseng, azaz ha a rendszer visszatér nyugalmi állapotába. Más szavakkal, ha véges energiájú bemenet esetén a kimenet energiája is véges lesz.

Vizsgáljuk meg a fenti szűrő stabilitását. Ehhez szükségünk lesz az egységimpulzus bemenet z-transzformáltjára. Az egységimpulzus bemenet:

$$X_n = \begin{cases} 1 & n = 0 \\ 0 & n \neq 0 \end{cases}. \tag{7}$$

A z-transzformált definíciója:

$$X(z) = \sum_{n=0}^{\infty} X_n z^n. \tag{8}$$

Így (7) z-transzformáltja $X(z) = 1$.

A kimenet z-transzformáltja (5) alapján:

$$Y(z) = \frac{\dfrac{1}{R_p} - \dfrac{1}{R_p} \cdot z}{1 - \dfrac{1}{R_p} \cdot z} \quad X(z) = \frac{\dfrac{1}{R_p} - \dfrac{1}{R_p} \cdot z}{1 - \dfrac{1}{R_p} z},$$
(9)

amely éppen az átviteli függvény, a $|z| = 1$ körön.

(9)-et sorbafejtve $Y(z)$-re a következő képletet kapjuk:

$$Y(z) = 1 + \left(\frac{1}{R_p} - 1\right) z + \left(\frac{1}{R_p^2} - \frac{1}{R_p}\right) z^2 + \ldots + \left(\frac{1}{R_p^n} - \frac{1}{R_p}\right) z^n + \ldots$$
(10)

a kimenet időtartományban tehát az

$$1; \quad \frac{1}{R_p} - 1; \quad \frac{1}{R_p^2} - \frac{1}{R_p}; \quad \ldots; \quad \frac{1}{R_p^n} - \frac{1}{R_p^{n-1}}; \quad \ldots$$
(11)

sorozat lesz.

Ha $R_p = 1$ a kimenet megegyezik a bemenettel, ekkor ugyanis $G(z) = 1$ lesz.
Ha $R_p > 1$ akkor:

$$\lim_{n \to \infty} \left(\frac{1}{R_p^n} - \frac{1}{R_p^{n-1}}\right) = (1 - R) \lim_{n \to \infty} \left(\frac{1}{R_p}\right)^n = 0$$

tehát a kimenet lecseng.

Végül ha $R_p < 1$ akkor $\dfrac{1}{R_p} > 1$, így a kimenet minden határon túl nő. A szűrő instabil.

A pólusokat tehát mindenkor az egységkörön kívül kell elhelyezni.

A zérus és pólushelyek az előző példákban a valós tengelyen voltak. Általában ezek komplex számok. Ilyen esetekben a megfelelő komplex konjugált értékeket is figyelembe kell venni a szűrő tervezésénél.

HOW THE NUMBER OF COVERAGES AFFECTS THE ATTENUATION OF MULTIPLES IN COMMON-DEPTH-POINT STACKING

T. BODOKY–I. POLCZ*

The attenuating effect of common-depth-point systems upon multiple reflexions was discussed in detail in a previous paper (BODOKY, 1970). Using the computational technique introduced there, it will be examined, what role the number of CDP traces has in the elimination of multiple reflexions. The principal aim will be to give criteria, upon which it can be decided, whether the advantages due to an increase of the percentage of coverage are proportional to the increase in measuring costs.

In order to characterize the multiple-attenuating efficiency of some type of stacked traces, resp. of a spread system, in the paper mentioned the ratio of transmitted, resp. total energy of the multiple was used. This ratio is given by the following relation:

$$\Phi(t_0, d) = \frac{\int_0^\infty [A(\omega)S(\omega)]^2 \, d\omega}{\int_0^\infty [fA(\omega)]^2 \, d\omega} ,$$

where Φ ratio of attenuated, resp. unattenuated multiple energy
       t_0 recording period
       d seismometer spacing
       f number of CDP traces
       ω circular frequency
       $A(\omega)$ spectrum of multiple reflexions
       $S(\omega)$ transfer function corresponding to the stacked trace; in detail:

$$S(\omega) = \sum_{i=1}^{f} e^{j\omega\tau_i(t_0, x)}$$

where $\tau_i(t_0, x)$ is the residual moveout of the i-th trace to be stacked,
       x seismometer-shotpoint distance.

Throughout the computations, the velocity function and spectrum characteristic to the Nyir region, described in the paper mentioned, were employed. To make calculations simple, the Φ functions were not determined for the entire $t_0 - d$ plane, but t_0 was kept fixed. This does not cause a loss of information whatever, since the functions are approximately independent of t_0 (BODOKY, 1970).

The Φ functions were computed as functions of d for $t_0 = 2$ sec, for 3-, 4-, 6- and 12-fold systems. The computations were carried out for a split-spread system (Fig. 1), for an end-on-system (Fig. 2) and for an offset-shotpoint system with 12 seismometer spacings (Fig. 3). The Φ functions obtained were represented in dB units. The Φ function of the individual systems is defined as the aritmetic mean of the Φ functions corresponding to different types of stacked traces occurring in the system.

It is apparent from the figures, that the cut-off frequency and slope is practically independent of the number of the coverages; a doubling of the latter improves the maximum attenuation by 3–6 dB, but the optimum zone shifts, according the cut-off steepness, towards greater seismometer spacings.
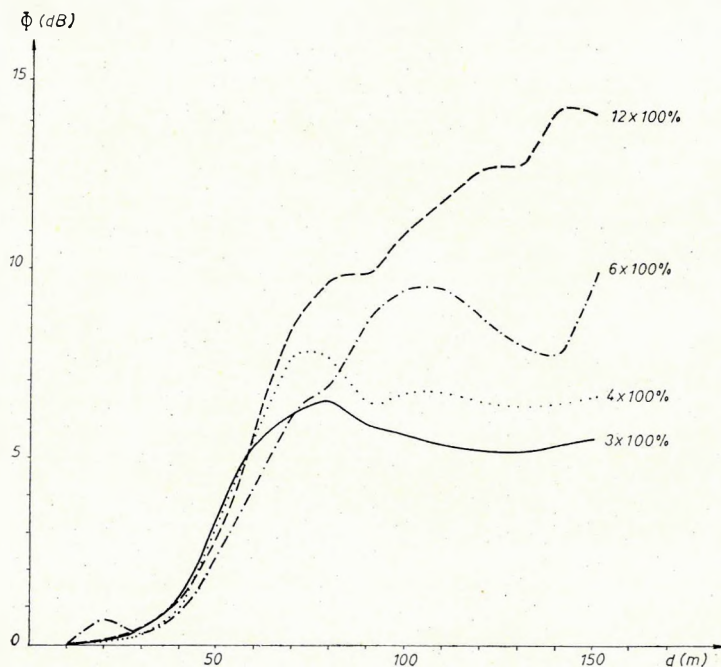
Fig. 1 Attenuating effect of a split-spread system upon multiple reflexions (in dB) as function of seismometer spacing, in 3-, 4-, 6- and 12-fold stacking

1. ábra. Középlövéses terítési rendszernek a többszörös reflexiókat csillapító hatása (dB-ben) a geofontávolság függvényében 3-, 4-, 6- és 12-szeres fedés mellett

Рис. 1. Зависимость степени подавления кратных отражений (в дб) от шага сейсмоприемников при 3-, 4-, 6- и 12-кратном перекрытии для установки с центральным положением ПВ
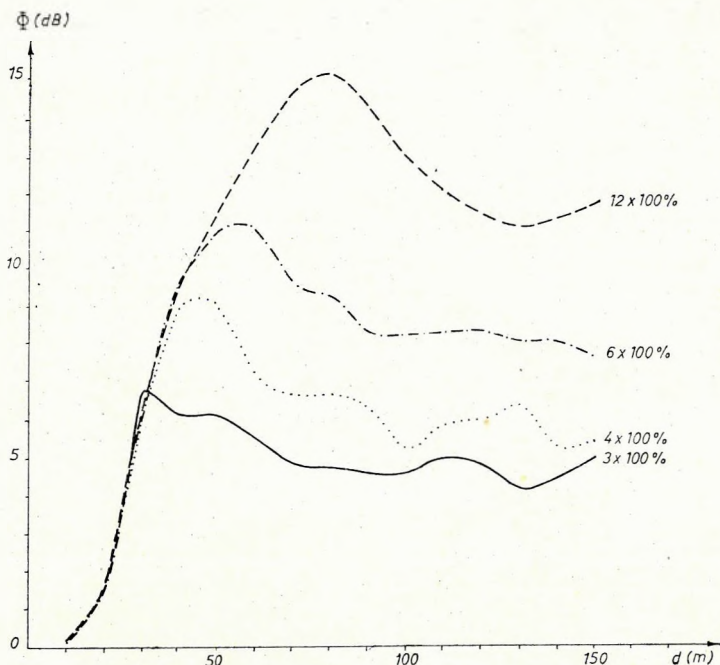
Fig. 2 Attenuating effect of an end-on spread system upon multiple reflexions (in dB) as function of seismometer spacing, in 3-, 4-, 6- and 12-fold stacking

2. ábra. Véglövéses terítési rendszernek a többszörös reflexiókat csillapító hatása (dB-ben) a geofontávolság függvényében 3-, 4-, 6- és 12-szeres fedés mellett

Рис. 2. Зависимость степени подавления кратных отражений (в дб) от шага сейсмоприемников при 3-, 4-, 6- и 12-кратном перекрытии с ПВ в конце установки

These results imply, that the suppression of multiples can be considerably improved by increasing the number of coverages, but only when other causes, first of all the noise level and energy conditions of the area do not prohibit a simultaneous increase in seismometer spacing. If short seismometer spacings lying in the cut-off range must be used, there will be no essential differences between the efficiencies of the different numbers of coverages. In such cases, the optimal number of coverages must be determined according to other aspects.

REFERENCE

Bodoky, T., 1970: A közös mélységpontos (CDP) rendszerek szűrőhatása és átviteli függvényeik. (The filtering effect of common-depth-point systems and their transfer functions; in Hungarian). Magyar Geofizika, XI. 6. pp. 209–218.
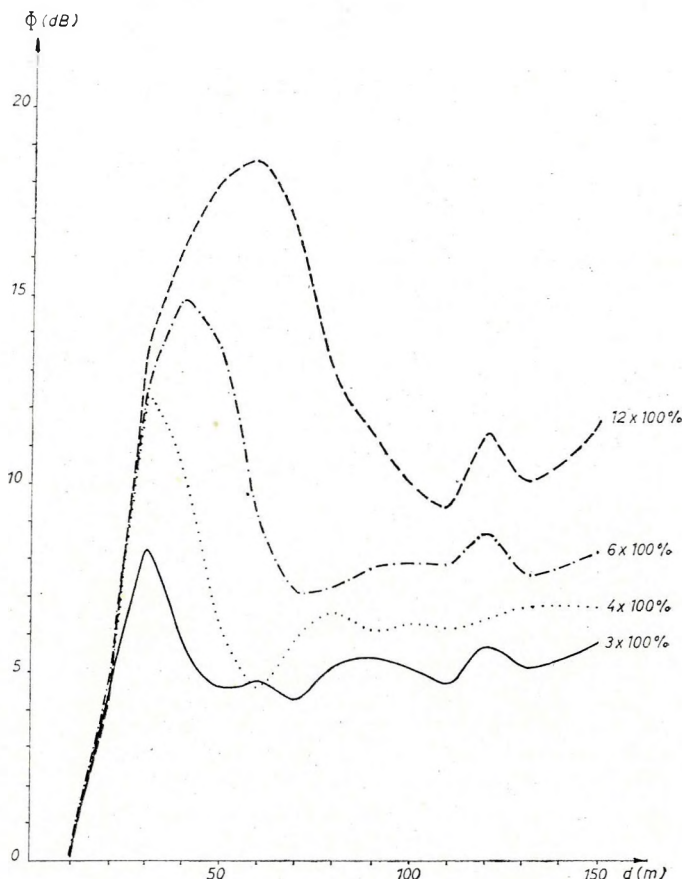
Fig. 3 Attenuating effect of a 12 seismometer-spacing offset-shotpoint system upon multiple reflexions (in dB) as function of seismometer spacing, in 3-, 4-, 6- and 12-fold stacking

3. ábra. 12 geofonköz offsettel kívülről lőtt rendszernek a többszörös reflexiókat csillapító hatása (dB-ben) a geofontávolság függvényében 3-, 4-, 6- és 12-szeres fedés mellett

Рис. 3. Зависимость степени подавления кратных отражений (в дб) от шага сейсмоприемников при 3-, 4-, 6- и 12-кратном перекрытии для системы наблюдений с ПВ, смещенным на расстояние, равное 12 шагам сейсмоприемников

A FEDÉSSZÁM ÉS A TÖBBSZÖRÖS REFLEXIÓK CSILLAPÍTÁSÁNAK KAPCSOLATA KÖZÖS MÉLYSÉGPONTOS ÖSSZEGEZÉSNÉL

BODOKY TAMÁS—POLCZ IVÁN

A többszörös fedésű közös mélységpontos rendszereknek a többszörös reflexiókat csillapító hatásával részletesen korábban foglalkoztunk (BODOKY, 1970). Az ott bemutatott számítási eljárás segítségével most megvizsgáljuk, hogy a fedésszámnak a többszörös reflexiók eltávolításában milyen szerepe van? Ennek ismeretében ugyanis konkrét esetekben el tudjuk dönteni, hogy a fedésszám növelésétől várható előnyök a mérési költségek növekedésével arányban állnak-e?

Az említett cikkben adott összegcsatorna típus, illetve terítési rendszer többszörös kioltási hatékonyságának jellemzésére a többszörös átengedett és teljes energiájának arányát használjuk. Ezt az arányt a következő összefüggés írja le:

$$\Phi(t_0, d) = \frac{\int\limits_0^\infty [A(\omega)S(\omega)]^2\, d\omega}{\int\limits_0^\infty [fA(\omega)]^2\, d\omega} \, ,$$

ahol Φ a csillapított és a csillapítatlan, többszörös energiaaránya,

t_0 a regisztrálási idő,

d a geofontávolság,

f a fedésszám,

ω a körfrekvencia,

$A(\omega)$ a többszörös reflexiók spektruma,

$S(\omega)$ az összegcsatorna átviteli függvénye; részletesebben

$$S(\omega) = \sum_{i=1}^{f} e^{j\omega\tau_i(t_0, x)} \, ,$$

ahol $\tau_i(t_0, x)$ az i-edik összegezendő csatorna maradék időkilépése,

x a geofon-robbantóponti távolság.

Számításainkhoz ezt az összefüggést használjuk fel.

Sebességfüggvényként és spektrumként az említett cikkben is használt nyírségi sebességfüggvényt és spektrumot alkalmazzuk. A számítások egyszerűsítése végett a Φ függvények meghatározását nem az egész $t_0 - d$ síkra végezzük el, hanem $t_0 - t$

2 sec értéknél rögzítjük. Ez információveszteséghez nem vezet, mert a függvények t_0-tól közelítőleg függetlenek. (BODOKY, 1970.).

Kiszámítottuk a Φ függvényeket d függvényében $t_0 = 2$ sec-ra, $f = 3$, $f = 4$, $f = 6$ és $f = 12$ fedésszám paraméterek mellett. A számításokat középlövéses rendszerre (1. ábra), véglövéses rendszerre (2. ábra) és egy 12 geofonköz offset-et alkalmazó külsőlövéses rendszerre (3. ábra) végeztük el. Az eredményül nyert Φ függvényeket dB-ben ábrázoltuk. Az egyes rendszerek Φ függvényén a rendre bennük szereplő összegcsatorna-típusok Φ függvényeinek számtani átlagát értjük.

Az ábrákat megvizsgálva megállapítható, hogy a levágás helye és meredeksége a fedésszámtól gyakorlatilag független; a fedésszám megkétszerezése a maximális csillapítást 3–6 dB-lel javítja, de az optimumzóna, a levágási meredekségnek megfelelően, a nagyobb geofontávolságok felé tolódik.

Eredményeinkből következően a többszörösök kioltása a fedésszám növelésével jelentékenyen javítható, de csak akkor, ha egyéb okok, elsősorban a terület zajnívója és energiaviszonyai nem akadályozzák meg, hogy egyúttal a geofontávolságot is növeljük. Ha mindenképpen a levágási szakaszra eső rövid geofontávolságokat kell használnunk, a különböző fedésszámok hatásossága közt lényeges különbség nincs. A fedésszámot ilyenkor más szempontok szerint kell meghatároznunk.

т. БОДОКИ—И. ПОЛЬЦ

СВЯЗЬ СТЕПЕНИ ПОДАВЛЕНИЯ КРАТНЫХ ОТРАЖЕНИЙ С КРАТНОСТЬЮ ПЕРЕКРЫТИЙ ПРИ СУММИРОВАНИИ ПО МЕТОДУ ОГТ

В работе рассматривается зависимость степени подавления кратных отражений при трех различных системах наблюдений от шага сейсмоприемников и кратности перекрытий.

Увеличение кратности перекрытий приводит к оптимальному повышению степени подавления кратных отражений только при одновременном увеличении шага сейсмоприемников.

THE EFFECT OF CHANGES IN WAVEFORM UPON CDP SUMMATION

T. BODOKY*

Essentially, stacking is a kind of filtering. It filters our random noises and, from among regular noises, multiple reflexions.

When using stacking for filtering out multiples, it is generally assumed that the waveform of multiples is entirely identical on the different channels. This, however, not always holds, not even as a rough approximation.

In the present paper, all the computations and notations are based on the velocity function and system of notations developed in the paper "Filtering effect of common-depth-point systems and their transfer functions" (BODOKY, 1970).

Computations were carried out for two types of stacking channels: a split-spread system (1,5, 2,5, 5,5, 6,5, 9,5, 10,5) and an offset-shotpoint system (12, 16, 20, 24, 28, 32). This special choice of stacking channels permits to obtain data, apart from the parameters investigated, about the role of the offset too.

In order to characterize the multiple transfer of various types of channels to be stacked, the function Φ is introduced. This is the ratio of transmitted, resp. total multiple energy:

$$\Phi(t_0, d) = \frac{\int_0^\infty [A(\omega)S(\omega, t_0, d)]^2 \, d\omega}{\int_0^\infty [fA(\omega)]^2 \, d\omega} \tag{1}$$

where t_0 = time of recording,
   d = seismometer spacing,
   ω = circular frequency,
   $A(\omega)$ = spectrum of the arrivals,
   $S(\omega, t_0, d)$ = the transfer function of stacking,
   f = number of coverages.

The detailed form of the transfer function is given by

$$S(\omega, t_0, d) = \sum_{i=1}^{f} c_i e^{j\omega\tau_i(t_0, d)} \tag{2}$$

where c_i = weight of the i-th channel,
   τ_i = residual moveout of the multiple reflexion arriving on the i-th channel.

In the computation of the Φ function the assumption on the identical form of the arrivals appears as their expression with identical weights and identical spectra. Thus, if we are investigating what kind of transfer variations could arise from the different forms of arrivals, the variations of the Φ functions due to deviations in spectra and in weights must be investigated.

Since the $\Phi(t_0, d)$ functions, in the paper mentioned, are approximately independent of t_0, i.e. the multiple-transfer of the stacked channel types discussed there is approximately time-independent it was sufficient to carry out the computations for a single t_0 value, say $t_0 = 2$ sec.

The first problem is that, if the weights of the channels are not assumed to be identical, the number of possible cases is infinite; namely an infinite number of weight series can be ordered to the channels to be stacked. The probability of occurrence of a certain weight series is so small that the knowledge of its transfer properties gives no practically usable information. Therefore a statistic approach was chosen and instead of dealing with individual weight series, statistical properties (expected value and standard deviation) of the Φ functions were investigated as function of the scattering of the weight series.

The expected value of channel weights is invariably assumed to be unity. This ensures, without restricting generality that the denominator on the right-hand side of Formula (1) remains unchanged. (Namely, the constant f in the denominator is the value of the transfer function $S(\omega)$ for $\tau_1 = \tau_2 = \ldots = \tau_f = 0$.)

If the weights c_i are treated as variables, Φ will be a function of $f + 1$ variables of the type $\Phi(d, c_1, \ldots, c_f)$. However, in order to get rid of the great number of independent variables, instead of variables $c_1, \ldots, c_f$, their scattering $\sigma(c)$ will be treated as a single independent variable,

$$\sigma^2(c) = \frac{1}{f} \sum_{i=1}^{f} (c_i - 1)^2.$$

Denoting the weight series by C_k (where index k refers to some given series), the scattering of the series will be denoted by $\sigma(C_k)$. The same $\sigma(C_k)$ scattering may correspond to many weight series C_k. Consequently, the expected value and standard deviation of the $\Phi[\sigma(C_k)]$ function of a given stacking channel type are for a fixed $\sigma(C_k)$ value and given values (t_0, d), as follows:

$$E\{\Phi(C_k)_{\sigma = \text{const}}\} = \frac{1}{n} \sum_{k=1}^{n} \Phi(C_k)_{\sigma = \text{const}} \tag{3}$$

and

$$\sigma^2\{\Phi(C_k)_{\sigma = \text{const}}\} = \frac{1}{n} \sum_{k=1}^{n} [\Phi(C_k)_{\sigma = \text{const}} - E\{\Phi(C_k)_{\sigma = \text{const}}\}]^2 \tag{4}$$

where n is the number of all such possible weight series, the scattering of which is exactly the constant chosen.

The course of the calculations was the following: first the value of Φ was calculated, according to relations (1) and (2), for six weight series of identical scattering for a given place (t_0, d), then the values of $E(\Phi)$ and $\sigma(\Phi)$ were determined from the

Φ values obtained, according to Formulae (3) and (4). The six weight series of identical scattering were selected from the permutations of an arbitrarily chosen series.

In Formulae (3) and (4), n represents the number of all appropriate weight series. In practical calculations, this theoretical requirement is not met, due to the number and way of generating of the weigth series used; therefore our results are only approximate.

The calculations were carried out with seven different values of weight scattering, in function of seismometer spacing $(d = 10$ m sampling interval, from 0 m to 150 m).

The $E\{\Phi[\sigma(c), d]\}$ function of the split-spread stacking channel type is shown in Fig. 1, its $\sigma\{\Phi[\sigma(c), d]\}$ function in Fig. 2. The same functions for the offset-shotpoint stacking channel type are shown in Figs. 3 and 4.
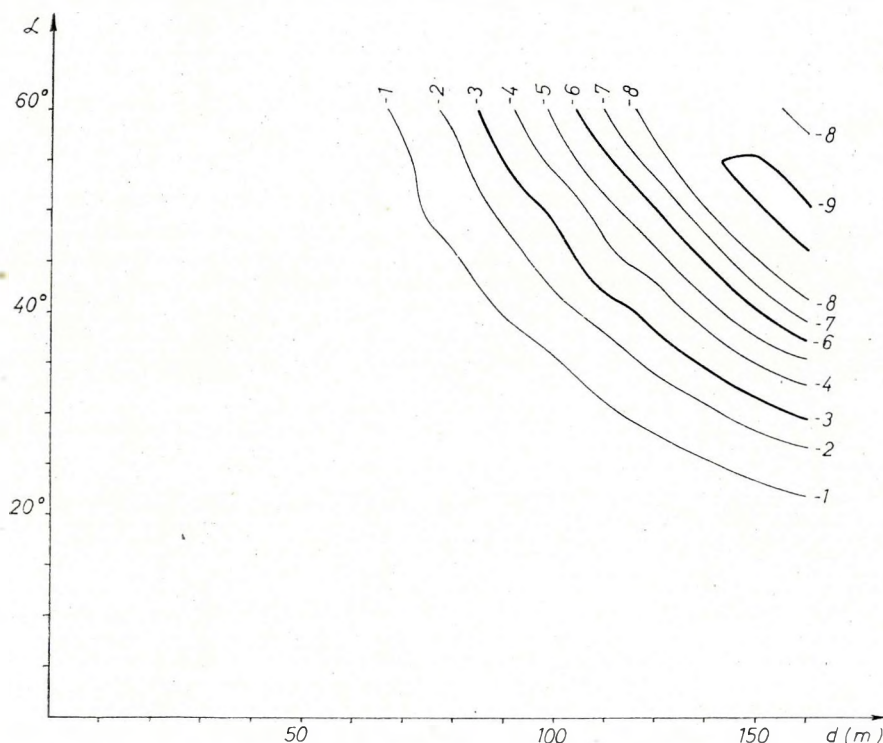
Fig. 1 The expected value (in dB) of the multiple-attenuation of the stacking channel type (1,5; 2,5; 5,5; 6,5; 9,5; 10,5) as a function of the scattering of channel weights [$\sigma(c)$] and of seismometer spacing (*d*)

1.ábra. Az (1,5; 2,5; 5,5; 6,5; 9,5; 10,5) összegcsatorna típus többszörös reflexió csillapításának várható értéke (dB-ben ábrázolva) a csatorna súlyok szórásának [$\sigma(c)$] és a geofontávolságnak (*d*) a függvényében

Рис. 1. Зависимость ожидаемой степени подавления кратных отражений (в дб) для суммотрассы типа (1,5; 2,5; 3,5; 6,5; 9,5; 10,5) от разброса весов каналов [$\sigma(c)$] и от шага сейсмоприемников (*d*)
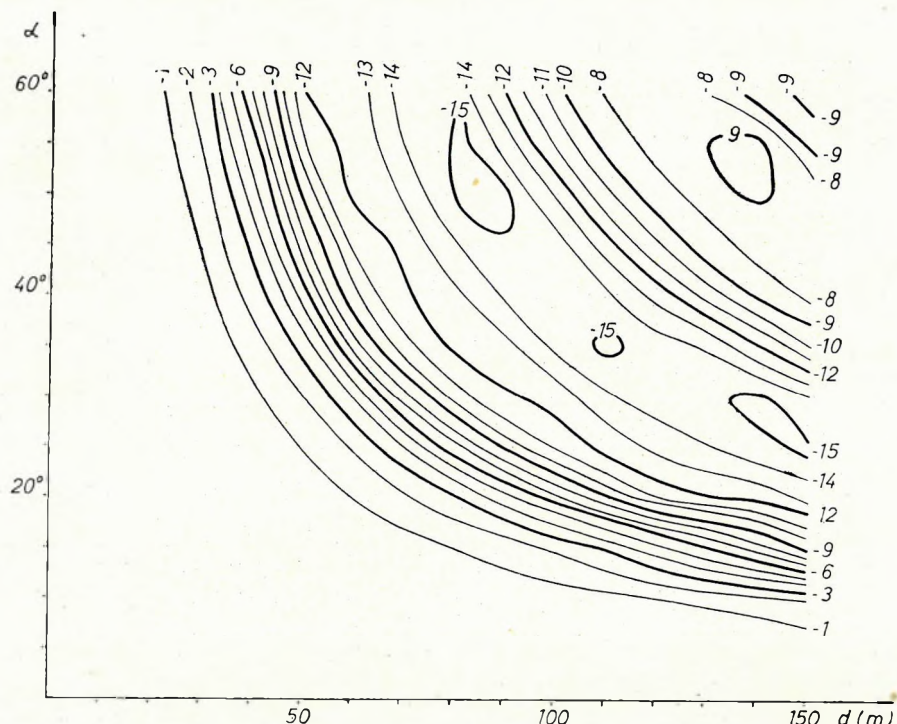
Fig. 2 The scattering of the multiple-attenuation of the stacking channel type
(1,5; 2,5; 5,5; 6,5; 9,5; 10,5) (in dB) as a function of the scattering of channel
weights [$\sigma(c)$] and of the seismometer spacing (*d*)

2. ábra. Az (1,5; 2,5; 5,5; 6,5; 9,5; 10,5) összegcsatorna típus többszörös reflexió
csillapításának szórása (dB-ben ábrázolva) a csatorna súlyok szórásának [$\sigma(c)$] és a
geofontávolságnak (*d*) a függvényében

Рис. 2. Зависимость разброса степени подавления кратных отражений (в дб) для сум-
мотрассы типа (1,5; 2,5; 5,5; 6,5; 9,5; 10,5) от разброса весов каналов [$\sigma(c)$] и от шага
сейсмоприемников (*d*)

The investigations concerning weight scattering were carried out also for the
scattering of the spectra of multiples to be stacked.

Under expected value and scattering of spectra, the expected value and scat-
tering of the peak-frequency a_{max} of the spectra will be understood. For simplicity's
and unambiguity's sake it was agreed upon that the spectra can be of a Ricker-
wavelet spectrum form only. This type of spectrum is described by

$$A(\omega) = \frac{\omega^p}{p} e^{\frac{1}{2} \left(\frac{\omega}{p}\right)^2} \tag{5}$$

where $p = \pi a_{max}$.

In order to make a comparison with the results of the paper used as initial
material possible, the value of $E(a_{max})$ was chosen for 30 cps.

Fig. 3 The expected value of the multiple-attenuation of the stacking channel type (12, 16, 20, 24, 28, 32) (in dB) as a function of the scattering of channel weights [$\sigma(c)$] and of the seismometer spacing (d)

3. ábra. A (12; 16; 20; 24; 28; 32) összegcsatorna típus többszörös reflexió csillapításának várható értéke (dB-ben ábrázolva) a csatorna súlyok szórásának [$\sigma(c)$] és a geofontávolságnak (d) a függvényében

Рис. 3. Зависимость ожидаемой степени подавления кратных отражений (в дб) для суммо-трассы типа (12, 16, 20, 24, 28, 32) от разброса весов каналов [$\sigma(c)$] и от шага сейсмоприемников (d)

Starting out again from Formula (1), $A(\omega)$ occurs both in the numerator and denominator of the right-hand side. As previously, instead of $A(\omega)$, $E\{A(\omega)\}$ will be written in the denominator. In the numerator, the product $[A(\omega)S(\omega)]$ can be written, after some rearrangements:

$$[S(\omega)A(\omega)] = \left(\sum_{i=1}^{I} e^{j\omega\tau_i} \right) A(\omega) e^{j\omega\tau_i}.$$

(The weights c_i are taken as of unit value).
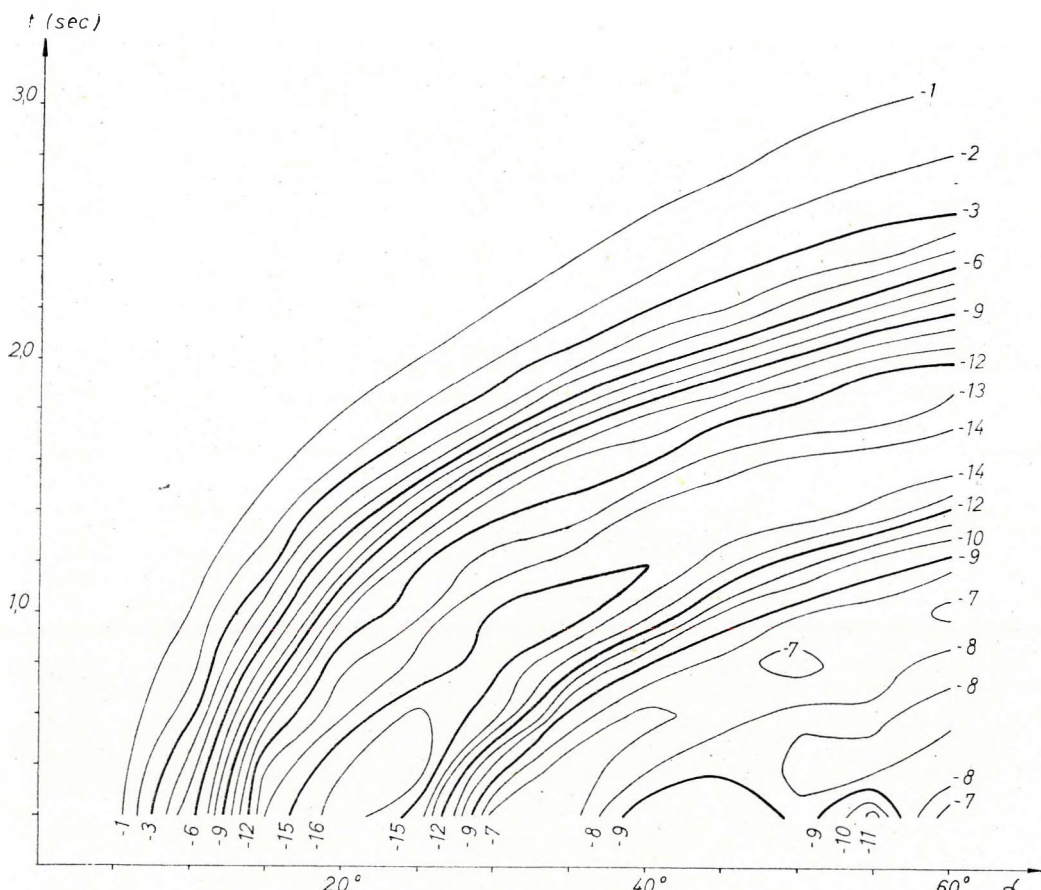
Fig. 4 The scattering of the multiple-attenuation of the stacking channel type (12, 16, 20, 24, 28, 32) (in dB) as a function of the scattering of channel weights [σ(c)] and of seismometer spacing (d)

4. ábra. A (12; 16; 20; 24; 28; 32) összegcsatorna típus többszörös reflexió csillapításának szórása (dB-ben ábrázolva) a csatorna súlyok szórásának [σ(c)] és a geofontávolságnak (d) a függvényében

Рис. 4. Зависимость разброса степени подавления кратных отражений (в дб) для суммотрассы типа (12, 16, 20, 24, 28, 32) от разброса веса каналов [σ(c)] и от шага сейсмоприемников (d)

Since it is assumed now that the arrivals have different spectra, also these spectra must be indexed. Thus, the right-hand side of (1) will be

$$\frac{\int_0^\infty \left[\sum_{i=1}^{f} A_i(\omega) e^{j\omega\tau_i} \right]^2 d\omega}{\int_0^\infty [f E\{A_i(\omega)\}]^2 d\omega}.$$

Accordingly, Φ will be, on a given place (t_0, d) a function of the form $\Phi[A_1(\omega),$ $A_2(\omega), \ldots, A_f(\omega)]$. Let also here possible spectrum series $A_1(\omega), A_2(\omega), \ldots, A_f(\omega)$ denoted by A_k, and their scattering by $\sigma(A_k)$. The same scattering can belong to an infinite number of spectrum series A_k, therefore the functions

$$E\{\Phi(A_k)_{\sigma=\text{const}}\} = \frac{1}{n} \sum_{k=1}^{n} \Phi(A_k)_{\sigma=\text{const}} \tag{6}$$

and

$$\sigma^2\{\Phi(A_k)_{\sigma=\text{const}}\} = \frac{1}{n} \sum_{k=1}^{n} [\Phi(A_k)_{\sigma=\text{const}} - E\{\Phi(A_k)_{\sigma=\text{const}}\}]^2 \tag{7}$$

can be calculated, at a given place (t_0, d) for a given type of channels to be stacked.

The calculations and generating spectrum series of identical scattering take place in the same way as in the case of weight series.

As the result of calculations, the $E\{\Phi[\sigma(A), d]\}$ function calculated for the split-spread stacking channel type is shown by Fig. 5. — the $\sigma\{\Phi[\sigma(A), d]\}$ function
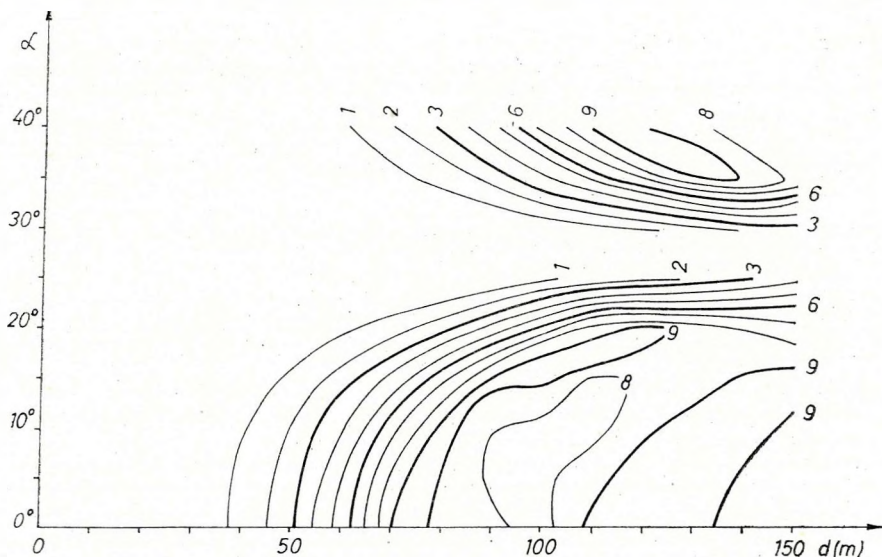

Fig. 5 The expected value of the multiple-attenuation of the stacking channel type (1,5; 2,5; 5,5; 6,5; 9,5; 10,5) (in dB) as a function of the scattering of channel spectra $[\sigma(a_{\text{max}})]$ and of seismometer spacing (d)

5. ábra. Az (1,5; 2,5; 5,5; 6,5; 9,5; 10,5) összegcsatorna típus többszörös reflexió csillapításának várható értéke (dB-ben ábrázolva) a csatorna spektrumok szórásának $[\sigma(a_{\text{max}})]$ és a geofontávolságnak (d) a függvényében

Рис. 5. Зависимость ожидаемой степени подавления кратных отражений (в дб) для суммотрассы типа (1,5; 2,5; 5,5; 6,5; 9,5; 10,5) от разброса спектров каналов $[\sigma(a_{\text{max}})]$ и от шага сейсмоприемников (d)
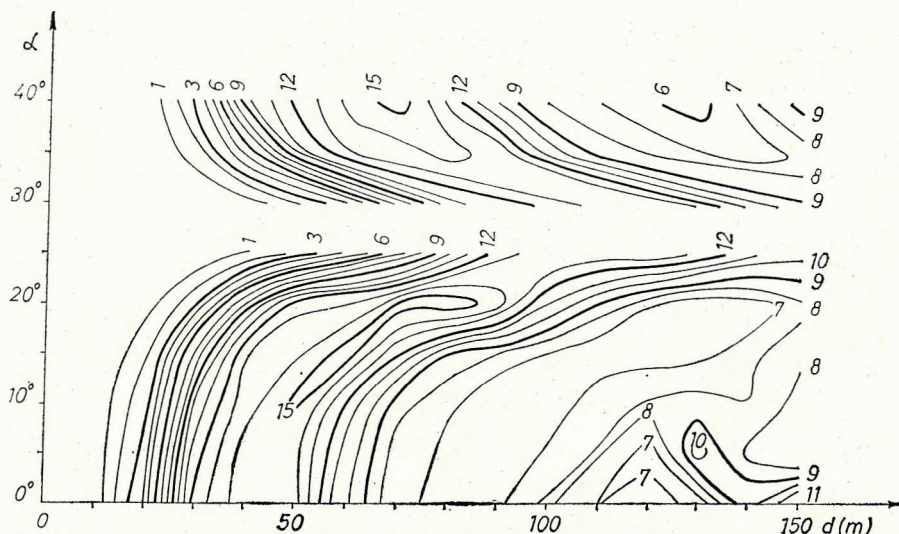
Fig. 6 The scattering of the multiple-attenuation of the stacking channel type
(1,5; 2,5; 5,5; 6,5; 9,5; 10,5) as a function of the scattering of channel spectra
$[\sigma(a_{max})]$ and of seismometer spacing (d)

6. ábra. Az (1,5; 2,5; 5,5; 6,5; 9,5; 10,5) összegcsatorna típus többszörös reflexió
csillapításának szórása (dB-ben ábrázolva) a csatorna spektrumok szórásának
$[\sigma(a_{max})]$ és a geofontávolságnak (d) a függvényében

Рис. 6. Зависимость разброса степени подавления кратных отражений (в дб) для сум-
мотрассы типа (1,5; 2,5; 5,5; 6,5; 9,5; 10,5) от разброса спектров каналов $[\sigma(a_{max})]$ и от
шага сейсмоприемников (d)

by Fig. 6. The same functions calculated for the offset-shotpoint spread system
are illustrated by Figs. 7 and 8.

Examining the resulting eight figures, following conclusions can be drawn;

— The expected value of multiple-attenuating of stacked channels decrease
slowly, practically insignificantly in case of an increasing scattering of the
weights, resp. spectra of the channels, the place of maximum extinction
being, however, independent of these quantities.

— The scattering of the multiple-attenuation of stacked channels is practically
insignificant, slightly growing with increasing scattering of weights, resp.
spectra of the arrivals to be stacked.

All in all, the multiple-attenuating effect of stacking is practically insensible
even against comparatively coarse form-variations of multiple reflexions.
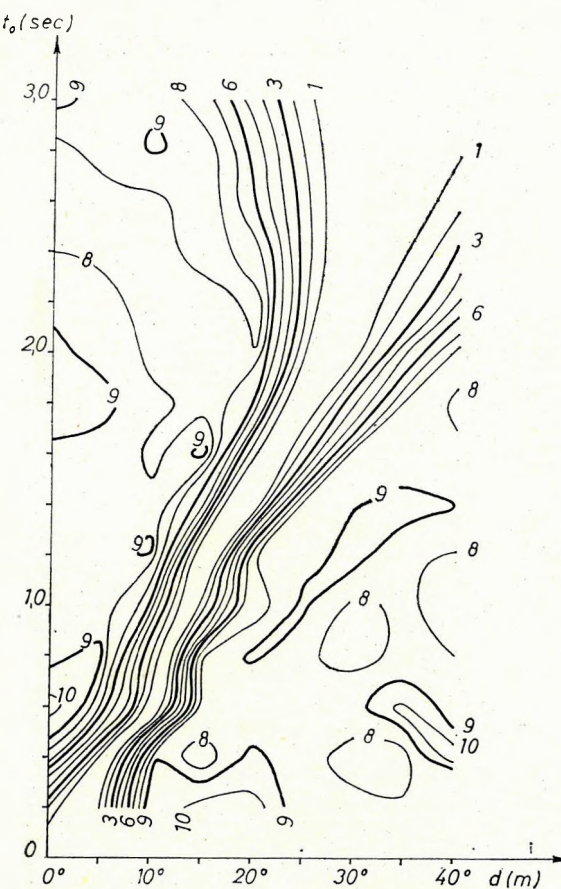
Fig. 7 The expected value of the multiple-
attenuation of the stacking channel type
(12, 16, 20, 24, 28, 32) (in dB) as a function
of the scattering of channel spectra $[\sigma(a_{max})]$
and of seismometer spacing (d)

7. ábra. A (12; 16; 20; 24; 28; 32) összeg-
csatorna típus többszörös reflexió csillapítá-
sának várható értéke (dB-ben ábrázolva)
a csatorna spektrumok szórásának $[\sigma(a_{max})]$
és a geofontávolságnak (d) a függvényében

Рис. 7. Зависимость ожидаемой величины по-
давления кратных отражений (в дб) для сум-
мотрассы типа (12, 16, 20, 24, 28, 32) от разб-
роса спектров каналов $[\sigma(a_{max})]$ и от шага
сейсмоприемников (d)
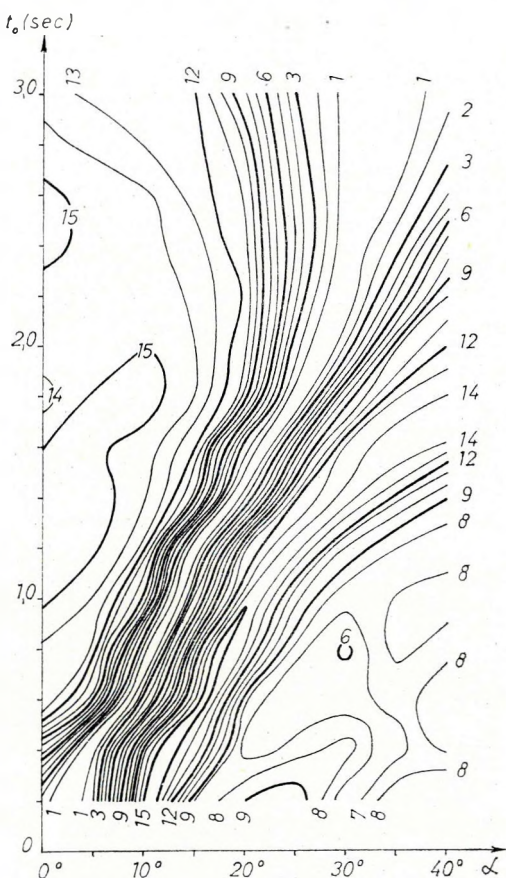
Fig. 8 The scattering of the multiple-attenu-
ation of the stacking channel type (12; 16;
20; 24; 28; 32) (in dB) as a function of the
scattering of channel spectra $[\sigma(a_{max})]$ and
of seismometer spacing (d)

8. ábra. A (12; 16; 20; 24; 28; 32) összeg-
csatorna típus többszörös reflexió csillapítá-
sának szórása (dB-ben ábrázolva) a csatorna
spektrumok szórásának $[\sigma(a_{max})]$ és a geo-
fontávolságnak (d) a függvényében

Рис. 8. Зависимость разброса степени подав-
ления кратных отражений (в дб) для суммо-
трассы типа (12, 16, 20, 24, 28, 32) от разброса
спектров каналов $[\sigma(a_{max})]$ и от шага сейсмо-
приемников (d)

REFERENCES

Bodoky, T., 1970: A közös mélységpontos (CDP) rendszerek szűrőhatása és átviteli függvényeik. (The filtering effect of common-depth-point (CDP) systems and their transfer functions; in Hungarian), Magyar Geofizika, Vol. XI, No. 6.

Ricker, N., 1953: The form and laws of propagation of seismic wavelets. Geophysics Vol. 18, No. 1.

BODOKY TAMÁS

A BEÉRKEZÉSEK ALAKVÁLTOZÁSAINAK HATÁSA
A KÖZÖS MÉLYSÉGPONTOS ÖSSZEGEZÉSNÉL

A tanulmányban a szerző kiszámítja — a számításokat két összegcsatorna típusra végezte el — a közös mélységpontos összegezés többszörös csillapításának várható értékét és szórását az összegezendő többszörös beérkezések amplitúdószórásának függvényében. Ugyanezt a vizsgálatot a többszörös beérkezések csúcsfrekvencia-szórásának függvényében is elvégzi, a spektrumokat Ricker-féle wavelet spektrum alakúnak tételezve fel.

A számítások eredményeként a következő megállapításokat teszi:

1. az összegcsatornák többszörös csillapításának várható értéke lassan, gyakorlati szempontból jelentéktelen mértékben csökken a csatornák súlyainak, illetve spektrumainak növekvő szórásainál; a maximális kioltás helye azonban független ezen mennyiségektől.

2. Az összegcsatornák többszörös csillapításának szórása az összegezendő beérkezések súlyainak, illetve spektrumainak növekvő szórásánál gyakorlati szempontból csak enyhén növekszik.

т. БОДОКИ

ВЛИЯНИЕ ИЗМЕНЕНИЙ ФОРМЫ ЗАПИСАННЫХ КОЛЕБАНИЙ
ПРИ СУММИРОВАНИИ ПО МЕТОДУ ОГТ

В работе вычисляются ожидаемые степень и разброс подавления кратных отражений при суммировании по методу ОГТ для двух типов суммотрасс в зависимости от разброса амплитуд суммируемых кратных отражений. Подобный анализ проводится и в зависимости от разброса максимальной частоты кратных отражений, причем предполагается, что спектры имеют форму спектров волн Рикера.

В результате проведенных вычислений делаются следующие выводы:

1. Ожидаемая степень подавления кратных отражений на суммотрассах снижается медленно, в практически незначительной мере с увеличением разброса весов и спектров каналов. Однако, место максимального подавления кратных волн не зависит от этих величин.

2. Разброс степени подавления кратных отражений на суммотрассах увеличивается в практически незначительной мере с увеличением разброса весов и спектров суммируемых волн.

AN ANALYSIS OF THE PROPAGATION OF SOUND WAVES IN POROUS MEDIA BY MEANS OF THE MONTE CARLO METHOD

G. KORVIN–I. LUX*

Introduction

In the last two decades an abundant literature has been published on the determination of sound velocity in porous media. The problem has been tackled both from theoretical and experimental side. The discrepancies which appear between theoretical considerations are mainly due to the difference in the number of parameters and the assumptions about the physical mechanism involved. As for experimental findings, their range of validity and accuracy depend on the experimental conditions and techniques. Extensive investigations have been reported on sound velocity measurements in marine sediments (SHUMWAY 1960, NAFE and DRAKE 1957). Among the empirical formulae proposed the most simple is that of WYLLIE–GREGORY–GARDNER (WYLLIE et al., 1956) which has found wide-spread application in applied geophysics. According to this formula:

$$\frac{1}{V_{av}} = \frac{\Phi}{V_{fl}} + \frac{1-\Phi}{V_{sol}},$$

where V_{av} is average sound velocity in the porous medium, V_{fl} and V_{sol} are velocities in the fluid and solid phase, respectively, and Φ denotes porosity. The physical meaning of this formula is that acoustic waves spend Φ per cent of the whole travel time in fluid, i.e. the waves propagate along a straight line in a porous medium. This assumption however, fails to take into account the basic principle of wave propagation, viz. that a wave always choose the path of the shortest travel-time between two given points (Fermat's principle), which is, in our case, not necessarily a straight line.

The aim of the present paper is to try to find a modification of Wyllie's formula which would obey Fermat's principle. The hypothesis that Fermat's principle be applicable for waves with wave length larger than the characteristic size of the inhomogeneities of the medium had been already put forward by WYLLIE et al. (1958).

The method

The problem was analysed in a two-dimensional approximation with a Monte Carlo simulation method. Random models of porous media, of a given area and predetermined porosity, were generated by computer and the path requiring the shortest time was searched by means of Ford's algorithm (cf. e.g. KAUFMAN, 1968). For a given velocity ratio 8 different porosity values were taken and for each porosity 50 models were computed. After this an explicit functional relationship best describing the experimental results has been established.

A straightforward approximation of porous media can be obtained if one considers a hexagonal lattice where each single hexagon is randomly filled with solid or fluid phase. In this model the wave can "move" from the centre of a hexagon to the centre of some neighbouring one and so, if a starting and a terminal point are given, the average velocity can be obtained by dividing the distance of these points by the time required to pass along the shortest broken line connecting them. A serious drawback of this method is that it allows the waves to propagate only in six directions (while, in reality, no such restriction exists).
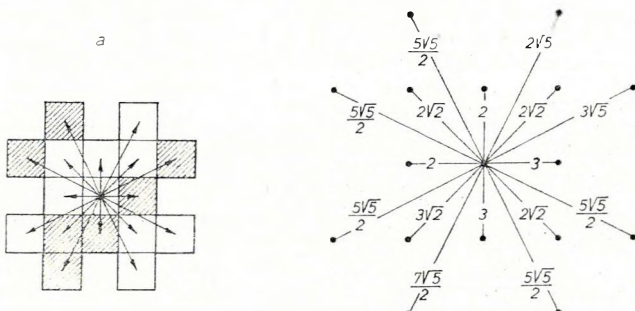
Fig. 1 a — a square and its "neighbours"; b — a portion of the graph corresponding to a (fictitious time scale, $\nu = 1/2$)

1. ábra. a — egy négyzet „szomszédai"; b — az a-nak megfelelő gráf részlete (fiktív időskála, $\nu = 1/2$)

Рис. 1. a) квадрат с «соседами»; δ) часть графа, соответствующего квадрату на рис. а (фиктивная шкала времени — $\nu = 1/2$)

In the present investigations we have adopted the more realistic square lattice approximation, where from each element the wave can continue its path in 16 directions (see Fig. 1a). Since the wave is imagined as propagating from centre to centre, it is enough to represent squares by their centres. Let us connect each centre by the 16 adjacent ones (i.e. with those points where the wave can "move in one step"). So, we obtain a configuration — a so-called graph — consisting of points and lines. Points are called vertices and the lines connecting them edges in the usual terminology of the theory of graphs. We attach to each edge the transit time necessary for the wave to make the distance between the points, and this value will be called the length of the edge. A portion of the graph corresponding to Fig. 1a is shown in Fig. 1b.

In order to construct porous media we generated uniformly distributed random numbers between 0 and 1 and the individual squares of the lattice were filled with fluid or solid phase according to whether the generated number had been less or greater than the porosity given. The generation of random numbers was performed with the method described by ADAMS and DENMAN (1966).

Each model consisted of 15×30 squares; for starting and terminal points of the path the two end-points of the longer axis of symmetry were taken (Fig. 2).

All computations reported in this paper were performed on the MINSK-32 computer of the ELGI.

Theoretical considerations

Let us denote the quotient $\dfrac{V_{fl}}{V_{sol}}$ by v and be

$$v_a = \frac{V_{fl}}{V_{av}} = G(v, \Phi).$$

We shall be concerned in this paper in the determination of the explicite form of the function $G(v, \Phi)$. It will be required that function $G(v, \Phi)$ should satisfy the following conditions:

1. $G(v, 0) = v$ — when no fluid-phase is present, $v_a = v$ i.e. $V_{av} = V_{sol}$

2. $G(v, 1) = 1$ — in the absence of solid medium $v_a = 1$, i.e. $V_{av} = V_{fl}$

3. $G(1, \Phi) = 1$ — i.e. if $V_{sol} = V_{fl}$ then $V_{av} = V_{sol} = V_{fl}$

4. $v \le G \le 1$ — i.e. the average velocity lies between the velocities of the two phases.

Fig. 2 A model with the corresponding shortest path ($\Phi = 0,3$)

2. *ábra.* Egy modell és a hozzá tartozó legrövidebb út ($\Phi = 0,3$)

Рис. 2. Модель с соответствующим кратчайшим путем ($\Phi = 0,3$)

It must be noted that inequality 4 is violated for large ($\Phi \ge 60\%$) porosities. In this case, namely, the sound velocity in the fluid-saturated medium may be less than in the fluid (HAMILTON 1956, SHUMWAY 1960, OFFICER 1958). Our results, therefore, will only apply for porosities less than 60 per cent but, of course, this covers the range most frequently encountered in geophysical practice.

An inherent approximation of the model is that material properties i.e. density, compressibility etc. of the individual phases are not taken into account.

The function $G(v, \Phi)$ will be sought for in the following form:

$$G(v, \Phi) = \frac{F(v, \Phi)\Phi + v(1 - \Phi)}{F(v, \Phi)\Phi + (1 - \Phi)},$$

where $F(v, \Phi)$ is some, for the time being unspecified, function. This functional form automatically satisfies conditions 1–4. For the special choice $F(v, \Phi) \equiv 1$ we receive back Wyllie's formula, since in this case

$$G(v, \Phi) = \frac{V_{fl}}{V_{av}} = \frac{\Phi + v(1 - \Phi)}{\Phi + 1 - \Phi} = \Phi + \frac{V_{fl}}{V_{sol}}(1 - \Phi),$$

$$\text{i.e. } \frac{1}{V_{av}} = \frac{\Phi}{V_{fl}} + \frac{1 - \Phi}{V_{sol}}.$$
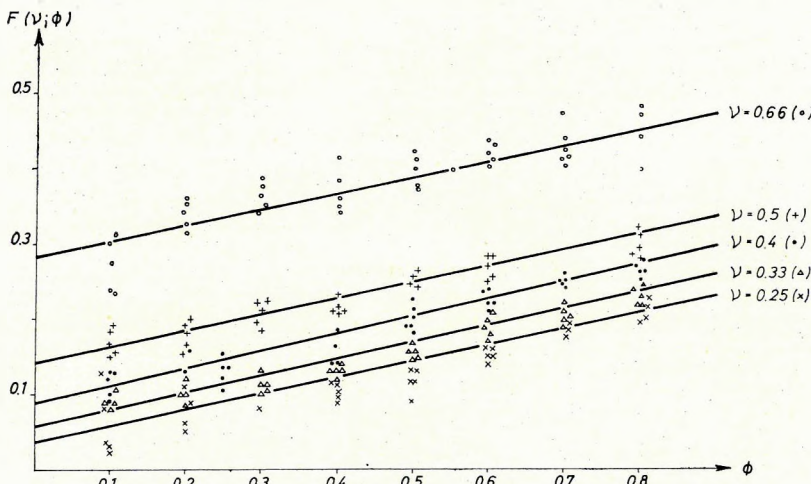
Fig. 3 Experimental values of function $F(v, \Phi)$ with the fitting straight lines. Each points plotted is the average of ten experiments

3. ábra. Az $F(v, \Phi)$ függvény értékei az illeszkedő egyenesekkel. Minden feltüntetett pont tíz kísérlet átlaga

Рис. 3. Величины функции $F(v, \Phi)$ с соответствующими прямыми. Каждая точка представляет собой среднюю величину результатов 10 вычислений

Results

The experiments were performed with $\nu = 0,66$; $0,5$; $0,4$; $0,33$; $0,25$, for each velocity ratio the porosity changed from $0,1$ to $0,8$ in $0,1$ steps. For any single pair (ν, Φ) 50 different models were generated.

The calculated values of the function $F(\nu, \Phi)$ are plotted in Fig. 3, where each point represents the average of 10 models. The values obtained are, for a given ν, in a linear relationship with porosity, i.e.

$$F(\nu, \Phi) \approx a(\nu) \cdot \Phi + b(\nu).$$

Fitting was performed according to the least mean square criterion. The slopes $a(\nu)$ and constant terms $b(\nu)$ figuring in the equation of the straight lines are shown in Fig. 4a and 4b, respectively. The slope of the straight lines is approximately constant

$$a(\nu) \approx 0,22$$

while the term $b(\nu)$ appears to have an exponential form:

$$b(\nu) \approx B(e^{\lambda \nu} - 1).$$

It is, of course, possible, that the constant $0,22$ and the parameters of the above exponential form of function $b(\nu)$ are not of universal validity but they are in connection with the special symmetries and size of the applied lattice model
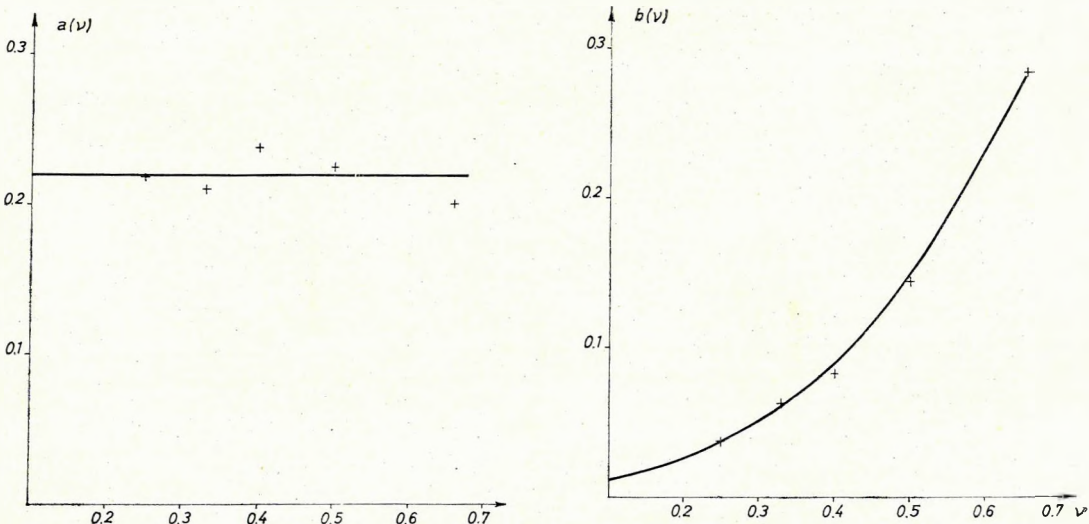
Fig. 4 a—the slope of the straight line $F(\nu, \Phi)$; *b*—the constant term of the straight line $F(\nu, \Phi)$

4. ábra. a — az $F(\nu, \Phi)$ egyenes iránytangense; *b* — az $F(\nu, \Phi)$ egyenes tengelymetszete

Рис. 4. a) Угловой коэффициент прямой $F(\nu, \Phi)$; *д)* Осевое сечение прямой $F(\nu, \Phi)$

Further possibilities of the method

In the computations reported, the effect of reflections and attenuation was not taken into account. Consequently, in actual measurements the arrival time of the first (recorded) pulse would not necessarily agree with the computed value, it will be greater. It was also neglected that the initial wave-form is not a spike and its shape can change during propagation due to the above-mentioned factors. The method of finding the shortest path can be improved so that it should yield the incident energy as well, by decreasing the energy at each phase-boundary according to the reflection coefficient and taking geometrical scattering into account. This version of the method may be useful for a Monte Carlo investigation of the occurrence of phase-skippings in sonic logging.

A further possibility is to extend the model to three dimensions. The method can be also adapted to the case of a medium consisting of many components, where the validity of the time-average equation is also taken for granted (TEGLAND, 1970). By an appropriate modification of the Monte Carlo method, in the generation of porous media, besides porosity, also the grain size distribution can be taken into account.

Summary

We have been concerned with the determination of the average velocity of sound waves propagating in porous media. Two-dimensional random models of porous media were generated by computer and the shortest path of acoustic waves between two given points was determined by means of Ford's algorithm. As a result of our experiments we obtained the following formula:

$$\frac{1}{V_{av}} = \frac{\dfrac{0,22}{V_{fl}}\,\varPhi + \dfrac{1-\varPhi}{V_{sol}} + \dfrac{b\left(\dfrac{V_{fl}}{V_{sot}}\right)}{V_{fl}}}{1 - 0,78\,\varPhi + b\left(\dfrac{V_{fl}}{V_{sol}}\right)}$$

where V_{av} = average velocity in the porous medium,

V_{fl} = velocity in the fluid phase,

V_{sol} = velocity in the solid phase,

$b\left(\dfrac{V_{fl}}{V_{sol}}\right)$ = is the exponential function illustrated in Figure 4b.

*

Appendix: Ford's algorithm for finding the shortest path of a graph

Suppose that we are given a connected graph*, to each edge of which there corresponds some positive distance value. Let the distance of disconnected vertices be $+\infty$. Let us denote the starting point of the path by x_0, its terminal point by S, and let the other vertices be, in an arbitrary order, $x_1, x_2, x_3, \ldots, x_k$.

We are going to attach a so-called potential value to each vertex, i.e. some value $\mu(x_i)$ to vertex x_i. The potential will be initially zero, while at the end of the algorithm it will be equal to the minimum distance from x_0 of the vertices in question.

In each step of the algorithm the graph will be split into two parts, let the subgraphs be denoted by A and B, respectively. Subgraph A will consist of those vertices whose minimum distance from X_0 had been already determined, and B of those for which this had not been done, i.e. whose potentials are not yet equal to the minimum distance. In the first step**

$$x_0 \in A \; ; \; \{x_1, x_2, x_3, \ldots, x_k, S\} \in B.$$

In course of the procedure subgraph A will be extended by elements from B until S itself is included in A. The extension of A with one more vertex is done as follows: let, in general,

$$x_a, x_b, \ldots, x_n \ldots \in A,$$
$$x_\alpha, x_\beta, \ldots, x_\nu \ldots \in B$$

and denote the distance of vetices $x_n \, x_v$ by τ_{nv}. Let us form now the value

$$\varepsilon_{nv} = \mu(x_n) + \tau_{nv}$$

for each pair of vetices $x_n \in A$, $x_v \in B$ and seek the value

$$E_{m\mu} = \min_{n, v} \varepsilon_{nv}.$$

The corresponding vertex x_μ will be inserted into subgraph A and its potential will be ε_{mu}. We have to show that the potential of any vertex in A will give the length of the shortest path connecting the given vertex with x_0.

Let the number of vertices belonging to A be l. If $l = 1$, then $A = \{x_0\}$ and $\mu(x_0) = 0$ for which the statement holds. Assume now, that

$$A = \{x_0, x_1, x_2, \ldots, x_{l-1}\}$$

and suppose the validity of the statement for these vertices. We proceed to show that the potential of the point x_μ which results according to the rules of the algorithm will also equal the length of the minimal path. Indeed,

$$\mu(x_u) = \mu(x_m) + \tau_{m\mu} = \min_{n, v} \left(\mu(x_n) + \tau_{nv}\right) \quad x_n \in A, \; x_v \in B.$$

---

* As to the basic principles and terminology of graph theory we refer to the monographs of KAUFMAN (1968) or BERGE (1957).
** The notation $x \in A$, frequently used in set-theory, means that x belongs to set A.

Since, by the induction hypothesis $\mu(x_n)$ is the length of the shortest path from x_0 to x_n, $\mu(x_n) + \tau_{nv}$ will be the length of some path from x_v through x_n to x_0. The value

$$\min_v \left(\mu(x_n) + \tau_{nv} \right)$$

is the length of a path which starts from a vertex in B, goes through x_n and terminates in x_0. Taking now the minimum in n we obtain the distance from x_0 to the nearest point in B, which was to be proved. The algorithm is finished as soon as vertex S gets incorporated to A.

There remains the problem how to determine the path itself. Let us choose vertex x_i for which

$$\mu(S) - \mu(x_i) = \tau_{Sx_i}$$

(it is possible, of course, that more than one such vertices exist which means that there are many, equally optimal paths), then x_i will precede S in the shortest path; we repeat then this procedure for x_i instead of S and obtain the next vertex etc., until x_0 will be reached.

REFERENCES

ADAMS, R. N.–DENMAN, E. D., 1966: Wave propagation and turbulent media. American Elsevier Publ. Co. New York, pp. 50–51.

BERGE, C., 1957: Théorie des graphes et ses applications. Dunod, Paris.

HAMILTON, E. L., 1956: Low sound velocities in high-porosity sediments. Journal of Acoustical Soc. Am. XXVIII. No. 1. p. 16.

KAUFMANN, A., 1968: Az operációkutatás módszerei és modelljei. Műszaki Könyvkiadó, Budapest. (Hungarian translation of the original: Méthods et modèles de la recherche operationelle, Dunod, Paris).

NAFE, J. E.–DRAKE, C. L., 1957: Variation with depth in shallow and deep water marine sediments of porosity, density and the velocities of compressional and shear waves. Geophysics, XXII. No. 3. pp. 523–552.

OFFICER, C. B., 1958: Introduction to the theory of sound transmission (with application to the ocean). McGraw–Hill, New York–Toronto–London, pp. 257–260.

SHUMWAY, G., 1960: Sound speed and absorption studies of marine sediments by a resonance method. I., II. Geophysics, XXV. No. 2. pp. 451–467, No. 3. pp. 659–682.

TEGLAND, E. R., 1970: Sand-shale ratio determination from seismic interval velocity. 23-rd Annual meeting of SEG and AAPG, Dallas, March 8–10, 1970.

WYLLIE, M. R. J.–GREGORY, A. R.–GARDNER, L. W., 1956: Elastic wave velocities in heterogeneous and porous media. Geophysics, XXI. No. 1, pp. 41–70.

WYLLIE, M. R. J.–GREGORY, A. R.–GARDNER, G. K. F., 1958: An experimental investigation of factors affecting elastic wave velocities in porous media. Geophysics, XXIII, No. 4. pp. 459–493 (480–484).

HANGHULLÁMOK TERJEDÉSÉNEK VIZSGÁLATA PORÓZUS KÖZEGBEN MONTE CARLO MÓDSZERREL

KORVIN GÁBOR – LUX IVÁN

A dolgozatban a porózus közegben terjedö akusztikus hullám átlagsebességének a porozitástól való függését vizsgáltuk. Feltételeztük, hogy a hullámhossznál jóval kisebb inhomogenitások esetére is alkalmazható Fermat-elve, vagyis a hullám a porózus közeg két pontja között mindig a legrövidebb idöt követelö utat választja.

A porózus közeg egy adott részét négyzetráccsal közelítettük, amelyet Monte Carlo módszerrel véletlen módon töltöttünk ki — a porozitásnak megfelelöen — folyadék, ill.

szilárd fázissal. A kapott modellben azután az operációkutatásból ismert Ford-algoritmussal határoztuk meg a legrövidebb utat. A két fázis sebességarányának 0,66; 0,5; 0,4; 0,33; 0,25 értékeire számítottunk modelleket a $\Phi = 0,1$; $0,2$; ...; 0,8 porozitásértékekre. Minden sebességarányra és porozitásértékre 50 — 50 modellt generáltunk és az átlagsebesség változásának statisztikus viselkedését a sebességarány és a porozitás függvényében határoztuk meg. A számításokat MINSZK — 32 számítógépen végeztük. A kísérletek eredményeképpen a következő formulához jutottunk;

$$\frac{1}{V_a} = \frac{\dfrac{0,22}{V_f}\,\Phi + \dfrac{1-\Phi}{V_{sz}} + \dfrac{b\left(\dfrac{V_f}{V_{sz}}\right)}{V_f}}{1 - 0,78\,\Phi + b\left(\dfrac{V_f}{V_{sz}}\right)}$$

ahol V_a a közegre vonatkozó átlagsebesség

       V_f a folyadékfázisra vonatkozó átlagsebesség

      V_{sz} a szilárd fázisra vonatkozó átlagsebesség

    $b\left(\dfrac{V_f}{V_{sz}}\right)$ a 4*b* ábrán látható, exponenciális menetű függvény.

АНАЛИЗ РАСПРОСТРАНЕНИЯ ЗВУКОВЫХ ВОЛН В ПОРИСТОЙ СРЕДЕ ПО МЕТОДУ МОНТЕ КАРЛО

Г. КОРВИН—И. ЛУКС

Постановка проблемы

За последнее десятилетие в ряде работ рассматривалась задача определения скорости распространения акустических волн в пористых средах. Решение задачи аппроксимировалось как с теоретической, так и с экспериментальной стороны. Расхождения полученных теоретических результатов вызваны различием учтенных параметров и допущенных физических механизмов (OFFICER, 1958; Петкевич—Вербицкий, 1970). Область действия результатов, полученных экспериментальным путем, определяются условиями проведения экспериментов. Большой объем экспериментов был проведен для определения скоростей волн в морских осадках. (SHUMWAY, 1960, NAFE и DRAKE, 1957.) Наиболее простое по форме выражение, полученное по экспериментам, предложено WYLLIE—GREGORY—GARDNER (WYLLIE и др., 1956). При вычислениях чаще всего применяется именно эта формула:

$$\frac{1}{V_{cp}} = \frac{\Phi}{V_{ж}} + \frac{1-\Phi}{V_T}$$

где V_{cp} — средняя скорость в пористой среде, $V_{ж}$ и V_T — скорости в среде жидкой и твердой фазы, соответственно и Φ — пористость. Формула выражает, что в пористой среде акустическая волна проводит $\Phi\%$ от всего времени своего пробега в жидкости, что однозначно с тем, что в пористой среде она также распространяется прямолинейно. Однако, это допущение не учитывает основного закона распространения волн, по которому между двумя любыми точками волна пробегает по пути, требующему наименьшего времени (принцип Ферма́та), а в нашем случае это не обязательно прямая линия.

Цель нашей работы сводится к видоизменению формулы Вилли с таким расчетом, чтобы она удовлетворила и принципу Ферма́та. Гипотеза о возможности применения при пористой среде принципа Ферма́та для волн, длина которых превосходит характерные размеры неоднородностей, была предложена WYLLIE и др. (1958).

Метод, применявшийся для решения проблемы

Поставленная проблема анализировалась с использованием метода Монте Карло, в двумерном приближении. При помощи ЭВМ была создана пористая модель с заданными поверхностью и пористостью и с случайным распределением. Путь между двумя точками, требующий наименьшего времени для пробега, находился при помощи алгоритма Форда (см. напр. KAUFMANN, 1968). Под пористостью подразумевается пропорция поверхности жидкости на заданной плоскости. Вычисления проводились для каждого скоростного соотношения с 8 величинами пористости на 50 моделях каждое. Для полученных таким образом результатов выбирались наиболее подходящие формы явных функций.

В первом приближении заданная плоскость рабзивалась гексагональной решеткой на шестиугольники, которые заполнялись случайно жидкостной и твердой фазой. Предполагалось, что из центра шестиугольника волна может перейти по прямой линии к центру соседнего шестиугольника; при этом средняя скорость получается путем деления расстояния между двумя точками на время, необходимое для пробега ломаной линии, соединяющей заданные таким образом начальную и конечную точки. Недостаток этой модели заключается в том, что из одной точки волна может распространяться только в шести направлениях (в то время как в действительности, само собой разумеется, это направление может быть любым).

Во втором приближении подобным образом применялась квадратная решетка, из элементов которой волна может распространяться по 16 направлениям, как это показано на рис. 1/а. Поскольку предполагается, что волна распространяется от центра до центра, четырехугольники могут быть представлены их центрами. Свяжем каждый центр с соседними с ним 16 остальными (в которые волна поступает «одним шагом»). Таким образом получается так назыв. граф, состоящий из пунктов и прямых. Прямые, связывающие точки графа называются по принятой терминологии дугами графа. К каждой дуге приурачивается время, необходимое для пробега волной расстояния между двумя точками и это называется длиной дуги или расстоянием между двумя пунктами. В этом графе предстоит определить серию наиболее коротких дуг, связывающих начальную точку с конечной. Часть графа, соответствующего рис. 1/а показана на рис. 1/б.

Пористая среда имитировалась путем случайной генерации (с равномерным распределением) чисел от 0 до 1, причем отдельные элементы заполнялись жидкостью или твердой фазой в зависимости от того, что указанные числа оказываются меньшими и бо́льшими по сравнению с величиной пористости. Генерация случайных чисел проводилась методом, использовавшимся авторами ADAMS и DENMAN (1966).

Каждая модель состояла из 15×30 квадратов, причем в качестве начальной и конечной точек волны выбирались две конечные точки более длинной оси симметрии. Подобная модель показана на рис. 2. Все вычисления проводились на ЭВМ Минск-32 Института.

Теоретические соображения

Применим обозначение v для отношения $\dfrac{V_{ж}}{V_T}$;

пусть будет

$$v_{cp} = \frac{V_{ж}}{V_{cp}} = G(v, \Phi).$$

Целью нашей работы является определение явной формы функции $G(v, \Phi)$.

К функции $G(v, \Phi)$ предъявляется требование удовлетворить следующим условиям:

1. $G(v, 0) = v$ т. е. при отсутствии жидкой фазы $v_{cp} = v$
   т. е. $v_{cp} = v_T$

2. $G(v, 1) = 1$ т. е. при отсутствии среды твердой фазы $v_{cp} = 1$
   т. е. $v_{cp} = v_{ж}$

3. $G(1, \Phi) = 1$ если $V_T = V_{ж}$, то $V_{cp} = V_T = V_{ж}$

4. $v \leqslant G \leqslant 1$,   средняя скорость приходится между скоростями, характерными для двух фаз.

Неравенство 4 на практике не выполняется при высоких величинах пористости ($\Phi \geqslant 60\%$). В этом случае (Hamilton, 1956; Shumway 1960; Officer, —1958) скорость распространения звуковой волны в породах, насыщенных жидкостью, может быть более низкой по сравнению со скоростью в жидкости. Полученные нами результаты могут использоваться применительно к величинам пористости $\Phi < 60\%$, т. е. они охватывают весь интересный для геофизики диапазон величин пористости. (Поскольку предполагалась приуроченность отдельных фаз к определенным местам — что не может быть действительным для частиц, плавающих в жидкости — предлагаемая модель не может применяться для случаев $\Phi \approx 1$.)

Дополнительное ограничение заключается в том, что моделью не учитываются вещественный состав, плотность и сжимаемость отдельных фаз.

Предстоит найти функцию $G(v, \Phi)$ в форме

$$G(v, \Phi) = \frac{F(v, \Phi) \cdot \Phi + v(1 - \Phi)}{F(v, \Phi) \cdot \Phi + 1 - \Phi}$$

где $F(v, \Phi)$ является пока неизвестной функцией. Данная форма функции автоматически выполняет условия 1-4. Следует заметить, что в случае $F(v, ф) = 1$ снова получается как раз формула Wyllie, так как в данном случае

$$G(v, \Phi) = \frac{V_{ж}}{V_{cp}} = \frac{\Phi + v(1 - \Phi)}{\Phi + 1 - \Phi} = \Phi + \frac{V_{ж}}{V_T}(1 - \Phi)$$

следовательно

$$\frac{1}{V_{cp}} = \frac{\Phi}{V_{ж}} + \frac{1 - \Phi}{V_T}.$$

Полученные результаты

Вычисления проводились для величин $v = 0{,}66$; $0{,}5$; $0{,}4$; $0{,}33$; $0{,}25$, причем для каждого соотношения скоростей величины Φ выбирались от $0{,}1$ до $0{,}8$ с шагом через $0{,}1$. Для каждой пары величин (v, Φ) были приняты по 50 моделей.

Подсчитанные величины функции $F(v, \Phi)$ представлены на рис. 3, причем одна точка соответствует средней по 10 моделям величине. Полученные величины при заданных v, как функции от Φ, хорошо совмещаются с прямой, т. е.

$$F(v, \Phi) = a(v) \cdot \Phi + b(v).$$

Совмещение проводилось по критерию погрешности наименьших квадратов. Угловые коэффициенты и осевые сечения прямых в функции от v показаны на рис. 4/а и 4/б. Угловые коэффициенты являются, с хорошим приближением, постоянными и равными

$$a(v) \approx 0{,}22$$

а кривая, определяемая осевыми сечениями, по имеющимся пунктам измерений, является экспоненциальной:

$$b(v) \approx B(e^{\lambda v} - 1).$$

Возможно, что численные величины входящей в формулу постоянной $0{,}22$ и параметров экспоненциальной кривой $b(v)$ не носят универсального характера, а связаны с специальной симметрией и размерами выбранной модели.

Направления дальнейшего усовершенствования метода

При вычислениях не учитывались эффекты отражений и поглощения. В связи с этим время вступления первого (регистрируемого) сигнала в экспериментах может не совпадать с вычисленным временем, а превышать его. Точно также не учитывалось, что исходной сигнал представлен не игловидным импульсом, причем форма сигнала сильно изменяется как раз по вышеуказанным причинам. В метод нахождения кратчайшего пути могут быть внесены изменения с таким расчетом, чтобы он определял и энергию вступления импульса путем снижения энергии, имеющейся у отдельных границ фаз в соответствии с коэффициентом отражения, а также, учета геометрического рассеяния. Таким образом метод Монте Карло может использоваться и для анализа скачков периодов, представляющих собой помехи в результатах акустического каротажа.

Другим возможным направлением усовершенствования метода является применение трехмерной модели.

Исследования могут быть распространены и на случай многокомпонентной среды, при котором также предполагается действие уравнения среднего времени (TEGLAND, 1970). Метод Монте Карло может быть изменен и с таким расчетом, чтобы при генерации среды, помимо пористости учитывалось и гранулиметрическое распределение.

Выводы

Проведенная работа преследовала цели определить средние скорости распространения акустических волн в пористых средах. Методом Монте Карло была создана двумерная пористая среда и с использованием алгоритма Форда на ЭВМ определялось время, необходимое для пробега акустической волной пути между двумя точками этой среды. В результате проведенной работы получена формула

$$\frac{1}{V_{cp}} = \frac{\dfrac{0{,}22}{V_{ж}}\,\varPhi + \dfrac{1-\varPhi}{V_T} + \dfrac{b\left(\dfrac{V_{ж}}{V_T}\right)}{V_{ж}}}{1 - 0{,}78\,\varPhi + b\left(\dfrac{V_{ж}}{V_T}\right)}$$

где V_{cp} — средняя для данной среды скорость

$V_{ж}$ — средняя скорость в жидкой фазе

V_T — средняя скорость в твердой фазе

$b\left(\dfrac{V_{ж}}{V_T}\right)$ — экспоненциальная функция, представленная на рис. 4б

Добавление: Алгоритм Форда для нахождения кратчайшего пути

Зададимся связным графом*, к каждой дуге которого приурачиваются положительные величины расстояний. Пусть будет расстояние не связанных между собой точек $+\infty$. Обозначим начальную точку пути x_0, а конечную точку — S. Пусть остальные точки, по любому порядку, будут $x_1, x_2, x_3 \ldots x_k$.

К каждой точке графа приурачиваются так назыв. потенциальные величины, так к точке x_i — величина $\mu(x_i)$. Сначала эта потенциальная величина равняется нулю, а в конце алгоритма она означает минимальное расстояние отдельных точек до точки x_0.

В процессе выполнения алгоритма граф разделяется на две части; обозначим эти частичные графы буквами A и B. В частичный граф A входят точки, минимальные расстояния которых до точки x_0 уже определены, а в частичный граф B — точки, для которых эти расстояния не определены, т. е. потенциалы которых еще не равняются минимальному расстоянию. Первый шаг:**

$$x_0 \in A\ \{x_1,\, x_2,\, \ldots x_k,\, S\} \in B.$$

В процессе данной операции частичный граф A дополняется элементами из частичного графа B до тех пор, пока в A не войдет и S.

---

* Относительно основ и терминологии теории графов см. напр. монографии Кауфмана (1968) или Бержа (1957).

** $X \in A$ — принятое в теории множеств обозначение того, что X входит в множество A.

А дополняется одной точкой следующим образом. Пусть будут в обобщенном виде

$$x_a, x_b, \ldots x_n \ldots \in A$$

$$x_\alpha, x_\beta, \ldots x_\nu \ldots \in B$$

а расстояние точек x_n, x_ν обозначим $\tau_{n\nu}$.

Зададимся величиной

$$\varepsilon_{n\nu} = \mu(x_n) + \tau_{n\nu}.$$

для каждой пары точек $x_n \in A$, $x_\nu \in B$.

Найдем величину

$$\varepsilon_{m\mu} = \min_{n, \nu} \varepsilon_{n\nu}.$$

Затем соответствующая точка x_μ вводится в частичный граф A и ее потенциал подбирается равным $\varepsilon_{m\mu}$. Необходимо показать, что так потенциал каждой точки в частичном графе A равен длине кратчайшего пути, соединяющего его с X_0.

Пусть количество точек в частичном графе A будет l. Если $l = 1$, то $A = \{x_0\}$ и $\mu(x_0) = 0$, для чего действительно указанное утверждение. Теперь предположим, что

$$A = \{x_0, x_1, \ldots x_{l-1}\}$$

и предположим правильность утверждения для этих точек; нетрудно видеть, что потенциал точки x_μ, полученной по правилам алгоритма, также равняется минимальной длине пути, так как

$$\mu(x_n) = \mu(x_m) + \tau_{m\mu} = \min_{n, \nu} [\mu(x_n) + \tau_{n\nu}].$$

Поскольку согласно исходному допущению $\mu(x_n)$ представляет собой длину кратчайшего из путей $x_n - x_0$, $\mu(x_n) + \tau_{n\nu}$ будет равняться длине пути, исходящего из x_ν через x_n до x_0. Величина

$$\min_\nu [\mu(x_n) + \tau_{n\nu}]$$

представляет собой длину кратчайшего пути, исходящего из одного из элементов частичного графа B через x_n до x_0. Если взять его минимум b n, получаем расстояние точки частичного графа B, располагающейся наиболее близко к x_0, т. е. длину кратчайшего из путей $x_\mu - x_0$, в чем и заключалось наше положение. Эта операция кончается введением точки S в частичный граф A.

После этого определение самого пути уже является простой задачей; находим точку x_i, для которой

$$\mu(S) - \mu(x_i) = \tau_{Sxi}.$$

(возможно, что имеется несколько таких точек; это означает, что существует несколько равно оптимальных путей) и эта точка находится на кратчайшем пути перед S. Затем подобным образом на месте S с x_i получаем предыдущую точку и т. д., пока не дойдем до x_0.

Rybár István
1886 — 1971

Nagy halottja van a magyar geofizikának: 1971. november 18-án R Y B Á R István Egyesületünk tiszteletbeli tagja, a Munkaérdemrend ezüst fokozata és az Eötvös Loránd emlékérem tulajdonosa, Eötvös Lorándnak hosszú éveken keresztül közvetlen munkatársa és kutatásainak méltó folytatója, elhunyt.

Rybár István 1886. május 7-én, Budapesten született. Iskoláit, beleértve az egyetemet is, itt végezte, majd a göttingai egyetemen Voigt Waldemar intézetében tovább képezte magát. Eötvös munkáiba már 1908-ban bekapcsolódott. Eleinte az Eötvös-ingával végzett terepmérésekben vett részt, 1912-ben Eötvös tanársegédje, majd adjunktusa, s 1915-ben az egyetem magántanára lett. Eötvös halála után Eötvös tanszékét Eötvös régebbi munkatársa, Tangl Károly kapta; Rybárt viszont rövidesen — 1922-ben — a gyakorlati fizika ny. r. tanárává, Tangl Károly halála után pedig 1924-ben Eötvös tanszékének, a kísérleti fizika tanszékének a tanárává nevezték ki, s itt 1950-ig működött. Nyugalomba helyezése azonban nem jelentette munkájának a megszakítását, hanem inkább az eredeti munkaterülethez való hatékonyabb visszatérést: még ugyanazon évben, 1950-ben az Eötvös Loránd Geofizikai Intézet tudományos tanácsadója lett, s mint ilyen dolgozott itt 75 éves koráig, 1961-ig.

Nyugalomba vonulása után is tevékenyen részt vett a Magyar Geofizikusok Egyesületének életében, amelynek alapító, tiszteleti és elnökségi tagja volt. Az Egyesület 1971 nyarán tartott elnökségi ülésén e sorok írójának jutott az a megtiszteltetés, hogy az Egyesület nevében a 85 éves Pista bátyánkat felköszönthesse. Akkor nem sejtettük, de nem is sejthettük, hogy alig néhány hónap múlva halálát kell gyászolnunk. A Magyar Geofizikusok Egyesülete, a Magyar Állami Eötvös Loránd Geofizikai Intézet és az Országos Kőolaj- és Gázipari Tröszt nagy halottjának búcsúztatása december 1-én volt a Farkasréti temetőben.

Rybár István tudományos munkássága igen nagy területet ölel fel. Értékes tanulmányai vannak pl. a spektrálanalízis és fényvisszaverődés terén. Legnagyobb jelentőségűek azonban — népgazdasági szempontból is — az Eötvös-inga továbbfejlesztései voltak; az automatikusan regisztráló Eötvös—Rybár-inga, az Auterbal

inga nemzetközi viszonylatban is hírnévre tett szert. Nem kevésbé fontosnak és nagyjelentőségűnek bizonyult 1954-ben készült E 54 ingája is, amely 1958-ban (egy másik magyar geofizikai műszerrel együtt) elnyerte a brüsszeli világkiállításon a geofizikai műszerek Grand Prix-jét. Tudományos érdemei elismeréséül a Magyar Tudományos Akadémia 1918-ban levelező, s 1931-ben rendes tagjává választotta. Az átszervezés következtében az Akadémia tanácskozó tagja lett, s 1952-ben kandidátusi fokozatot kapott. Nagy elégtételt és örömet jelentett számára, hogy tudományos elismeréséül kérése és külön vizsga nélkül, az Akadémia 1957-ben a fizikai tudományok doktorává minősítette.

Rybár István neve a magyar geofizika történetével elválaszthatatlanul összeforrt, s ez nevét és munkásságát az utánunk következő generációk számára is híven megőrzi!

<div align="right">Tárczy-Hornoch Antal</div>

<div align="center">*</div>

Great sorrow has befallen the Hungarian geophysics: on the eighteenth of november, 1971, István RYBÁR, Honorary Member of the AHG, holder of the "Silver Medal of Work" and of the "Roland Eötvös Memorial Medal" who participated for a long time in Eötvös' work and later continued it, deceased.

István Rybár was born in Budapest, 7, May, 1886. Here he got his education — including the academic career. He performed his postgraduate work in the Institute of Waldemar Voigt, Göttingen, Germany.

1908 is the year when he rendered his first services to Eötvös. In the beginning he was in charge of the field measurements. In 1912 he was appointed to the Department of Experimental Physics of the University "Péter Pázmány" (the present University "Roland Eötvös") as lecturer, later as Assistant Professor and Associate Professor.

He did not follow Eötvös in the Chair immediately for it had been offered to Károly Tangl, an earlier associate of Eötvös, while István Rybár was appointed as full time Professor of Practical Physics in 1922. After the death of Tangl, however, in 1924 István Rybár followed him in the Chair of the Experimental Physics until his retirement in 1950.

His retirement actually meant an active "retirement" to his original activity. In the same year he became a Scientific Adviser of the ELGI where he worked until his age of 75, in 1961.

Even after his final retirement he actively participated in the life of the AHG, being its foundation, honorary and presidential member.

In a Presidential Session in 1971 the undersigned had the honour to congratulate to the 85th birthday of our *Uncle Pista.* Nobody thought then that in a few months we are to mourn for him.

The funeral sponsored by the AHG, ELGI and NOGT took place on the first of December, 1971.

His scientific activity covered a wide range, including spectrum analysis and optical geometry. The most significant achievement of his, however, was—economically too—the development of the Eötvös torsion balance. The automatic *Auterbal* has gained international recognition. Another type: the E 54 was awarded with the Grand Prix of Geophysical Instruments at the World Exhibition of Brussels, in 1958.

As an acknowledgement he was elected in 1918 as Corresponding Member, and in 1933 as Ordinary Member of the Academy of Sciences.

The name of István Rybár has become inseparable from the history and development of the Hungarian geophysics and it will pass through times for generations to come.

Antal TÁRCZY-HORNOCH

Weikko Aleksanteri Heiskanen
1895 — 1971

W. A. HEISKANEN professzor 1971. október 23-án meghalt. Emlékét kegyelettel megőrizzük.

M. Állami Eötvös Loránd Geofizikai Intézet

∗

Professzor W. A. HEISKANEN deceased on the 23-th of October, 1971. We keep his memory in deep reverence.

Hungarian Geophysical Institute Roland Eötvös

GEOPHYSICAL TRANSACTIONS
VOL. XX.

CONTENTS

GEOFIZIKAI KÖZLEMÉNYEK
XX. KÖTET

СОДЕРЖАНИЕ ТОМА XX ЖУРНАЛА
«ГЕОФИЗИЧЕСКИЙ БЮЛЛЕТЕНЬ»

Az „ERDÖL-ERDGAS-ZEITSCHRIFT (MARITIME ROHSTOFFGEWIN-NUNG)"-nek a moszkvai 1971. évi 8. Olaj-Világkongresszusára készült különkiadása a „Kőolaj- és földgáz Európában".

Neves szerzők (Prof. Dr. H. Boigk, A. Caspari okl. bányamérnök, Dr. H. U. Hark és H. Schöneich bányászati főfelügyelő) tájékoztatnak a szárazföldön, valamint az európai selfterületeken folyó kutatások legújabb állásáról. A beszámolókat számos térkép és grafikon egészíti ki. Egyéb időszerű témák, többek között: előkészítés és szállítás (Dr. N. G. Graf mérnök), automatizálás a kőolaj- és földgáztermelésnél (Fr. Schlemm mérnök) stb.

A különkiadás angol nyelven készült, valamennyi tájékoztatónak német- és orosz-nyelvű összefoglalója is van.

Ára: 84.— ö.S., (12.— DM, Urban-Verlag, 1041, Bécs, pf. 116).

„Erdöl und Erdgas in Europa" Sonderheft der ERDOEL-ERDGAS-ZEITSCHRIFT (MARITIME ROHSTOFFGEWINNUNG) zum 8. Welt-Erdöl-Kongress Moskau 1971. Namhafte Autoren (Prof. Dr. H. Boigk und Dipl. Berging. A. Caspari sowie Dr. H.-U. Hark und Bergoberinspektor H. Schöneich) berichten über den neuesten Stand der Explorationen auf dem Festland und in den Schelfgebieten Europas. Die Beträge sind mit zahlreichen Karten und Graphiken ausgestattet. Weitere aktuelle Themen sind u.a. Aufbereitung und Transport (Dr. Ing. N. G. Graf) sowie die Automatisierung bei der Förderung von Erdöl und Erdgas (Ing. Dr. Fr. Schlemm).

Das Sonderheft ist in englischer Sprache herausgegeben, alle Beiträge enthalten zusätzlich deutsche und russische Zusammenfassungen.

Preis: ö.S. 84,— (DM 12,— Urban-Verlag, 1041 Wien, Postfach 116.)

„Oil and Gas in Europa" special edition of the ERDÖL-ERDGAS-ZEITSCHRIFT (MARITIME ROHSTOFFGEWINNUNG) for the 8th World Oil Congress, Moscow 1971. Distinguished authors (Prof. Dr. H. Boigk, A. Caspari Ph. D. in mining engineering and mine superintendent H. Schöneich) report on the newest results of explorations in European inland and shelf-regions. The papers are supplemented with numerous maps and diagrams. Of considerable interest are discussions of recent topics in oil and gas processing and transportation (N. G. Graf Ph. D. in eng.) and automatization (Fr. Schlemm Ph. D. in eng.).
The special edition is published in English, with German and Russian summaries for each paper.

Price: Ö.S. 84,— (DM 12, Urban-Verlag, 1041 Wien, POB 116).

«Нефть и Газ в Европе» (Erdöl und Erdgas in Europa) является отдельным выпуском журнала „Erdöl-Erdgas-Zeitschrift (Maritime Rohstoffgewinnung)" изданным по поводу 8-го мирового Конгресса по нефти, состоявшегося в 1971 г. в г. Москве.

Выдающиеся авторы (проф. д-р Х. Боигк, и горн. инж. А. Каспари, а также д-р Х. У. Харк и главный горный инспектор Х. Шэнеих) дают информацию о настоящем состоянии разведочных работ, проводящихся на суше и в шельфовых областях Европы. Работы сопровождаются рядом карт и графических материалов. Прочие актуальные темы, рассматриваемые в выпуске: подготовка месторождений, транспорт (инж. д-р Н. Г. Граф), автоматизация в области разработки нефтяных и газовых месторождений (инж. Фр. Шлемм) и т. п.

Отдельный выпуск издан на английском языке и все работы имеют резюме на немецком и русском языках.

Цена: 84 австр. шилинга (DM 12.— Urban-Verlag, 1041 Wien, Postfach 116)

If you want to advertise in our paper (circulating in 55 countries), please call on our Editorial Office: Budapest, XIV., Columbus u. 17–23. Tel: 632-835.
Postal address: Budapest, 70, P.O.B. 35, Cables: ELGI, Budapest.

* * *

Please mention *Geophysical Transactions* when answering advertisers.

* * *

The *Geophysical Transactions* is a quarterly and can be subscribed at *Kultura* Foreign Trading Company, Budapest, I., Fő u. 32.

При желании публиковать объявления в нашем журнале, циркулирующем в 55 странах, просьба обратиться к редакции по адресу: Budapest. XIV, Columbus u, 17-23,
телефон: 632-835. Почтовый адрес: Budapest, 70, pf, 35,
Телеграфиный адрес: ELGI, Budapest

* *

При ответе на объявления просьба ссылаться на «Геофизический буллетень».

* *

Подписка на журнал «Геофизический буллетень» принимается в Внешнеторговом предприятии «Культура», г. Будапешт.
Почтовый адрес: Budapest I, Fő u, 32,

Ha hirdetni óhajt 55 országban cirkuláló lapunkban, szíveskedjék Szerkesztőségünket megkeresni. Budapest, XIV., Columbus u. 17–23. Telefon: 632-835. Levélcím: Budapest, 70 pf. 35. Távirati cím: ELGI, Budapest.

* * *

Ha hirdetésünkre válaszol, szíveskedjék a *Geofizikai Közlemények*re hivatkozni.